SYNTHESIS, REACTIVITY, AND APPLICATIONS OF BENZIMIDAZOLE THIONES AND SELONES

by

Lizeth Hernandez

A thesis submitted to the faculty of
The University of North Carolina at Charlotte
in partial fulfillment of the requirements
for the degree of Master of Science in
Chemistry

Charlotte

2016

Approved by:

_____
Dr. Daniel Rabinovich

_____
Dr. Daniel S. Jones

_____
Dr. Thomas A. Schmedake

_____
Dr. Inna Sokolova

ABSTRACT

LIZETH HERNANDEZ. Synthesis, reactivity, and applications of benzimidazole thiones and selones (Under the direction of DR. DANIEL RABINOVICH)

Benzimidazole-2-thiols and their transition metal complexes have been the focus of intense research due to their potential applications in bioinorganic and organometallic chemistry. Within this field of research, the synthesis and reactivity of benzimidazole thiones and selones bearing secondary alkyl substituents on both nitrogen atoms, iPr_2bimE (E = S, Se), is described in this thesis. In order to investigate the significance of steric hindrance, the analogue of iPr_2bimS bearing methyl substituents on the nitrogen atoms, Me_2bimS, is also explored. In pursuance of establishing the coordination chemistry of these N-heterocyclic sulfur- and selenium- containing ligands, their reactivity towards closed-shell d^{10} metal ions such as copper(I), gold(I), and mercury(II) is examined. The structural differences and similarities among the iPr_2bimE (E = S, Se) and Me_2bimS complexes will be highlighted and the complete characterization of copper(I), gold(I), and mercury(II) complexes is discussed, including detailed structural information obtained using X-ray crystallography. Moreover, the enhanced selenophilicity of mercury, relative to its thiophilicity, is investigated using a combination of ^{1}H NMR spectroscopy and electrospray ionization mass spectrometry (ESI-MS).

ACKNOWLEDGEMENTS

It is my pleasure to thank everyone who has guided and helped me over the last two years. My deepest appreciation goes to Dr. Daniel Rabinovich. Throughout the years, I have been privileged to know him as a research advisor, mentor, instructor, and friend. Not only did he see my true potential from the very beginning, DR was the first individual who encouraged me to pursue a career pathway in chemistry and allowed me to recognize that chemistry was indeed a perfect match for me. From the basics in scientific research to valuable life lessons, DR has taught me all. The trust, respect, and rapport that DR so naturally builds with us is such an exceptional gift. A good mentor is one who influences a student inside the classroom, a great mentor is one who extends his influence outside of the classroom….without a doubt, DR is an exceptional mentor! I thank him for believing in me, guiding me, and preparing me to face any challenges that come my way. Your hard work, patience, and persistence is admirable and I am deeply appreciative of the extra push that you have given me to reach my maximum potential, even if it has involved a couple of "I am not impressed" talks in your office. Ultimately, I thank you for it all and could have not asked for a better mentor!

I would also like to express my gratitude to the entire DR Group. It has been you all that have made my research experience so enjoyable. John, you are an exceptional chemist and an extraordinary being. Don't ever lose your drive and willingness to help others get things done and impart your passion for science. I know that you are going to do great things in life, and please never forget about us when you do end up making it on the cover of JACS one day. Jerrod, it was a pleasure to share some time getting to know you. Thank you for the much deserved breaks, phone charging stations, and most

importantly candy access that you brought to the group. I wish you the best of luck in all of your academic ventures! Please keep in touch. Kara and Grace, I will forever be grateful for everything that you two have done. It was a pleasure to teach you, train you, and most of all, get to know you both. My words for you two lovely ladies are to dream big, believe in yourself, stay focused, and know that you can do anything! Marissa, you have so much going on for you. I have always admired your work ethic and ability to do it all! You are honestly a supermom, your children are all very lucky to have such a strong, intelligent mother that I know cares for them very much. I wish you great success in everything that you do. Margaret, congratulations future Dr. Kocherga!! You are a brilliant chemist and I know you will achieve more success as you continue on to your future goals. Thanks to Jill, Alex, Ashley, Diego, and Yana for making the lab such a wonderful place to spend my days in, it has been a privilege meeting you all in the DR group. I would also like to thank Sophie Whitemeyer, Thomas R. Groenhout, and Christian Joseph for their extraordinary contributions to my research in the summer of 2015. You are all curious individuals that remind me so much of my younger self, and I know that you will all continue to impress those around you and make us proud.

I would like to extend my appreciation towards my other thesis committee members, Dr. Schmedake, Dr. Jones, and Dr. Sokolova, for their commitment and time. Dr. Jones has been truly helpful over the past year! I greatly appreciated learning single crystal X-ray diffraction from him and will forever be grateful for all the Diet Coke he supplied me with. I also want to thank Dr. Vivero-Escoto for his help with the biological testing. I am very grateful for the one-on-one training that he provided, it was truly a great pleasure to work in his cell lab. I would also like to acknowledge Prof. James Golen

(University of Massachusetts Dartmouth) and Dr. Eric Reinheimer (Rigaku) for solving all the crystal structures presented in this thesis.

Moreover, I am extremely grateful to the entire faculty and staff of the chemistry department at UNC Charlotte for making my journey here so memorable. Robin, thank you for all the good advice, instruction with the Toshiba, great laughs and awesome conversations that we have had over the years. I would also like to thank MONICA! Thank you so much for all of your guidance in the teaching laboratories. You are an amazing, wonderful, incredible person with an impeccable work ethic. It was been a pleasure to have your guidance and assistance these past two years. Dr. Merkert and Dr. Carlin thank you very much for solving all of my instrument-related queries.

Finally, and most importantly, I would like to thank my family and friends. I am simply blessed to be surrounded with such an amazing group of people. Joel and Carlitos thank you for keeping me grounded every evening. Mami and Papi, thank you for all of your encouragement and prayers throughout the years. Your love, encouragement, and support have played a critical role in getting me to this point. Thank you all for always reminding me that it is OK to dream and dream big, los amo! Damian, my fiancé, you have been such a support system these past two years. I am such a lucky woman to have such a supportive, strong, caring man by my side…te amo.

TABLE OF CONTENTS

LIST OF FIGURES

LIST OF TABLES

LIST OF SCHEMES

LIST OF EQUATIONS

LIST OF ABBREVIATIONS

DCM	Dichloromethane
DMSO	Dimethyl sulfoxide
EA	Elemental Analysis
ESI-MS	Electrospray Ionization Mass Spectrometry
h	Hour(s)
HSAB	Hard and Soft Acids and Bases
IR	Infrared
NHC	N-Heterocyclic Carbene
NHT	N-Heterocyclic Thione
NHSe	N-Heterocyclic Selone
Mes	2, 4, 6-trimethylphenyl (mesityl)
Xy	2, 6-dimethylphenyl (2, 6-xylyl)
Dipp	2, 6-diisopropylphenyl
NMR	Nuclear Magnetic Resonance
THF	Tetrahydrofuran
XRD	X-Ray Diffraction
CT	Charge Transfer
ROS	Reactive Oxygen Species
HeLa	Cervical Cancer Cell

CHAPTER 1: INTRODUCTION

1.1 Thiones and Selones

Thiones and selones, $R_2C=E$ (E = S, Se), are sulfur and selenium analogues of ketones (E = O).[1] Since carbon, sulfur and selenium show similar electronegativities, the C=E bonds (E = S, Se) are less polar than the ketone bond but are more polarizable.[1] Some of the most investigated thioketones have found applications in the pharmaceutical, herbicide, polymer, and pesticide industries.[2-4] Regarding the chemistry of chalcogenoketones, over the past twenty years about 80% of scientific papers have focused on thioketones, while selenoketones and telluroketones accounting for much less, roughly 16% and 4%, respectively.[1]

1.2 N-Heterocyclic Carbenes

Over the past few decades, stable carbenes have received a great deal of attention from a number of researchers.[5] In the singlet carbene compounds, a carbon center bears a lone pair of electrons in an sp^2 hybridized orbital while a *p* orbital remains vacant (Figure 1.1). N-heterocyclic carbenes (NHCs) are a specific form of this class of compound, where the carbene is located on an N-heterocyclic scaffold (Figure 1.2).[6] While these species were initially not widely applied in chemistry, they have now been employed in a broad range of fields, including organocatalysis[7] and organometallic chemistry[8]. Hundreds of different NHCs are now in the literature, and much has been learned about their reactivity.

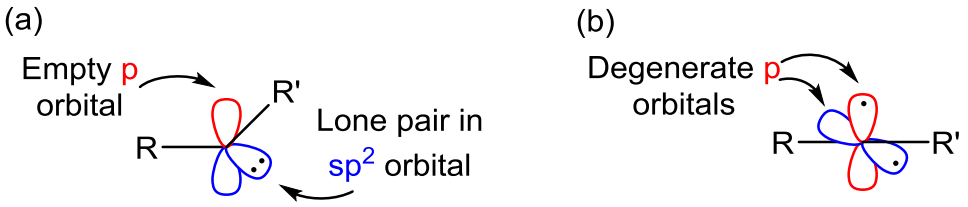

Figure 1.1. (a) singlet carbenes; (b) triplet carbenes

The chemistry of N-heterocyclic carbenes has long been limited to metal coordination compounds derived from azolium precursors, a development that was started by Öfele and Wanzlick in 1968.[9,10] Since free carbenes are now available through the work of Arduengo (1991), a renaissance in this area of chemistry has occurred.[11-13] A leading motive is the advantages of N-heterocyclic carbenes as ligands in organometallic catalysts, where they extend the scope of application reached by phosphines (functionalized, chiral, water-soluble, and immobilized derivatives).

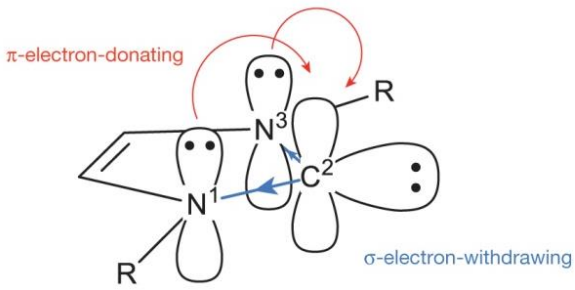

Figure 1.2. N-heterocyclic carbenes[6]

The remarkable stability of NHCs may be explained by the steric and electronic effects of their structural features (Figure 1.2). NHCs generally feature bulky substituents on the nitrogen atoms adjacent to the carbene carbon that help to kinetically stabilize the species by sterically disfavoring dimerization to the corresponding olefin. Structurally, the cyclic nature of NHCs favors the singlet state by forcing the carbene carbon into a bent, more sp^2- like arrangement. However, the electron stabilization provided by the

nitrogen atoms is a much more important factor in determining their overall stability (Figure 1.2). The adjacent σ–electron withdrawing and π–electron donating nitrogen atoms stabilize NHCs both by donating electron density into the empty *p*-orbital of the carbene carbon and by lowering the energy of the occupied σ–orbital.[6] Due to such structural features, NHCs are strong σ-donors and poor π-acceptors and thus are workhorses of organic and organometallic chemistry, rivalling phosphines and ancillary ligands in transition metal catalysis and offering new possibilities in main-group chemistry and organocatalysis.[6-8]

1.3 N-Heterocyclic Thiones

The reaction of an NHC with elemental chalcogens affords chalcogenones.[14-18] N-heterocyclic thiones (NHTs), in particular, are versatile S-donor ligands whose interaction with soft Lewis acids are feasible and result in the formation of a rich variety of coordination compounds ranging from mono and dinuclear complexes to polynuclear networks.[20, 21] Similarly to NHCs, N-heterocyclic thiones are good σ-donors and therefore, nucleophilic in character. Common NHTs known in the literature consist of imidazole thiones, benzimidazole derived thiones, and thiazole derived thiones (Figure 1.3).[22-24]

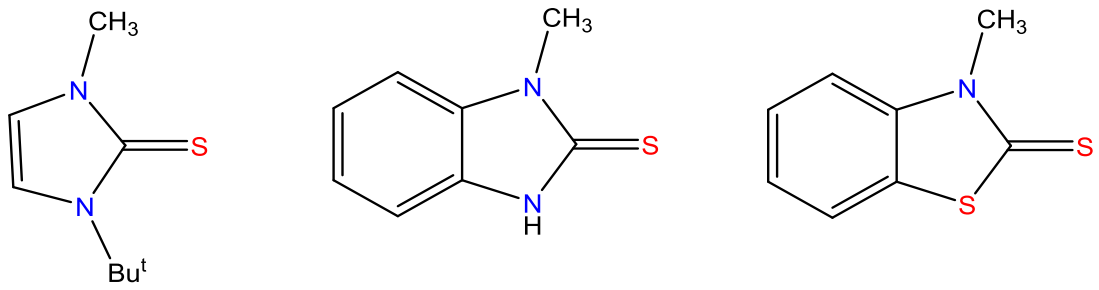

Figure 1.3. Common N-heterocyclic thiones

Heterocyclic thiones have attracted considerable interest as ligands in metal complexes because of their relevance in biological systems.[25,26] This is due to the notion that they are potentially bidentate or multifunctional donors with either the exocyclic sulfur or heterocyclic nitrogen atom available for coordination. Moreover, the thio-amide group exhibits thione-thiol tautomerization, with the thione form dominating in aqueous media and the thiol form in non-aqueous media (Figure 1.4). Based on this tautomerization, NHTs form a variety of coordination compounds having a wide range of applications as analytical reagents, medical and biologically active molecules, and metal corrosion inhibitors.

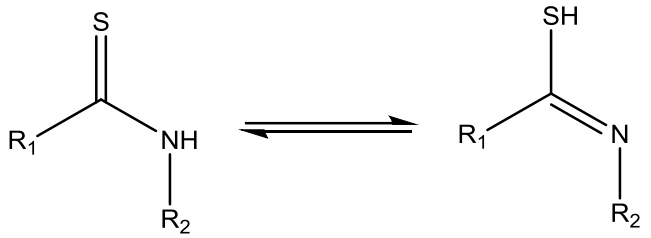

Figure 1.4. Thione-thiol tautomerization of NHTs

1.4 N-Heterocyclic Selones

Within the last 25 years, the chemistry of organoselenium compounds has attracted much attention because of their importance as synthetic tools,[27] but especially as a result of their biological,[28] agricultural,[29] and medicinal activities.[30] In particular, N-heterocyclic selones have contributed to the remarkable growth of interest in organoselenium chemistry, however, their coordination chemistry is less developed than that of N-heterocyclic thiones. N-heterocyclic selones reported in literature have proven to be useful antioxidant,[31] antiviral, [32] and anticancer [33] compounds, as well as enzyme inhibitors.[34] Therefore, efficient and safe syntheses for such Se-heterocycles are highly desirable. On the other hand, preparation of selenium-containing heterocycles often

involves the use of toxic selenium reagents, which are difficult to handle and store. For this reason, new synthetic approaches using easily accessible, more stable, and less toxic selenium reagents are of high interest. Examples of a variety of current N-heterocyclic selones reported in the literature are depicted in Figure 1.5.[35-38]

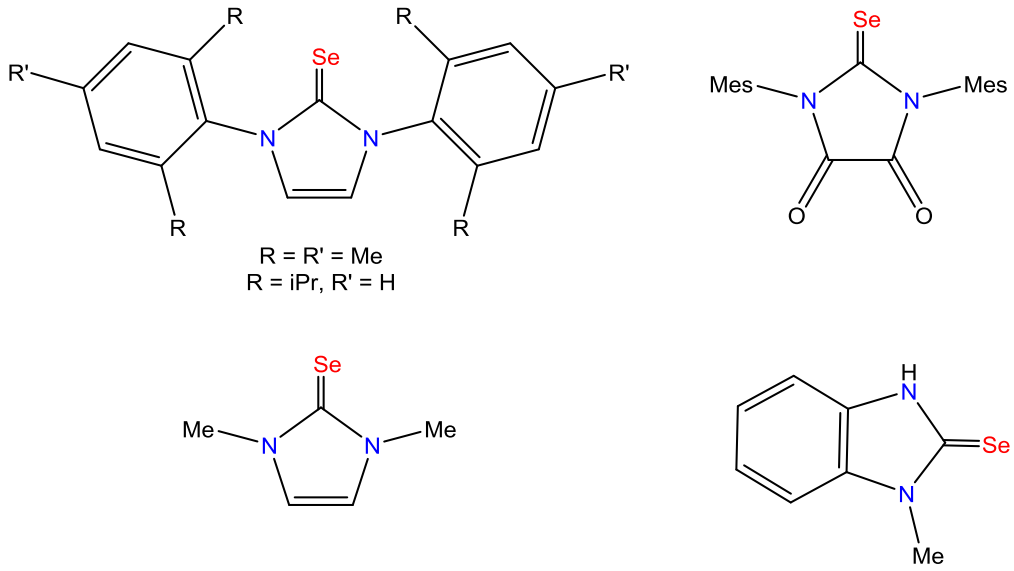

Figure 1.5. Structures of N-heterocyclic selones reported in literature

1.5 Benzimidazole Thiones and Selones

Benzimidazoles are an extension of the well elaborated imidazole system and are known for their commercial and biological importance as pharmaceuticals, veterinary anthelmintics and fungicides. Literature survey shows that among the benzimidazole derivatives, 2-substituted ones are found to be pharmacologically more potent and hence the design and synthesis of 2-substituted benzimidazoles is an active area of research as a large variety of these compounds have been found to possess antiulcer, anthelmintic, anti-inflammatory, antispasmodic, antihistaminic, antimicrobial, and anticancer activities. Moreover, benzimiazolin-2-chalcogenones have been synthesized from their elemental chalcogens and, less commonly, by the utilization of other chalcogen sources such as

CSe_2, thiophosgene, etc.[39-41] Benzimidazole-2-thione, the most studied benzimidazole-2-chalcogenone, is effective in preventing the dissolution of carbon-steel in acidic media[42] and corrosion of brass and aluminum in alkaline solutions.[43,44]

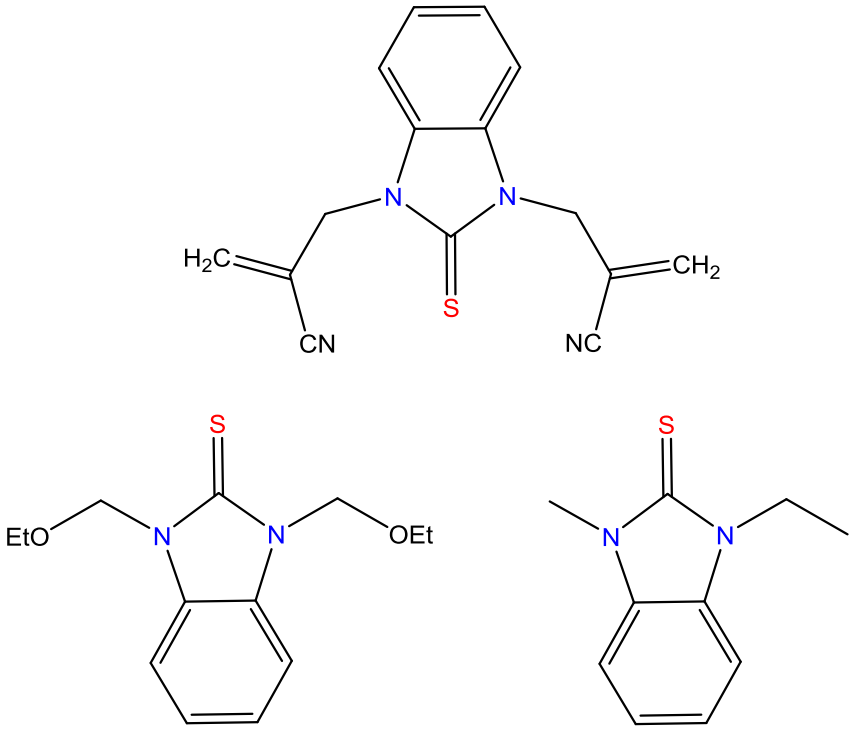

Figure 1.6. Examples of primary disubstituted benzimidazole thiones

In contrast to the numerous studies pertaining to benzimidazole-2-thione, there are few corresponding investigations of its disubstitued and/or selone analogues. Such examples of disubstituted derivates reported so far predominately contain benzimidazolin-nitrogen atoms that are bonded to a primary carbon (Figure 1.6)[45-47] where very few examples are reported for derivatives containing secondary or tertiary alkyl or aryl substituents (Figure 1.7).[48,49]

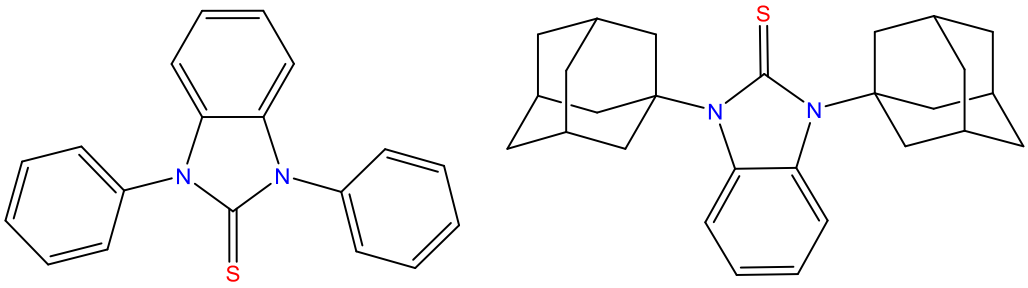

Figure 1.7. Examples of benzimidazole thiones bearing aryl or tertiary alkyl substituents

Studies pertaining to benzimidazole selones are rare where the bulk majority reported in literature so far are monosubstituted (Figure 1.8).[50-53] Metal complexes of non-substituted and monosubstituted benzimidazole chalcogenones have been synthesized and structurally characterized for mercury(II),[54-56] copper(I),[57-64] and gold(I)[65-67] (Figure 1.9).

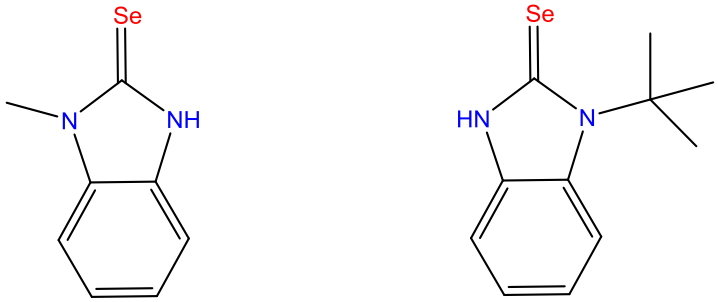

Figure 1.8. Examples of benzimidazole selones

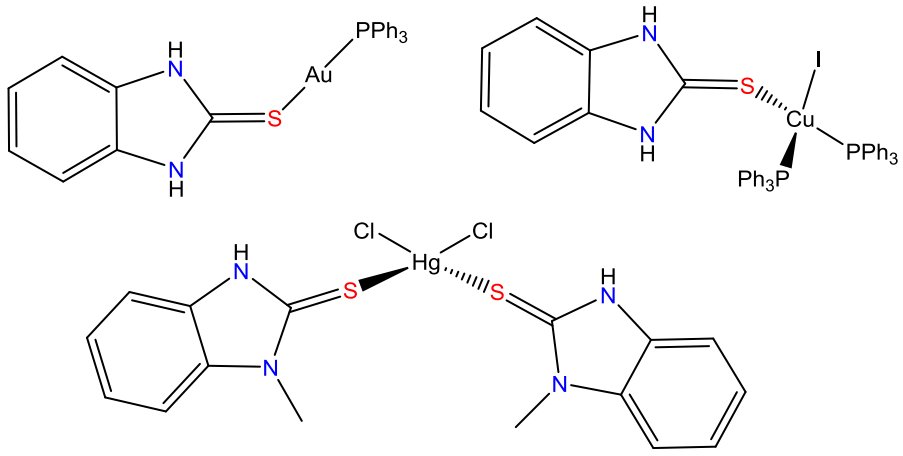

Figure 1.9. Selected examples of metal benzimidazole chalcogenone complexes

The synthesis of a disubstitued benzimidazole thione, Me_2bimS, and selone, iPr_2bimSe, is of particular interest to this thesis due to their remarkable stability, structurally rigid backbone, and aromatic delocalized electron system. The synthesis of Me_2bimS has been reported via treatment of benzimidazole-2-thione with dimethylcarbonate, as shown in Scheme 2.1.[68] However, this reaction produces three methylated products with relatively low yields that must separated from each other.

Scheme 2.1. Reported Synthesis of Me_2bimS[68]

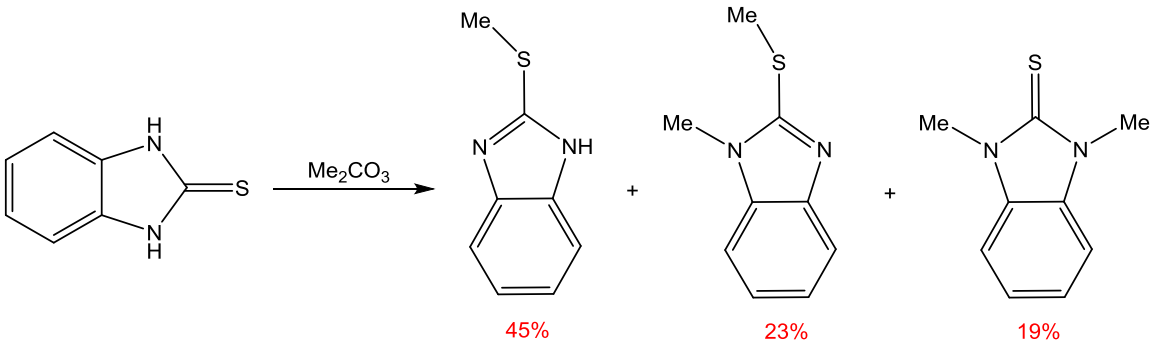

The synthesis of iPr_2bimSe has been reported via two different reaction routes in the literature, as shown in Scheme 2.2.[70] One route involves the treatment of its NHC precursor salt, [iPr_2bimH]Br, with disodium diselenide and potassium tert-butoxide to produce the respective ligand in a relatively low yield. The other synthetic route also involves the use of [iPr_2bimH]Br, however, it is reacted with elemental selenium and bis(trimethylsilyl)amine. Advantages of this second synthetic route include the isolation of the pure product in good yield, however, it incorporates expensive starting reagents and is a thermally sensitive reaction.

Scheme 2.2. Reported Syntheses of iPr_2bimSe[70]

(a)

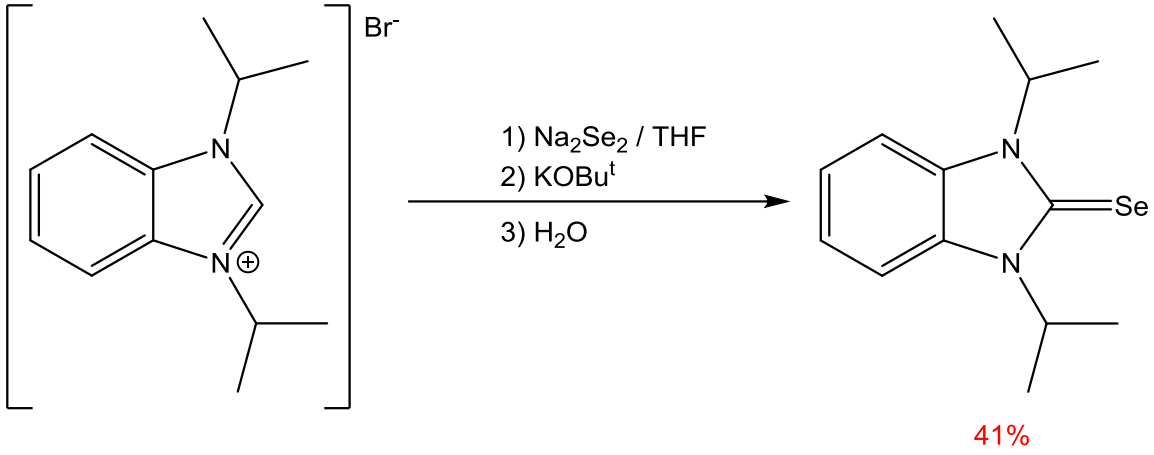

(b)

1.6 Research Objectives

The main objective of this research lies in the synthesis of monodentate benzimidazole derived R_2bimE ligands bearing methyl or isopropyl substituents (R = Me, ^{i}Pr) and either sulfur or selenium donor moieties (E = S, Se), as shown in Figure 1.10. Most disubstituted benzimidazole thiones and selones reported so far contain primary alkyl groups on the nitrogen atoms.[45-47] A secondary carbon attached to the nitrogen is desirable since it increases the steric bulk of the benzannulated ligand and therefore

extends the scope of its application in catalysis. Notably, the iPr_2bimSe and Me_2bimS have previously been synthesized and iPr_2bimSe has been structurally characterized.[68-72] However, there are no examples of structurally characterized metal complexes that feature such benzimidazole thione and selone ligands. Here, we describe improved syntheses of Me_2bimS[68-71] and iPr_2bimSe[72] and synthesis of the new iPr_2bimS ligand.

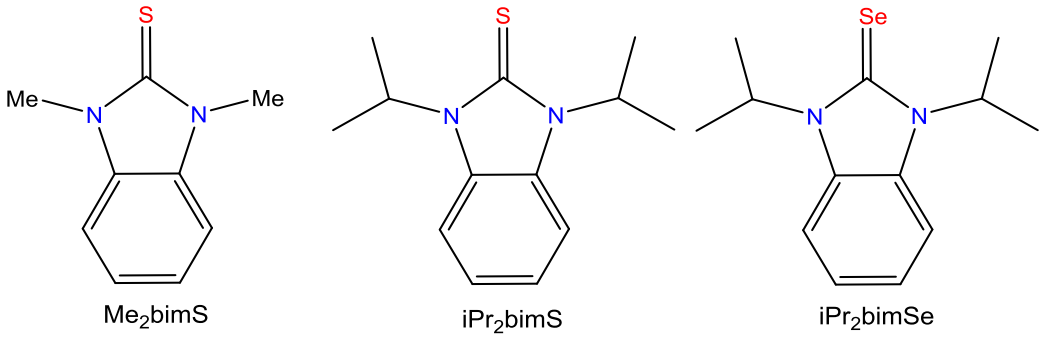

Figure 1.10. The R_2bimE ligands (R = Me, E = S; R = ^{i}Pr, E = S, Se)

The reactivity of these ligands towards elemental iodine and bromine will help understand how they behave in the presence of oxidizing agents. Moreover, in order to establish the coordination chemistry of these NHT and NHSe ligands, their reactivity with closed-shell d^{10} metal ions such as mercury(II), copper(I) and gold(I) were chosen because of their simple electronic configuration. Therefore, such diamagnetic complexes can be readily characterized using spectroscopic techniques such as nuclear magnetic resonance. Since these complexes are convenient probes to assess the coordination preferences of the R_2bimE ligands, the characterization of some of the new complexes by single-crystal X-ray diffraction will also be pursued with the goal of comparing metal coordination in a sulfur-rich environment versus the selenium-rich environment provided by the iPr_2bimSe ligand.

Additionally, selenium, being a softer donor than sulfur, has been shown to exhibit higher affinity than sulfur for metals like mercury and copper.[71-75] Consequently, competition studies between thione and selone analogues with soft Lewis acids such as Hg(II) and Cu(I) can be used to confirm the greater selenophilicity of the iPr_2bimSe ligand over the thiophilicity of the Me_2bimS and iPr_2bimS ligands. Moreover, a preliminary study of the potential anticancer properties of selected copper(I) complexes of the R_2bimE ligands against HeLa cancer cells will help evaluate if they are viable anticancer agents.

CHAPTER 2: RESULTS AND DISCUSSION

2.1 Synthesis and Characterization of R_2bimE

The combination of benzimidazole with a relatively weak base, large excess of alkylating agent, and prolonged reaction time yielded benzimidazolium salts (Scheme 2.3), which are the key intermediates in the syntheses of the R_2bimE (R = Me, E = S; R = ^{i}Pr, E = S, Se) ligands.[76] Treatment of these salts with a slight excess of potassium carbonate and elemental sulfur or gray selenium in refluxing methanol or ethanol for 24-48 hours afforded the corresponding ligands (Scheme 2.4).

Scheme 2.3. Synthesis of Intermediate Salt

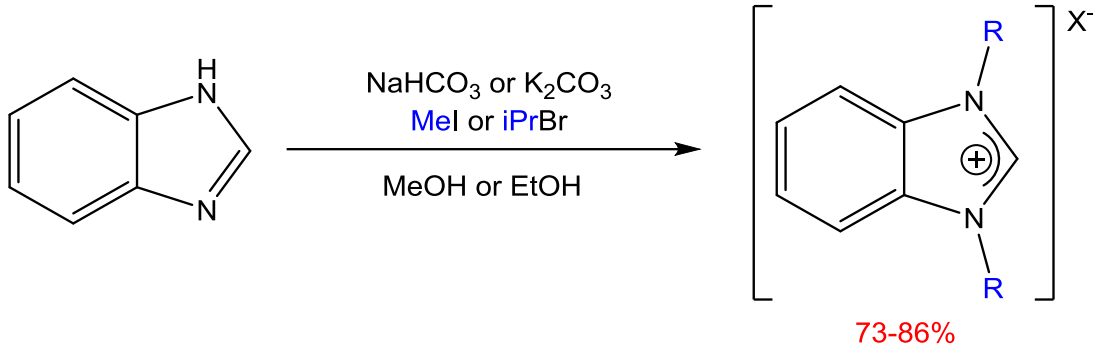

Scheme 2.4. Synthesis of R_2bimE (R= Me, E = S; R = ^{i}Pr, E = S, Se)

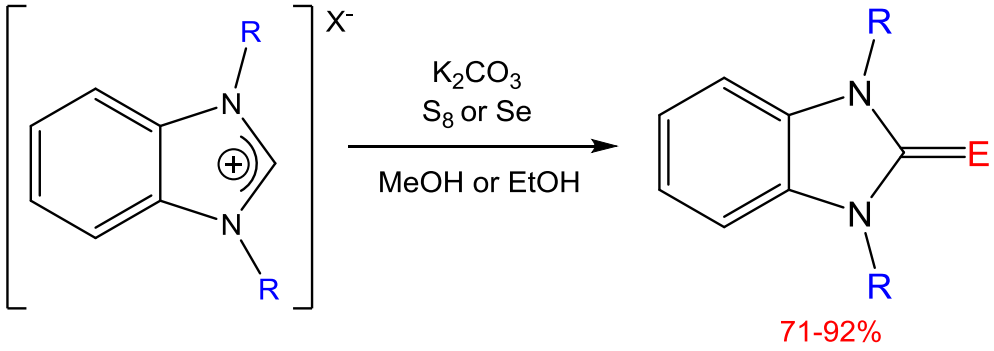

It is proposed that the base in the reaction, K_2CO_3, abstracts the methine proton from the imidazole ring. Consequently, the π-electrons forming the double bond move back onto the more electronegative nitrogen, and as a result forms a reactive carbene that quickly incorporates the sulfur or selenium atom. Through this improved synthesis, the iPr_2bimS, iPr_2bimSe, and Me_2bimS ligands have successfully been isolated in 71-92% yields and fully characterized by different analytical and spectroscopic techniques, including elemental analysis (CHN) and IR and NMR spectroscopies.

The ^{1}H NMR spectra of Me_2bimS (Figure 2.1) in d_6-DMSO depicts three distinct peaks, one corresponding to the methyl substituent (δ 3.70 ppm) and two corresponding to the inequivalent protons located on the benzene ring (δ 7.22-7.30 & 7.40-7.48 ppm). Moreover, the aromatic hydrogens depict an AA'BB' splitting pattern that is common for ortho disubstituted benzenes containing chemically equivalent but magnetically inequivalent protons.[77]

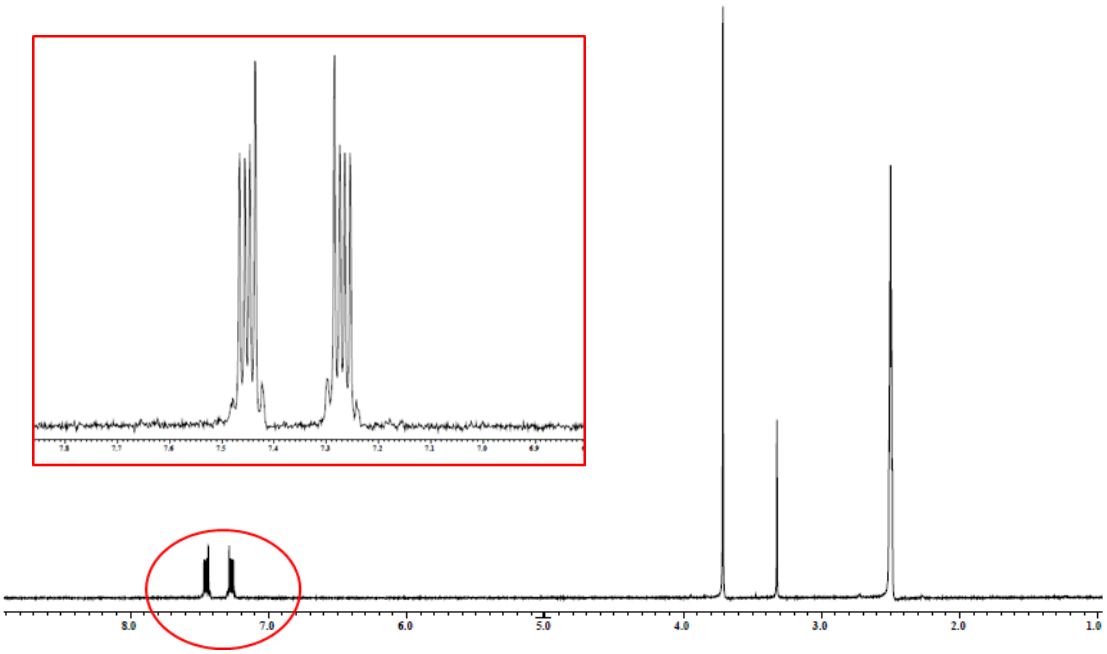

Figure 2.1. ^{1}H NMR spectrum of Me_2bimS in d_6-DMSO.

Similarly, the ^{1}H NMR spectrum of the iPr_2bimE ligands (E = S, Se) in d_6-DMSO (Figures 2.2 and 2.3) depicts four distinct peaks, two corresponding to the isopropyl substituents (δ 1.50-1.52 & 5.57-5.74 ppm) and the remaining two to the aromatic ring protons (δ 7.18-7.31 & 7.64-7.81 ppm). Notably, the two inequivalent aromatic protons present in the Me_2bimS ligand are closer in distance to each other (δ 7.22-7.30 & 7.40-7.48 ppm) than those present in the iPr_2bimS ligand (δ 7.18-7.31 & 7.64-7.81 ppm). Difference in rotation of the isopropyl substituents may account for the slight asymmetry observed in the aromatic protons in comparison to the methyl ligand. Moreover, the isopropyl septet observed in the spectra of the corresponding iPr_2bimE (E = S, Se) ligands is unexpectedly deshielded for iPr_2bimSe (δ 5.74 ppm) in comparison to iPr_2bimS (δ 5.57 ppm); an observation that defies the conventional trend as selenium is less electronegative than sulfur and should therefore have a shielding effect.

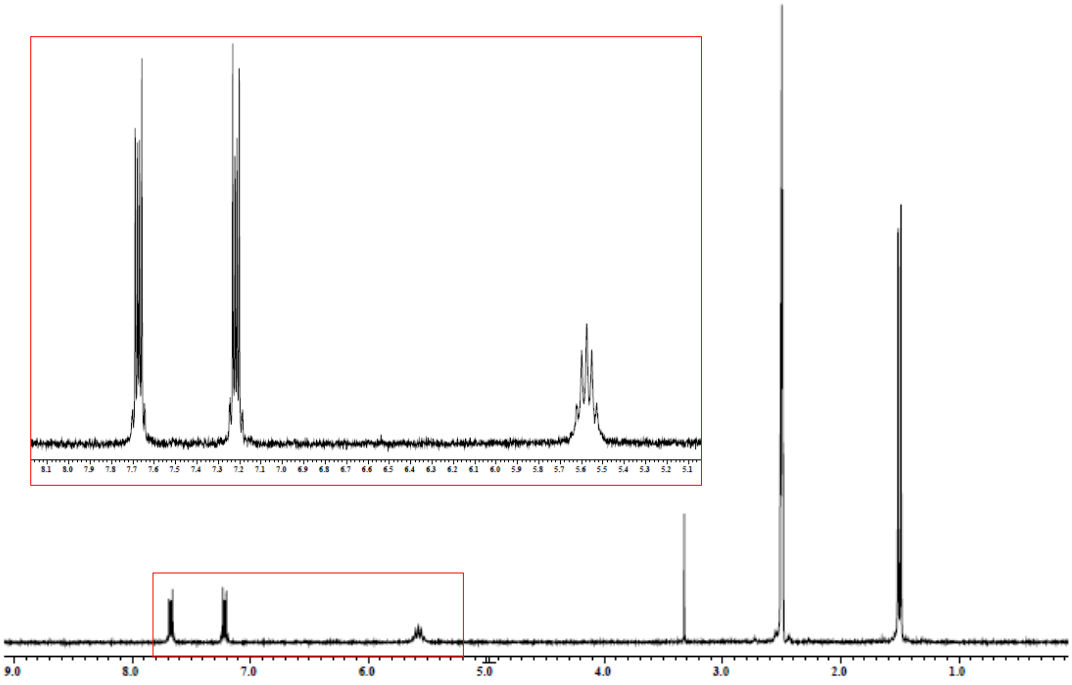

Figure 2.2. ^{1}H NMR spectrum of iPr_2bimS in d_6-DMSO.

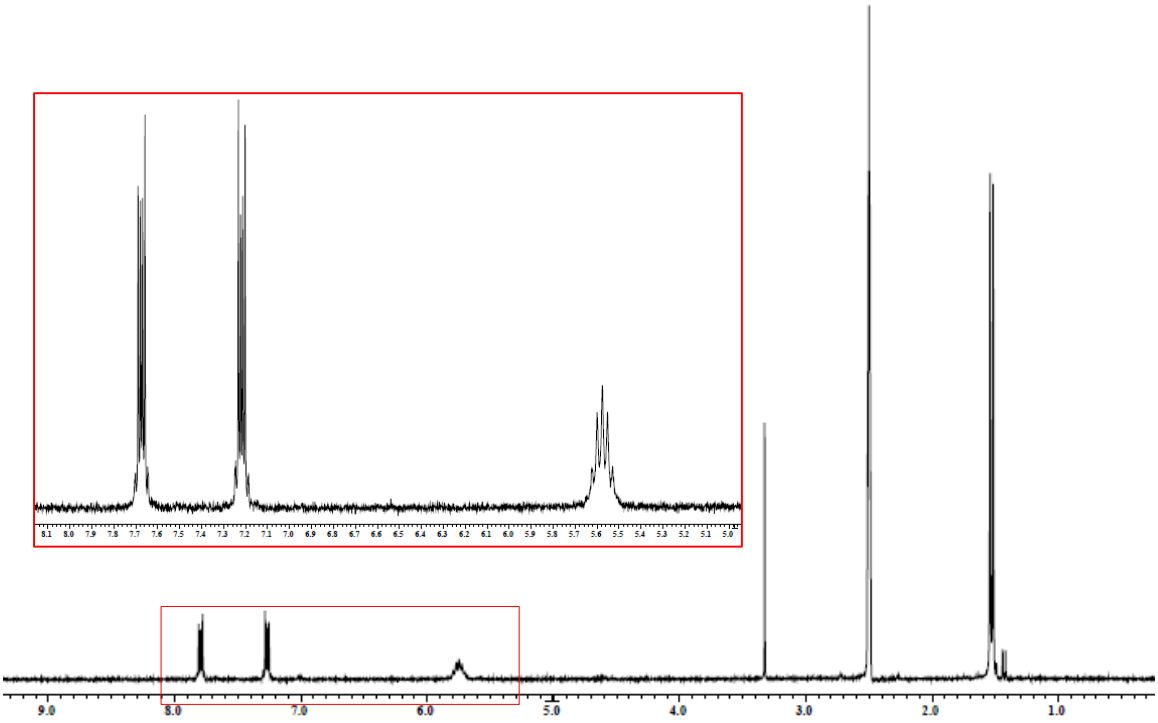

Figure 2.3. ^{1}H NMR spectrum of iPr_2bimSe in d_6-DMSO.

The formation of either the thione or selone on the benzimidazole ring is implied by the absence of the peak located at around 10 ppm originally observed in the ^{1}H NMR spectra of the benzimidazolium intermediates (Figure 2.4). Similarly, the shifting of the respective isopropyl and methyl peaks upfield when compared to the intermediate denotes the incorporation of the electron rich sulfur or selenium. ^{1}H NMR data in other solvents including acetone and acetonitrile demonstrate similar chemical shifts with variations in the pattern at which the peaks appear.

The ^{13}C NMR spectrum in d_6-DMSO shows the nine expected peaks for Me_2bimS, similarly, the iPr_2bimE (E = S, Se) ligands shows thirteen peaks. The thione/selone carbon is the furthest downfield as it is electron deficient resulting from its position with the two flanking nitrogens. The isomerism of these heterocyclic ligands

results in the electron density being drawn towards the respective chalcogen, in turn making it a strong electron-releasing donor atom.

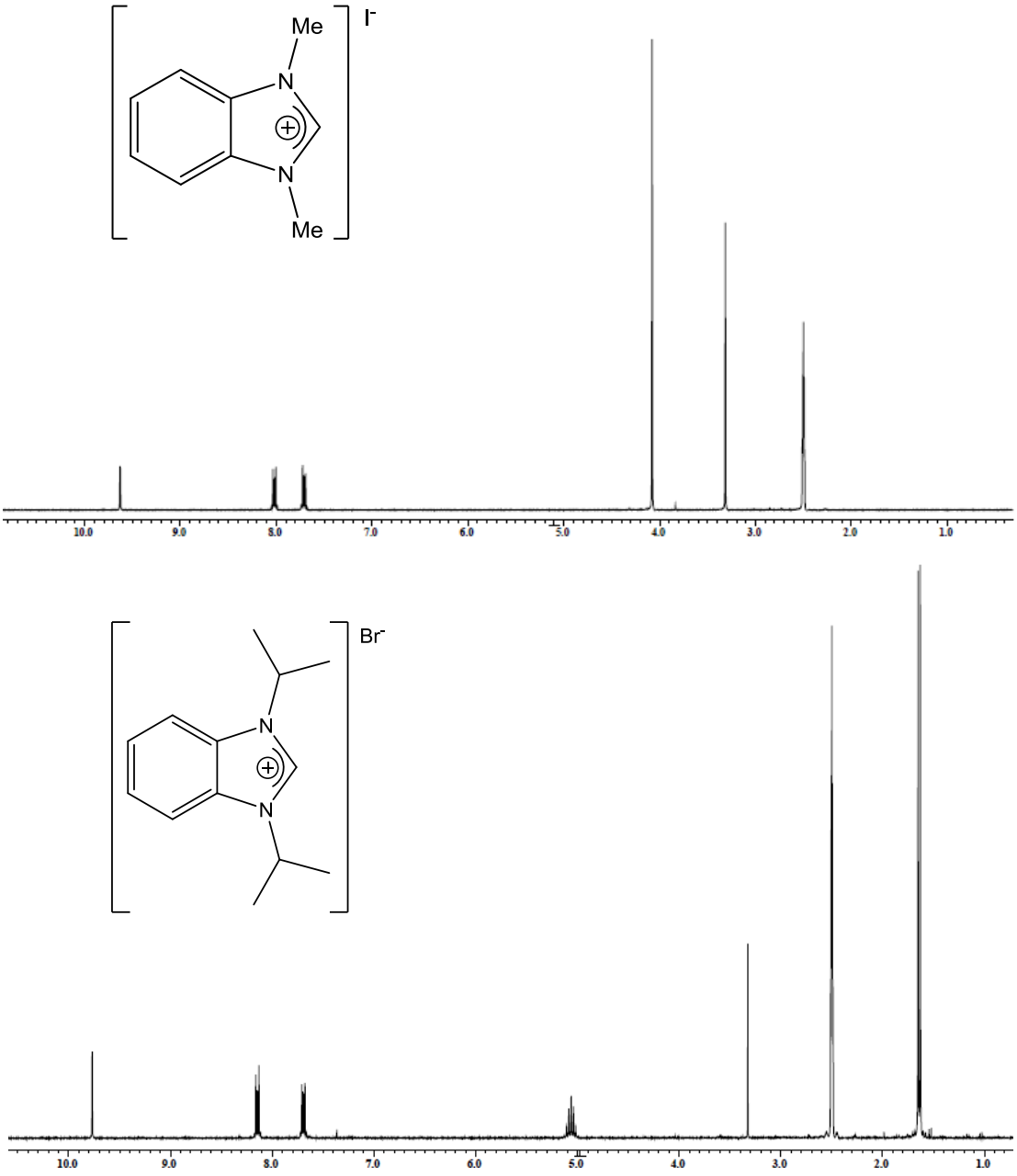

Figure 2.4. ^{1}H NMR spectra of [R_2bimH]X (R = Me, X = I; R = ^{i}Pr, X = Br) in d_6-DMSO.

Single crystals of iPr_2bimE (E = S, Se) suitable for X-ray diffraction studies were grown at room temperature by slow evaporation of the respective solutions in acetone. The

molecular structures are shown in Figure 2.5 with selected bond lengths and angles shown in Table 2.1.

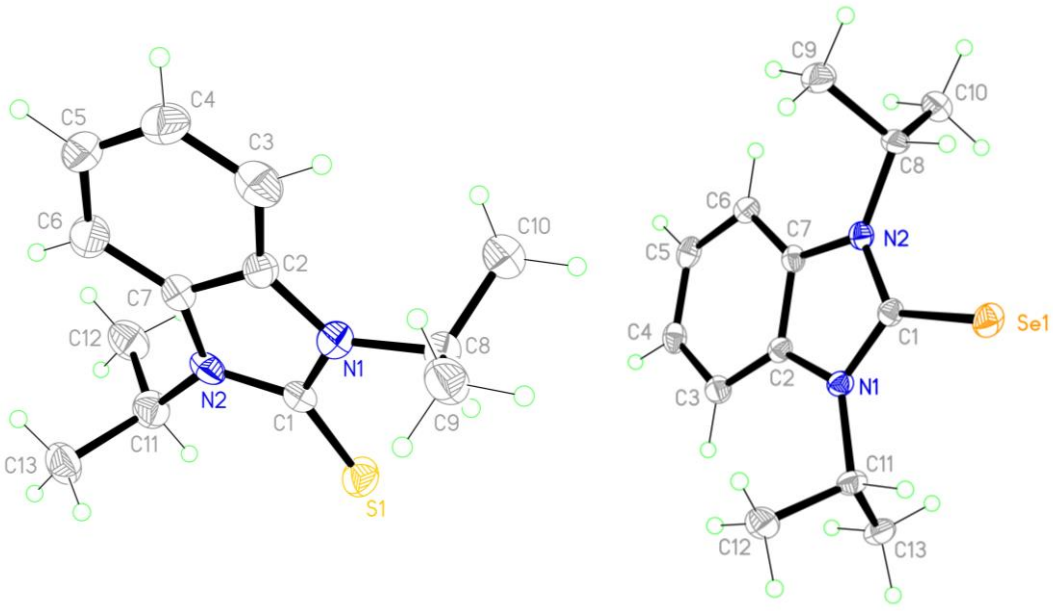

Figure 2.5. Molecular structures of iPr_2bimE (E = S, Se)

Table 2.1. Selected bond lengths (Å) and angles (°) for iPr_2bimE (E = S, Se)

	E = S	E = Se
E(1)–C(1)	1.670(5)	1.845(16)
N(1)–C(1)	1.382(7)	1.367(2)
N(2)–C(1)	1.354(7)	1.362(2)
N(2)–C(1)–E(1)	127.2(4)	126.30(12)
N(1)–C(1)–E(1)	126.5(4)	126.21(12)
C(1)–N(1)–C(2)	110.6(4)	109.45(13)
C(1)–N(2)–C(7)	110.2(4)	109.59(13)

The iPr_2bimS ligand crystallized in the orthorhombic system with a C–S bond length of 1.670 Å. This value is intermediate between the known C–S single (1.81 Å) and double bond (1.55 Å) lengths reported for most thione compounds.[78] Similarly, the C–Se bond length of 1.845 Å for the iPr_2bimSe ligand is intermediate between the known

C=Se double bond length of 1.689 Å for carbon diselenide[79] and the known average C–Se single bond length of 1.916 Å from organoselenium compounds found in the literature.[80-83] This intermediate bond length value between the predicted C–S/C–Se single and double bond values is a direct result of the resonance behavior apparent at the heterocyclic thione/selone region, illustrated in Figure 2.6.

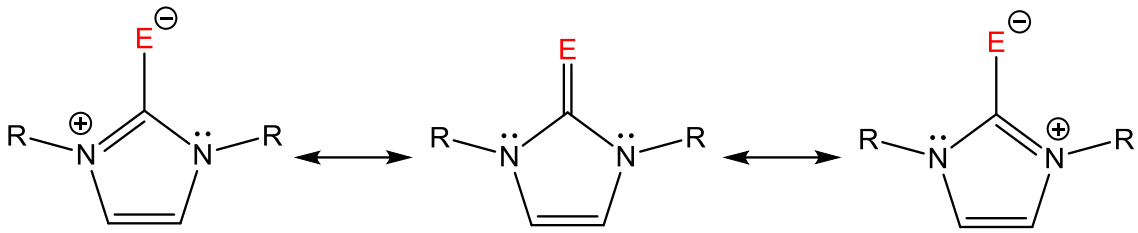

Figure 2.6. Resonance within the heterocyclic thione/selone region of R_2bimE (E = S, Se)

2.2 Halogen Compounds

A variety of compounds containing group 16 donor atoms, namely sulfur and selenium, have been known to exhibit rich structural diversity and reactivity with dihalogen and interhalogen species.[84-87] Hypervalent compounds have thus become of interest and are studied for their superconducting ability which has potential applications as electrical conductors and synthetic antithyroid agents.[88-94] Diiodine derivatives (R_2bimE)I_2 (R = Me, E = S; R = ^{i}Pr, E = S, Se) were prepared by reacting equimolar amounts of the ligands and I_2 for 21-24 h in THF, diethyl ether, or dichloromethane (Scheme 2.5). The resulting hypervalent compounds are isolated as air-stable microcrystalline brown solids in 65-81% yields. Previously, Devillanova *et al.* had reported the synthesis and thermodynamic characterization of (Me_2bimS)I_2[51] in dichloromethane and recently Singh *et al.* reported the synthesis of (iPr_2bimSe)I_2 in tetrahydrofuran in 77.6% yield.[70]

Scheme 2.5. Synthesis of $(R_2bimE)I_2$ (R = Me, E = S; R = ^{i}Pr, E = S, Se)

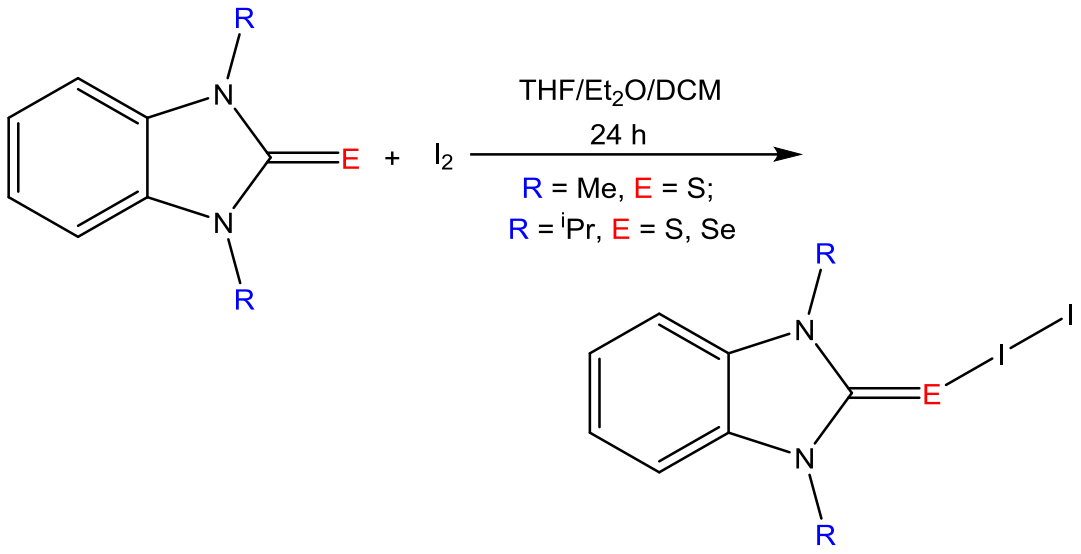

A single orange crystal of the new $(iPr_2bimS)I_2$ compound suitable for X-ray diffraction, was obtained at room temperature by layering with hexanes a solution of the compound in ethyl acetate (Figure 2.7). Selected bond lengths and angles are summarized in Table 2.2. The ligand reacts with molecular iodine to produce a charge-transfer (CT) product that has a severely bent geometry around the sulfur atom with a linear S–I–I fragment (178.97°) and a severely bent geometry around the sulfur atom depicted by the C-S-I bond angle (94.78°). Moreover, it was found that the C–S bond distance is slightly longer than that of the free ligand (1.709 *vs* 1.670 Å). The selone derivative, $(iPr_2bimSe)I_2$, reported in 2013 by Singh and coworkers yielded a similar structure featuring a linear Se–I–I fragment parallel to the region of coordination.[70] Moreover, the interaction between chalcogen-donor molecules (E = S, Se) and dihalogens (X_2) to give adducts containing an almost linear E–X–Y fragment can be seen as a charge-transfer process.[50,51] The charge-transfer process occurs via the transfer of charge density from a lone pair of electrons on the donor atom to the empty σ* orbital of the halogen species,

producing a lowering in the X–X bond order.[14] The consequent increase in the X–X bond length can be finely tuned by using donors of different strengths, which means changing the chalcogen-donor atom or its chemical environment.

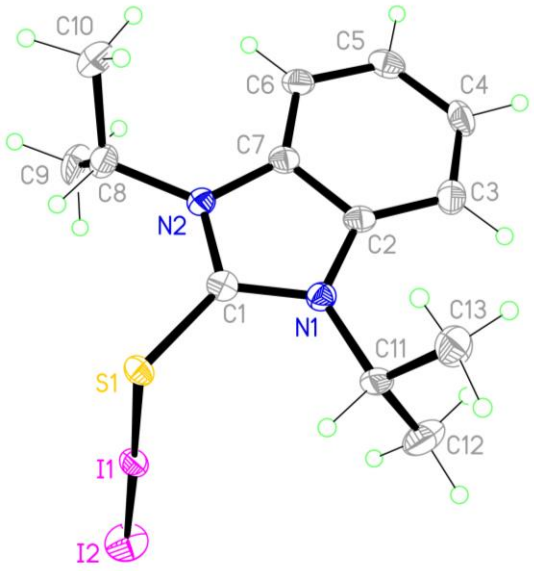

Figure 2.7. Molecular structure of (iPr_2bimS)I_2

Table 2.2: Selected bond lengths (Å) and angles (°) for (iPr_2bimS)I_2

S(1)–C(1)	1.709(4)	C(1)–S(1)–I(1)	94.78(13)
S(1)–I(1)	2.755(10)	S(1)–I(1)–I(2)	178.97(2)
I(1)–I(2)	2.850(5)	S(1)–C(1)–N(1)	125.6(3)

The formation of hypervalent compounds from heterocyclic selones and I_2 has been investigated in more detail than those with Br_2.[50,51,70,86-90] The dibromide derivative of iPr_2bimSe was prepared in dichloromethane for one hour and the resulting yellow solid was isolated in 82% yield (Scheme 2.6). Singh *et al.* recently reported a crystal structure of this compound in which the selenium moiety binds to the Br_2 molecule in a T-shaped geometry forming an oxidative-addition product.[70] This ‘T-shaped” geometry

around the selenium moiety is also reported in similar compounds that are known as stable donor/acceptor adducts.[14,90]

Scheme 2.6. Synthesis of (iPr_2bimSe)Br_2

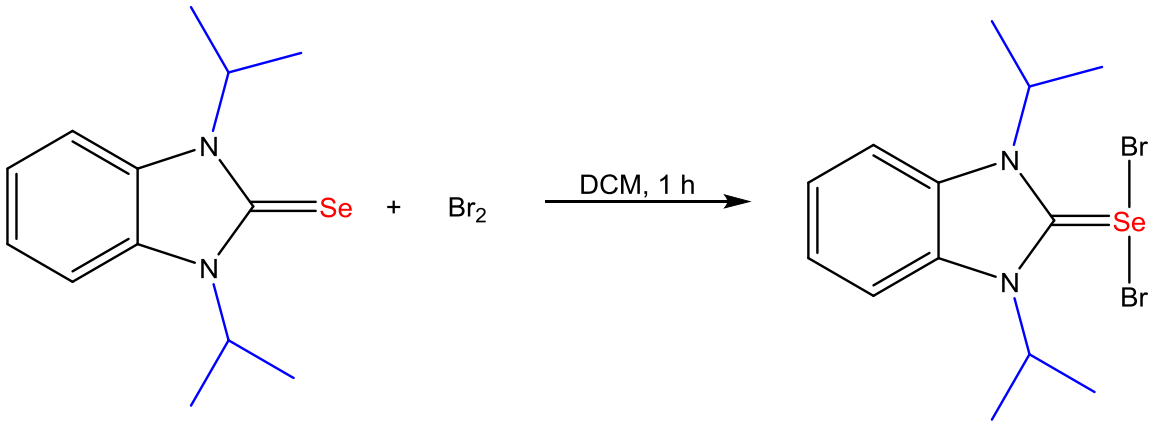

It is known that organoselenyl chlorides, RSeCl, are unstable because they can easily undergo dismutation or disproportionation reactions. Moreover, chlorination agents have a superior ability to oxidize substrates, in comparison to the abilities of dibromine, diiodine, and interhalogen reagents, which hinders the synthesis of these compounds. The stabilization of RSeCl compounds can be achieved by addition of a second chloride[95] as well as by the use of bulky substituents[96] or by functionalization of an organic ligand to provide a donor atom for intramolecular coordination.[97] Few examples of (NHSe)Cl_2 compounds have been reported in literature where all exhibit a T-shape geometry around the selenium atom.[38, 70a, 95b, 98] In attempts to prepare a benzimidazole selone dichloride, we treated iPr_2bimSe with thionyl chloride in dichloromethane at room temperature (Scheme 2.7). The resulting (iPr_2bimSe)Cl_2 was isolated in 47% yield and its purity was confirmed by elemental analysis. This is an improved synthesis as Singh *et al.* reported

the preparation of this compound at 55% yield, however, the use of the more toxic chlorine gas was employed in their synthesis.[70]

Scheme 2.7. Synthesis of (iPr_2bimSe)Cl_2

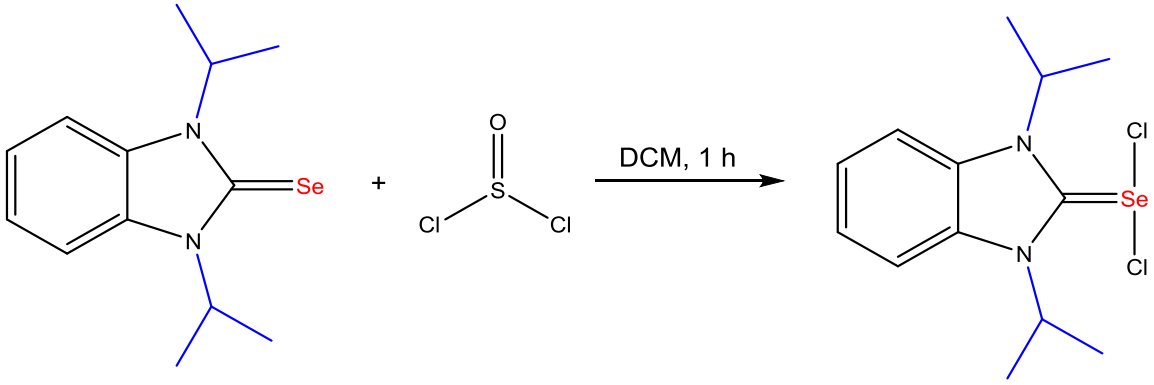

Other known (NHSe)Cl_2 compounds reported by Devillanova *et al.* also involve the use of chlorine gas as a starting reagent.[98] Khrustalev *et al.* reports synthesis of similar (NHSe)Cl_2 compounds utilizing sulfuryl chloride, SO_2Cl_2, as the chlorinating agent.[38] Moreover, Ragogna *et al.* report synthesis of dichloride derivatives by treatment of chalcogen tetrahalides (SeX_4 and TeX_4) with neutral donor ligands such as $^nBu_3P$.[95b] Notably, there are no reported instances that incorporate the use of thionyl chloride, $SOCl_2$, for the synthesis of (NHSe)Cl_2 compounds.

2.3 Synthesis and Characterization of Mercury(II) Complexes

In order to gain insight into the steric and electronic effects of N-heterocyclic thione and selone ligands to its coordination chemistry, we want to examine a series of complexes derived from mercury(II) halides. While the toxicological properties of mercury are often associated with its high affinity for sulfur,[99a] its toxicity has also been attributed to its impact on the biochemical roles of selenium,[99b] which is an important antioxidant element in the human body. Thus, in view of the proposal that the toxicity of

mercury is linked to its impact on the biochemical roles of sulfur and selenium, it is pertinent to further develop the coordination chemistry of mercury in an environment that features such two chalcogens.[74]

Mercury(II) complexes of R_2bimE (R = Me, E = S; R = ^{i}Pr, E = S, Se) were prepared by reacting the respective ligand with a mercury halide salt (HgX_2, X = Cl, Br, I) in either a 1:1 or 1:2 molar ratio, as illustrated in Scheme 2.8. Notably, these are the first coordination complexes of the R_2bimE (R = Me, E = S; R = ^{i}Pr, E = S) ligand system.

Scheme 2.8. Synthesis of Mercury(II) Complexes

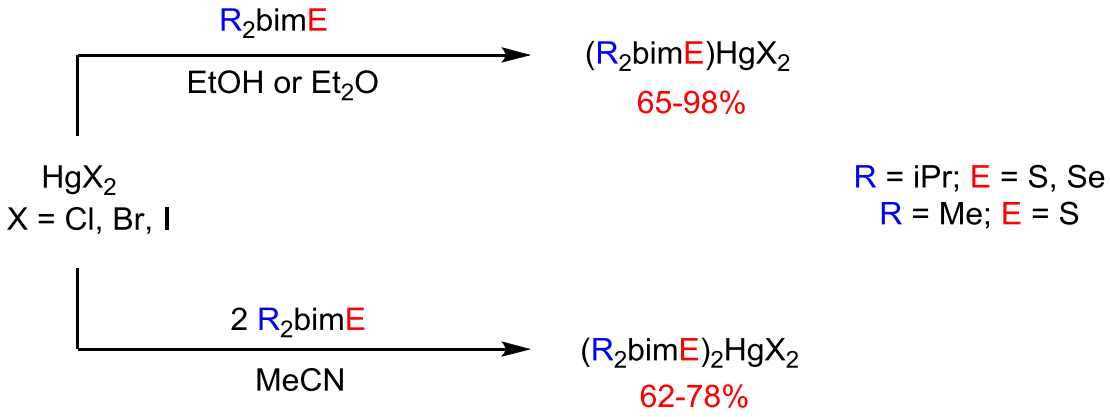

The 18 new complexes were isolated in *ca*. 62-98% yield and are all air-stable white or pale yellow solids that dissolve in polar solvents such as dimethyl sulfoxide, dichloromethane, acetonitrile, and tetrahydrofuran but are insoluble in water and ethyl acetate. Moreover, all mercury(II) complexes prepared so far are less soluble than the free ligand and have been characterized by elemental analysis, IR spectroscopy, NMR spectroscopies, and electrospray ionization mass spectrometry (ESI-MS).

The NMR spectra of these complexes exhibit similar patterns to those of their corresponding R_2bimE (R = Me, E = Se; R = ^{i}Pr, E = S, Se Se) ligands, however, all

peaks tend to be shifted downfield in comparison to the free ligand. Moreover, the ^{1}H NMR spectra for the various Hg(II) halide complexes are all similar to each other despite the speculation that the direct coordination of the halides to the metal could influence the chemical shifts with their electron density. Furthermore, a representative ESI-MS spectrum of a 1:2 mercury complex is depicted in Figure 2.8 and the ESI-MS data for all the mercury(II) complexes are summarized in Table 2.3. All ESI-MS experiments conducted at a cone voltage of 30 V in acetonitrile showed that a chloride anion is cleaved. Moreover, the $[L_2HgCl]^+$ cation is the prevalent species for all 1:2 mercury complexes. Surprisingly, this $[L_2HgCl]^+$ peak was also observed in the ESI-MS spectra for the $(iPr_2bimS)HgX_2$ (X = Cl, Br, I) complexes. Further experiments will have to be conducted to determine whether this peak is a product of fragmentation alone or fragmentation and contribution from equilibrium between the 1:1 and 1:2 species.

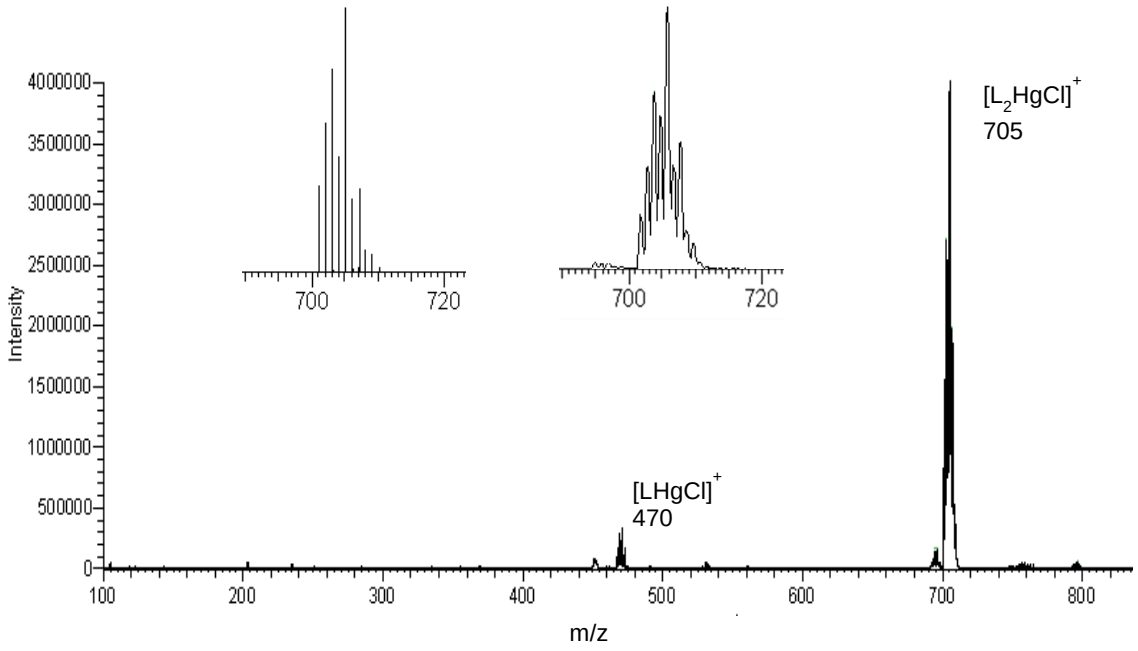

Figure 2.8. ESI-MS spectrum of $(iPr_2bimS)_2HgCl_2$ at cone voltage of 30 V.

Table 2.3: ESI-MS Data of $(iPr_2bimS)_nHgX_2$ Complexes (n = 1, 2; X = Cl, Br, I)

Complex	m/z $[LHgX]^+$	m/z $[L_2HgX]^+$
$(Me_2bimS)HgCl_2$	414	593
$(Me_2bimS)HgBr_2$	459	637
$(Me_2bimS)HgI_2$	506	684
$(Me_2bimS)_2HgCl_2$	414	593
$(Me_2bimS)_2HgBr_2$	459	637
$(Me_2bimS)_2HgI_2$	505	684
$(iPr_2bimS)HgCl_2$	470	705
$(iPr_2bimS)HgBr_2$	515	749
$(iPr_2bimS)HgI_2$	562	796
$(iPr_2bimS)_2HgCl_2$	470	705
$(iPr_2bimS)_2HgBr_2$	515	749
$(iPr_2bimS)_2HgI_2$	562	796
$(iPr_2bimSe)HgCl_2$	517	799
$(iPr_2bimSe)HgBr_2$	562	843
$(iPr_2bimSe)HgI_2$	609	890
$(iPr_2bimSe)_2HgCl_2$	517	799
$(iPr_2bimSe)_2HgBr_2$	562	843
$(iPr_2bimSe)_2HgI_2$	609	890

2.3.1 Molecular Structures of $(Me_2bimS)HgX_2$ (X = Cl, Br, I)

Molecular structures of $(Me_2bimS)HgX_2$ (X = Cl, Br, I) were determined using single crystals obtained at room temperature by slow evaporation of solutions of the complexes in methanol (X = Cl) or tetrahydrofuran (X = Br, I). As expected the Me_2bimS ligand coordinates in a monodentate fashion; however, due to the less bulky methyl substituents, it has an enhanced tendency to form dinuclear and polymeric complexes as illustrated in Figures 2.9 and 2.10. Selected bond lengths and angles are shown in Table 2.4. Evidently, the $(Me_2bimS)HgX_2$ (X = Cl, Br) complexes are polymeric, with a –Hg–X– repeating unit and a thione and a terminal halide also bound to

each mercury center. Calculation of the τ_4 (Equation 2.1) index, where α and β are the two largest angles around the metal center, for $(Me_2bimS)HgX_2$ (X = Cl, Br) complexes resulted in the numerical values of 0.77 and 0.78, respectively, which indicates a geometry around the metal center to be intermediate between the ideal seesaw (0.64) and trigonal pyramidal (0.85) geometries for both complexes.[100]

$$\tau_4 = \frac{360 - (\alpha + \beta)}{141} \tag{2.1}$$

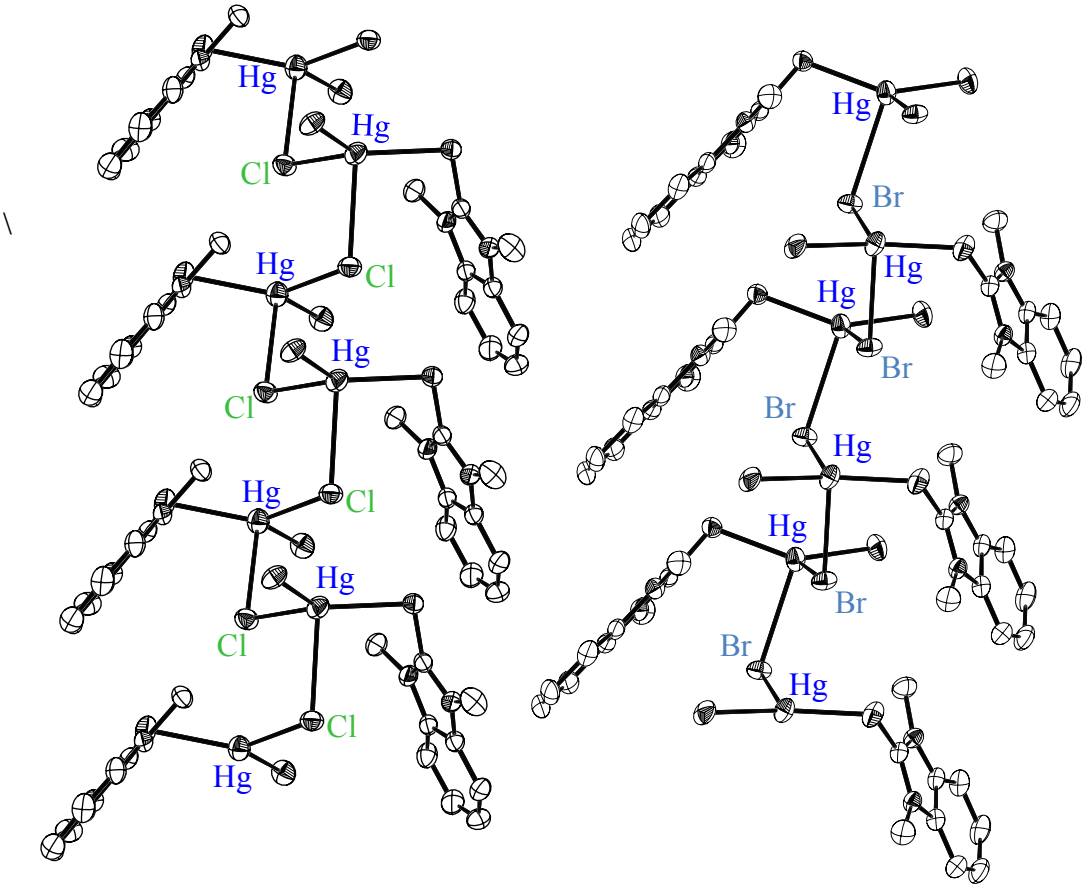

Figure 2.9. Molecular structures of $(Me_2bimS)HgX_2$ (X = Cl, Br)

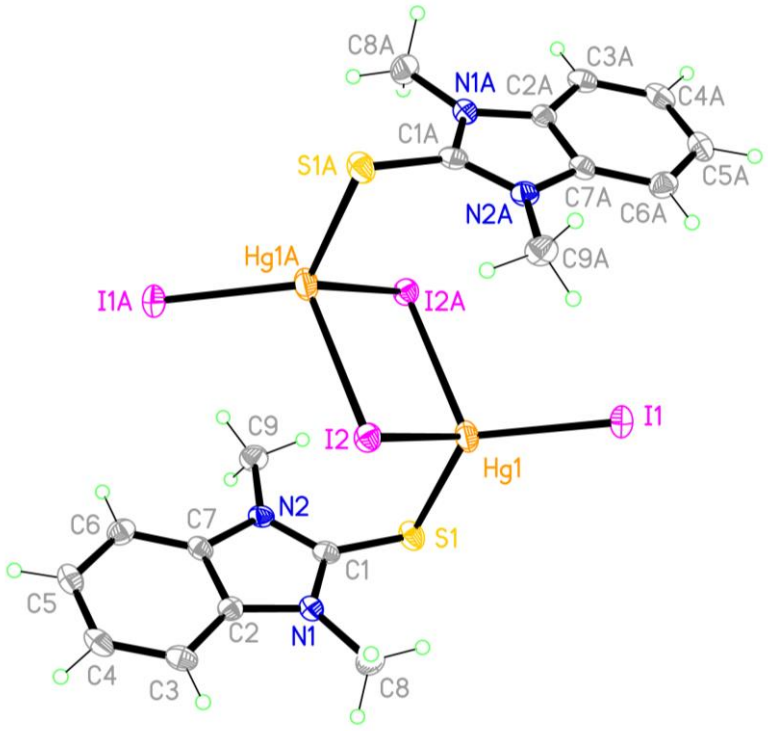

Figure 2.10. Molecular structure of $(Me_2bimS)HgI_2$

Table 2.4: Selected Bond Lengths (Å) and Angles (°) for $(Me_2bimS)HgX_2$ (X = Cl, Br, I)

	X = Cl	X = Br	X = I
Hg(1)–X(1)	2.4335(12)	2.5416(4)	2.6798(3)
Hg(1)–X(2)	2.5345(12)	2.6554(4)	2.8708(3)
Hg(1)–S(1)	2.4287(12)	2.4475(10)	2.5003(11)
S(1)–C(1)	1.716(4)	1.712(4)	1.719(4)
X(2)–Hg(1)–X(1)	106.82(4)	107.269(15)	113.174(10)
X(2)–Hg(1)–S(1)	124.62(5)	124.11(3)	105.06(3)
X(1)–Hg(1)–S(1)	126.60(4)	125.59(3)	123.98(3)
X(2)#1–Hg(1)–S(1)	93.22(4)	94.16(3)	105.83(3)
X(1)–Hg(1)–X(2)#1	103.84(4)	104.716(14)	109.795(10)
X(2)–Hg(1)–X(2)#1	86.67(3)	88.327(10)	94.940(9)

Moreover, the $(Me_2bimS)HgI_2$ structure is different from its chloro- and bromo-analogues as it is dimeric with two bridging and two terminal iodides. Consequently, the mercury center is surrounded by one sulfur atom and three iodides in a distorted seesaw

geometry (τ_4 = 0.67). This geometry differs from the ones observed with the isostructural (Me_2bimS)HgX_2 (X = Cl, Br) complexes, whose τ_4 were calculated to be 0.77 and 0.78, respectively, indicating an intermediate geometry between the ideal seesaw (0.64) and trigonal pyramidal (0.85) geometries. Additionally, the Hg-S bond distances in (Me_2bimS)HgX_2 (X = Cl, Br I), 2.43, 2.45, and 2.50 Å, respectively, increase in length as the halide becomes larger (Cl < Br < I). The decreased electronegativity and larger size of the halide weakens the Hg-X and Hg-S. This observation is also seen in the Hg-S bond lengths of the (iPr_2bimS)HgX_2 complexes (X = Cl, Br I) as 2.43 Å < 2.54 Å < 2.68 Å.

2.3.2 Molecular Structures of (Me_2bimS)$_2HgX_2$ (X = Cl, Br, I)

Single crystals of (Me_2bimS)$_2HgX_2$ (X = Cl, Br, I) suitable for X-ray diffraction studies were obtained by the slow evaporation of solutions of the compounds in dichloromethane (X = Cl), acetonitrile (X = Br), or tetrahydrofuran (X = I); the structures are shown in Figures 2.11 and 2.12. Selected bond lengths and angles are listed in Table 2.5. All three 1:2 complexes are monomeric in the solid state. The coordination sphere of the mercury center is composed of two thione sulfur atoms and two halogen atoms.

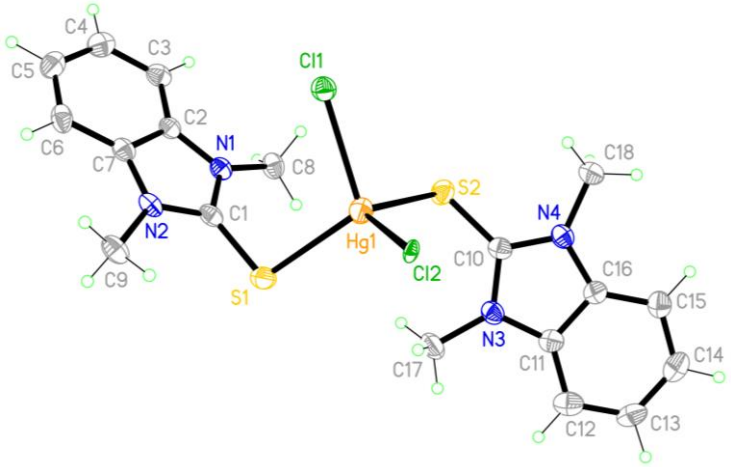

Figure 2.11. Molecular structure of (Me_2bimS)$_2HgCl_2$

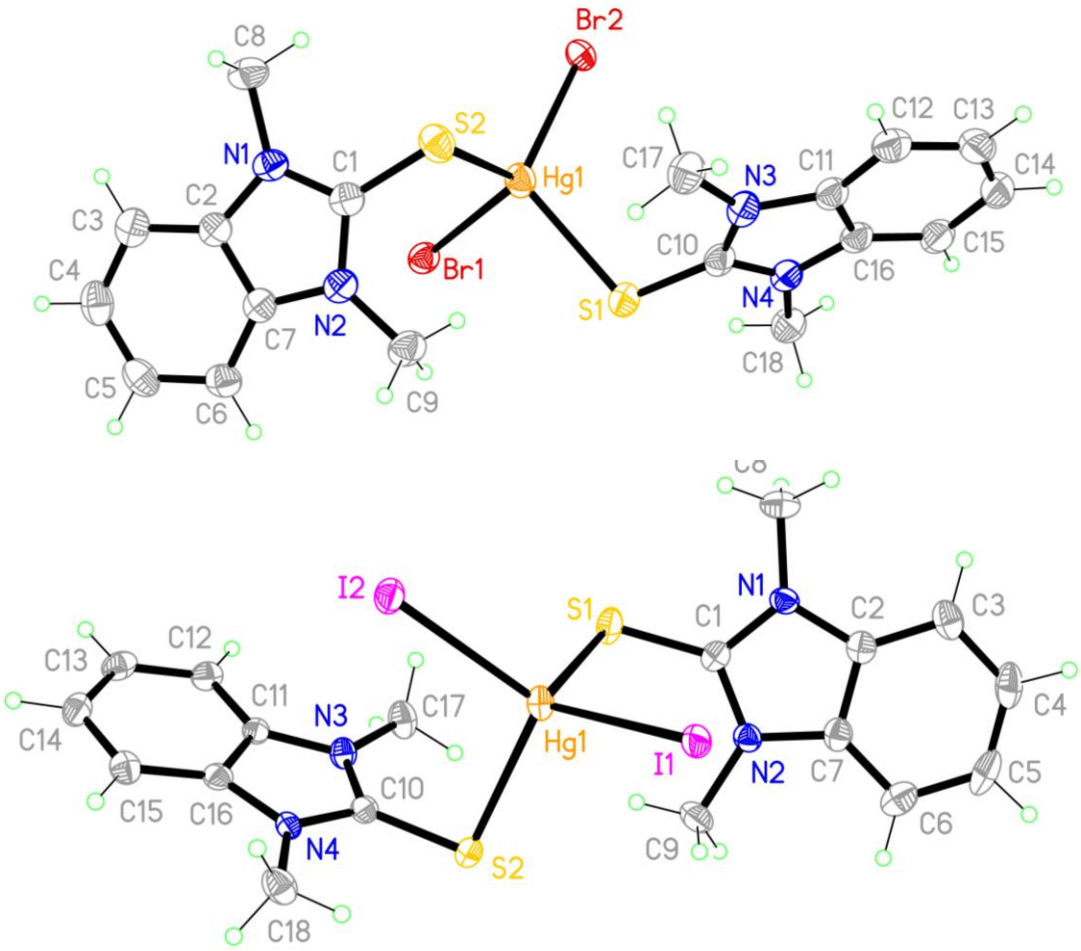

Figure 2.12. Molecular structures of $(Me_2bimS)_2HgX_2$ (X = Br, I)

Interestingly, the three Hg-S bond distances for the $(Me_2bimS)_2HgX_2$ complexes (X = Cl, Br, I) are slightly different from each other with no apparent trend (2.57, 2.55, and 2.61 Å, for X = Cl, Br, I, respectively). The S–Hg–S bond angles in $(Me_2bimS)_2HgX_2$ (X = Cl, Br, I) [114.2, 112.4 and 106.8 °, for X = Cl, Br, I, respectively] decrease with increasing size of the halogen atom. In contrast, the X–Hg–X bond angles slightly increase (111.0, 113.8 and 126.0°, respectively) as the size of the halogen increases. The geometry of the mercury center in $(Me_2bimS)_2HgX_2$ (X = Cl, Br) complexes are distorted tetrahedral with τ_4 = 0.95 and 0.94, respectively. Moreover,

calculation of the τ_4 index around the metal center for $(Me_2bimS)_2HgI_2$ yielded a numerical value of 0.88 which indicates that this complex exhibits a trigonal pyramidal geometry.

Table 2.5: Selected Bond Lengths (Å) and Angles (°) for $(Me_2bimS)_2HgX_2$ (X = Cl, Br, I)

	X = Cl	X = Br	X = I
Hg(1)–X(1)	2.5427(15)	2.6412(5)	2.7286(3)
Hg(1)–X(2)	2.5016(12)	2.5799(5)	2.7360(4)
Hg(1)–S(1)	2.5314(16)	2.5946(12)	2.6428(11)
Hg(1)–S(2)	2.5744(16)	2.5482(12)	2.6075(11)
S(1)–C(1)	1.708(7)	1.707(5)	1.701(4)
S(2)–C(10)	1.699(7)	1.701(5)	1.708(4)
X(2)–Hg(1)–X(1)	110.97(5)	113.766(17)	126.003(11)
X(2)–Hg(1)–S(1)	112.08(5)	114.15(3)	105.73(2)
X(1)–Hg(1)–S(1)	107.37(5)	96.57(3)	103.04(2)
X(2)–Hg(1)–S(2)	115.60(5)	111.69(3)	110.44(2)
X(1)–Hg(1)–S(2)	95.07(5)	107.27(3)	103.53(2)
S(1)–Hg(1)–S(2)	114.17(6)	112.36(4)	106.80(4)

2.3.3 Molecular Structures of $(iPr_2bimS)HgX_2$ (X = Cl, Br, I)

Molecular structures of $(iPr_2bimS)HgX_2$ (X = Cl, Br, I) were determined using single crystals obtained at room temperature by slow evaporation of a solution of the complex in ethanol (X = Cl) or methanol (X = I), and by slow diffusion of diethyl ether into a solution of the complex in chloroform (X = Br). The ligand coordinates in a monodentate fashion to form mostly dinuclear and mononuclear complexes, as depicted in Figures 2.13 and 2.14, with selected bond lengths and angles shown in Table 2.6. The $(iPr_2bimS)HgX_2$ (X = Cl, Br) are dimeric species with two bridging and two terminal halides; consequently, one sulfur atom and three halides are arranged around the mercury

center. Calculation of the four-coordinate trigonality index τ_4 (Equation 2.1) for (iPr_2bimS)HgX_2 (X = Cl, Br) complexes resulted in the numerical values of 0.76 and 0.80, respectively, which indicates a geometry around the metal center to be intermediate between the ideal seesaw (0.64) and trigonal pyramidal (0.85) geometries for both complexes.[100] The relatively larger size of iodide atom in comparison to its neighboring halides, causes the (iPr_2bimS)HgI_2 to present a monomeric structure with a trigonal planar geometry around the metal center. This complex is also structurally different from the dimeric Me_2bimS derivative, however, despite the change in nuclearity between the (iPr_2bimS)HgI_2 and (Me_2bimS)HgI_2, their C-S (2.50 Å *vs* 2.53 Å) and Hg-S (1.721 Å *vs* 1.719 Å) bond lengths are relatively similar.

(a)

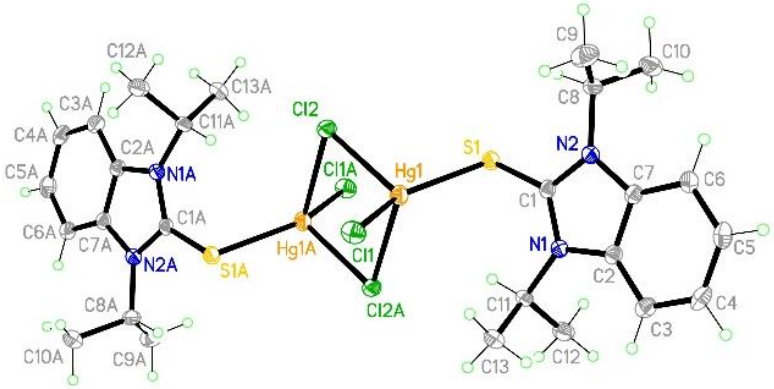

(b)

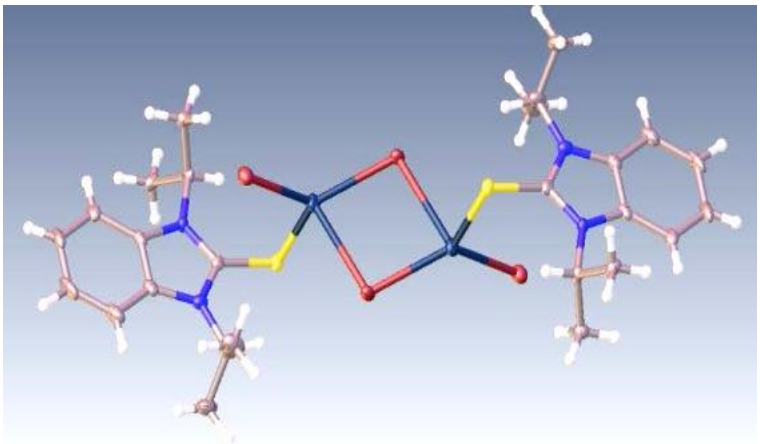

Figure 2.13. Molecular structures of (iPr_2bimS)HgX_2; (a) X = Cl, (b) X = Br

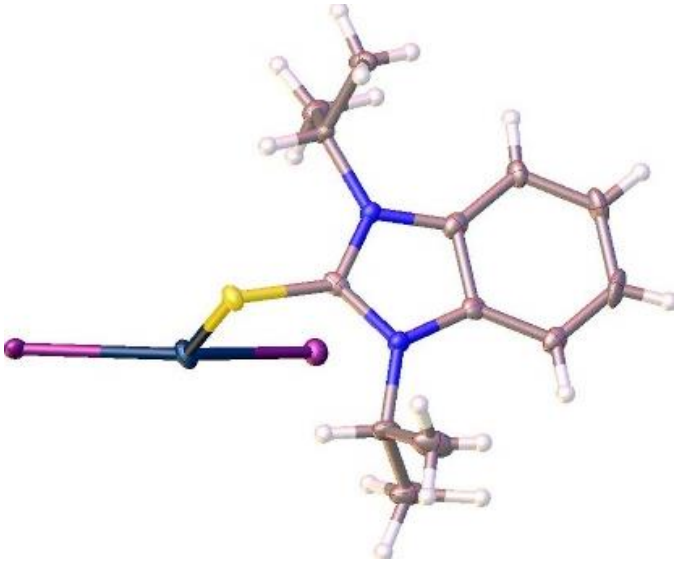

Figure 2.14. Molecular structure of (iPr_2bimS)HgI_2

Table 2.6: Selected bond lengths (Å) and angles (°) for (iPr_2bimS)HgX_2 (X = Cl, Br, I)

	X = Cl	X = Br	X = I
Hg(1)–X(1)	2.3836(6)	2.5378(4)	2.7268(5)
Hg(1)–X(2)	2.5919(6)	2.5669(3)	2.6966(5)
Hg(1)–S(1)	2.4325(6)	2.5035(7)	2.5332(12)
N(1)–C(1)	1.355(3)	1.348(3)	1.391(7)
S(1)–C(1)	1.741(2)	1.725(3)	1.721(5)
X(2)–Hg(1)–X(1)	110.65(2)	131.404(12)	133.515(13)
X(2)–Hg(1)–S(1)	99.47(2)	115.500(18)	110.54(3)
X(1)–Hg(1)–S(1)	142.74(2)	109.808(17)	111.75(3)

Additionally, the C-S bond distances in (iPr_2bimS)HgX_2 (X = Cl, Br, I) [1.74, 1.73, and 1.72 Å, respectively] increase in length relative to the C-S bond in the free iPr_2bimS ligand (1.67 Å). In turn, the C-S bond lengths slightly decrease as the covalent radii of the corresponding halide increases. Although the dimeric (iPr_2bimS)HgX_2 complexes (X = Cl, Br) are isostructural to each other, there exists a significant difference

between their Hg-S bond lengths [2.43 Å vs 2.50 Å], their X-Hg-X bond angles [110.7° vs 131.4°], and their X-Hg-S bond angles [99.5-142.7° vs 109.8-115.5°].

2.3.4 Molecular Structures of $(iPr_2bimS)_2HgX_2$ (X = Cl, Br, I)

Similarly, single crystals of $(iPr_2bimS)_2HgX_2$ (X = Cl, Br, I) suitable for X-ray diffraction studies were obtained by the slow evaporation of a solution of the compound diethyl ether (X = Cl) and by slow diffusion of hexanes into a solution of the complex in dichloromethane (X = Br, I); the structures are shown in Figure 2.15 and selected bond lengths and angles are listed in Table 2.7. Similarly to the Me_2bimS derivatives, all three 1:2 complexes are monomeric in the solid state where the coordination sphere of the mercury center is composed of two thione sulfur atoms and two halogen atoms. Moreover, the Hg-S bond lengths in $(iPr_2bimS)_2HgX_2$ (X = Cl, Br, I) shorten and thus become stronger as the electronegativity of the corresponding halide increases and its covalent radii decreases (2.55, 2.56, and 2.63 Å, for X = Cl, Br, I, respectively]. The S–Hg–S bond angles (124.9, 122.5 and 103.6º, respectively) decrease with increasing size of the halogen atom. In contrast, the X–Hg–X bond angles slightly increase (119.1, 120.1, and 121.2º, respectively) as the size of the halogen increases. The geometry of the mercury center in the $(iPr_2bimS)_2HgX_2$ (X = Cl, Br) complexes are distorted trigonal pyramidal confirmed with τ_4 = 0.88 and 0.83, respectively. Moreover, calculation of the τ_4 index around the metal center for $(iPr_2bimS)_2HgI_2$ yielded a numerical value of 0.90 which indicates that this complex exhibits a geometry intermediate between an ideal trigonal pyramidal (0.85) and tetrahedral (1.00) geometry.

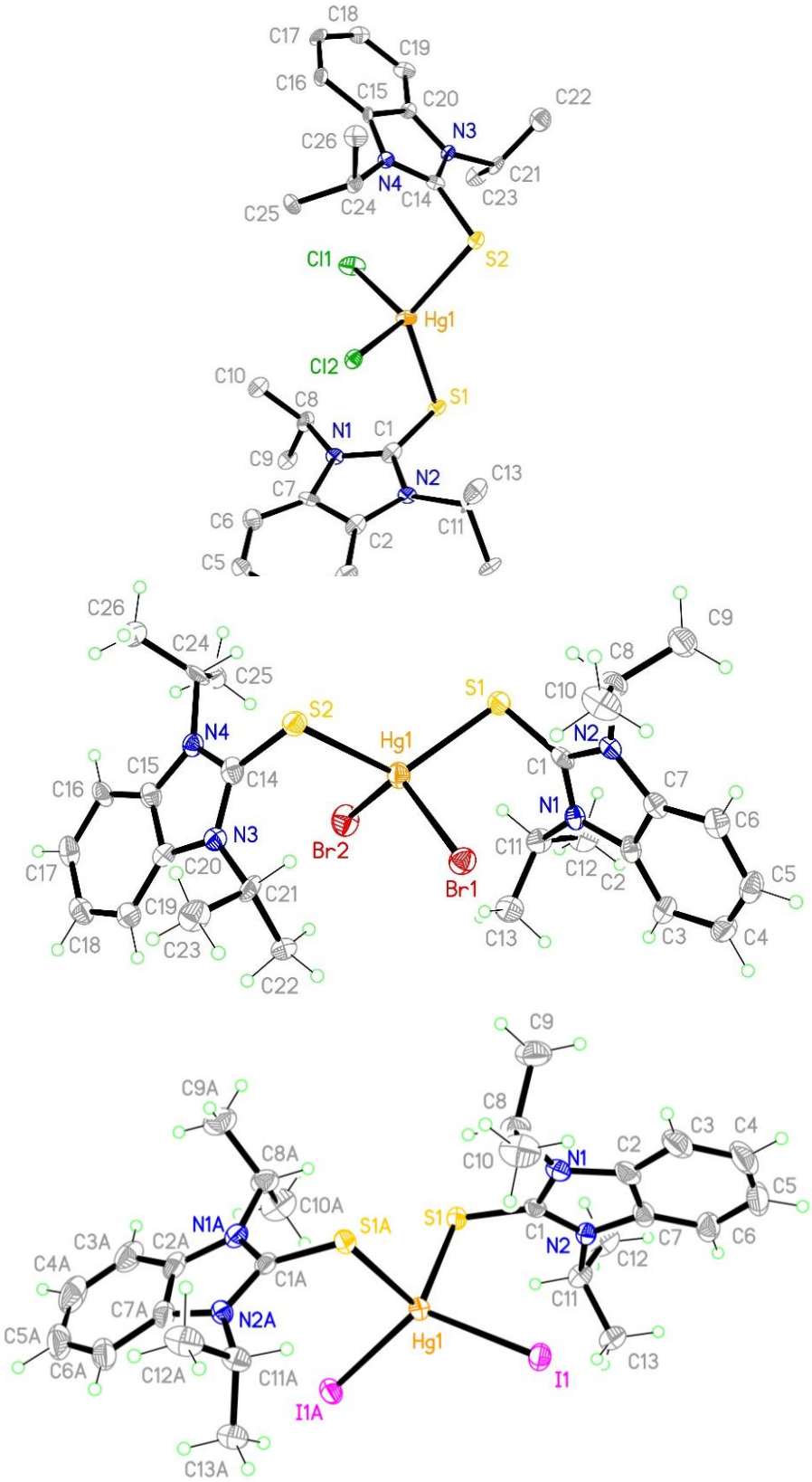

Figure 2.15. Molecular structures of $(iPr_2bimS)_2HgX_2$ (X = Cl, Br, I)

Table 2.7: Selected Bond Lengths (Å) and Angles (°) for $(iPr_2bimS)_2HgX_2$ (X= Cl, Br, I)

	X = Cl	X = Br	X = I
Hg(1)–X(1)	2.5082(18)	2.6046(6)	2.7490(2)
Hg(1)–X(2)	2.5092(18)	2.5972(6)	2.7490(2)
Hg(1)–S(1)	2.5539(19)	2.5713(15)	2.6288(8)
Hg(1)–S(2)	2.5523(18)	2.5636(13)	2.6288(8)
S(1)–C(1)	1.714(8)	1.717(6)	1.716(3)
S(2)–C(14)	1.721(7)	1.716(6)	1.717(4)
X(2)–Hg(1)–X(1)	119.06(6)	120.70(2)	121.178(12)
X(2)–Hg(1)–S(1)	100.92(7)	106.55(4)	112.314(18)
X(1)–Hg(1)–S(1)	105.84(6)	100.34(4)	103.168(18)
X(2)–Hg(1)–S(2)	104.54(6)	104.18(3)	103.169(18)
X(1)–Hg(1)–S(2)	102.97(6)	103.96(3)	112.315(18)
S(1)–Hg(1)–S(2)	124.88(6)	122.45(5)	103.58(4)

2.3.5 Molecular Structures of $(iPr_2bimSe)HgX_2$ (X = Cl, Br, I)

Molecular structures of $(iPr_2bimSe)HgX_2$ (X = Cl, Br, I) were determined using single crystals obtained at room temperature by slow evaporation of a solution of the complex in dichloromethane (X = Cl, Br) and tetrahydrofuran (X = I). The ligand coordinates in a monodentate fashion to exclusively form dinuclear complexes, shown in Figures 2.16 and 2.17, with selected bond lengths and angles shown in Table 2.8. The $(iPr_2bimSe)HgX_2$ complexes (X = Cl, I) are dimeric species with two bridging and two terminal halides; consequently, one selenium atom and three halides are arranged around the mercury center. Notably, the $(iPr_2bimSe)HgBr_2$ complex is dinuclear with bridging selone moieties coordinated to two metal centers that are each surrounded by two terminal bromides. The rare bridging mode for the selone in $(iPr_2bimSe)HgBr_2$ is one of the first examples of a dinuclear bridging selone for any metal.[22c, 101] Calculation of the four-coordinate geometry index for $(iPr_2bimSe)HgCl_2$ resulted in the numerical value of

0.74, which indicates a geometry around the metal center to be intermediate between the ideal seesaw (0.64) and trigonal pyramidal (0.85) geometry. Whereas calculation of τ_4 for (iPr_2bimSe)HgX_2 (X = Br, I) resulted in the numerical values of 0.81 and 0.83, respectively, which depicts a trigonal pyramidal geometry around the mercury coordination sphere. In turn, the (iPr_2bimSe)$HgCl_2$ complexes are isostructural to their sulfur counterparts. In contrast, mercury(II) prefers a four-coordinate geometry in the presence of the softer selenium donor moiety present in the dimeric (iPr_2bimSe)HgI_2 species than the three-coordinate geometry present in the monomeric (iPr_2bimS)HgI_2 complex.

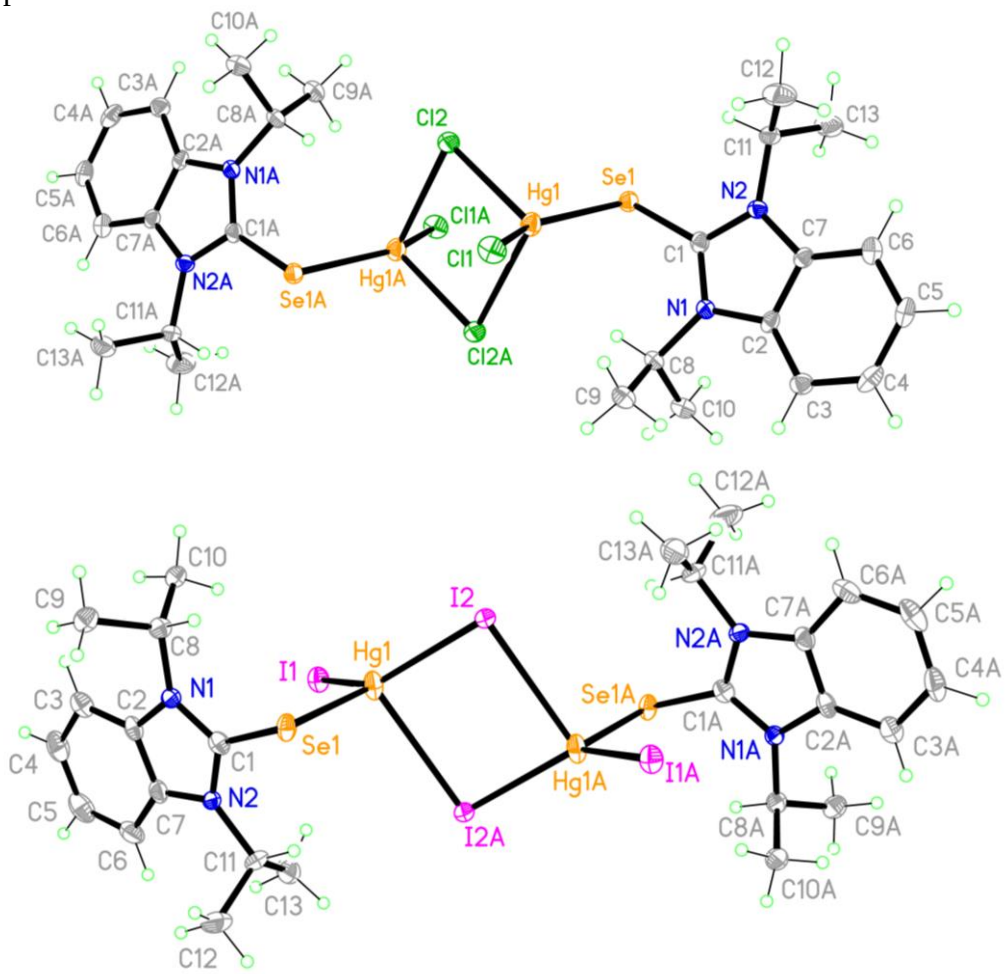

Figure 2.16. Molecular structures of (iPr_2bimSe)HgX_2 (X= Cl, I)

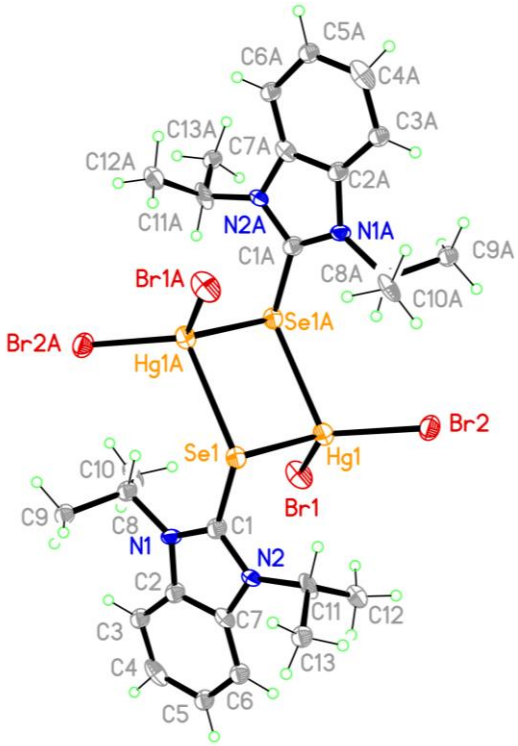

Figure 2.17. Molecular structure of (iPr_2bimSe)$HgBr_2$

Table 2.8: Selected Bond Lengths (Å) and Angles (°) for (iPr_2bimSe)HgX_2 (X= Cl, Br, I)

	X = Cl	X = Br	X = I
Hg(1)–X(1)	2.3783(8)	2.544(3)	2.7109(3)
Hg(1)–X(2)	2.6046(8)	2.575(3)	2.7436(3)
Hg(1)–Se(1)	2.5112(3)	2.580(3)	2.6097(4)
Se(1)–C(1)	1.883(3)	1.910(2)	1.880(4)
X(2)–Hg(1)–X(1)	109.91(3)	126.95(9)	130.899(11)
X(2)–Hg(1)–Se(1)	97.44(2)	111.05(8)	112.789(12)
X(1)–Hg(1)–Se(1)	145.42(2)	119.25(8)	112.502(12)
X(1)–Hg(1)–X(2)#1	98.73(3)	98.77(8)	100.221(9)
Se(1)–Hg(1)–X(2)#1	101.294(19)	103.64(7)	101.781(12)
X(2)–Hg(1)–X(2)#1	91.61(2)	85.39(8)	88.237(9)

Similar to its sulfur analogues, the C-Se bond lengths also weaken in the coordinated Hg(II) complex (1.88, 1.91, and 1.88 Å, for X = Cl, Br, I, respectively) in relation to the C-Se bond for the free iPr_2bimSe ligand (1.85 Å). However, this effect is to a lesser degree than that the one observed in its sulfur derivatives where no apparent

trend is observed between the C-Se bond lengths themselves. Similarly to its sulfur counterparts, the Hg-Se bond lengths in (iPr_2bimSe)HgX_2 (X = Cl, Br, I) increase [2.51, 2.58, and 2.61 Å, for X = Cl, Br, I, respectively] and the X-Hg-X bond angles also increase [109.9, 127.0, and 130.9° for X = Cl, Br, I, respectively] as the electronegativity of its corresponding halide decreases. However, the weaker Hg-Se bond present in the bromide complex (2.58 Å) is unusually stronger than that observed for the iodide complex (2.61 Å) despite the fact that the former depicts a bismonodentate coordination mode. The shorter bond distance observed is due to opposing effects derived from the rare bridging selone; as one would expect a weaker Hg-Se bond due to the decreased electron donation from the selenium atom and a stronger Hg-Se bond due to the presence of four, rather than two, terminal electron withdrawing halogens.

2.3.6 Molecular Structures of (iPr_2bimSe)$_2HgX_2$ (X = Cl, Br, I)

Single crystals of (iPr_2bimSe)$_2HgX_2$ (X = Cl, Br, I) suitable for X-ray diffraction studies were also obtained by slow evaporation of solutions of the compounds in dichloromethane (X = Cl), acetonitrile (X = Br), or tetrahydrofuran (X = I), as shown in Figure 2.18 with selected bond lengths and angles listed in Table 2.9. Similarly to the iPr_2bimS derivatives, the 1:2 complexes are monomeric in the solid state where the coordination sphere of the mercury center is composed of two thione sulfur atoms and two halogen atoms. The geometry of the mercury center in the (iPr_2bimSe)$_2HgX_2$ (X = Cl, Br) complexes are distorted trigonal pyramidal confirmed with τ_4 = 0.83 and 0.85, respectively. The (iPr_2bimSe)$_2HgI_2$, however, depicts a distorted tetrahedral/trigonal pyramidal geometry confirmed by the calculated τ_4 index. These geometries are similar to

those observed on their sulfur analogues as the τ_4 indexes for $(iPr_2bimS)_2HgX_2$ (X = Cl, Br, I) were calculated to be 0.88, 0.83, and 0.90 respectively.

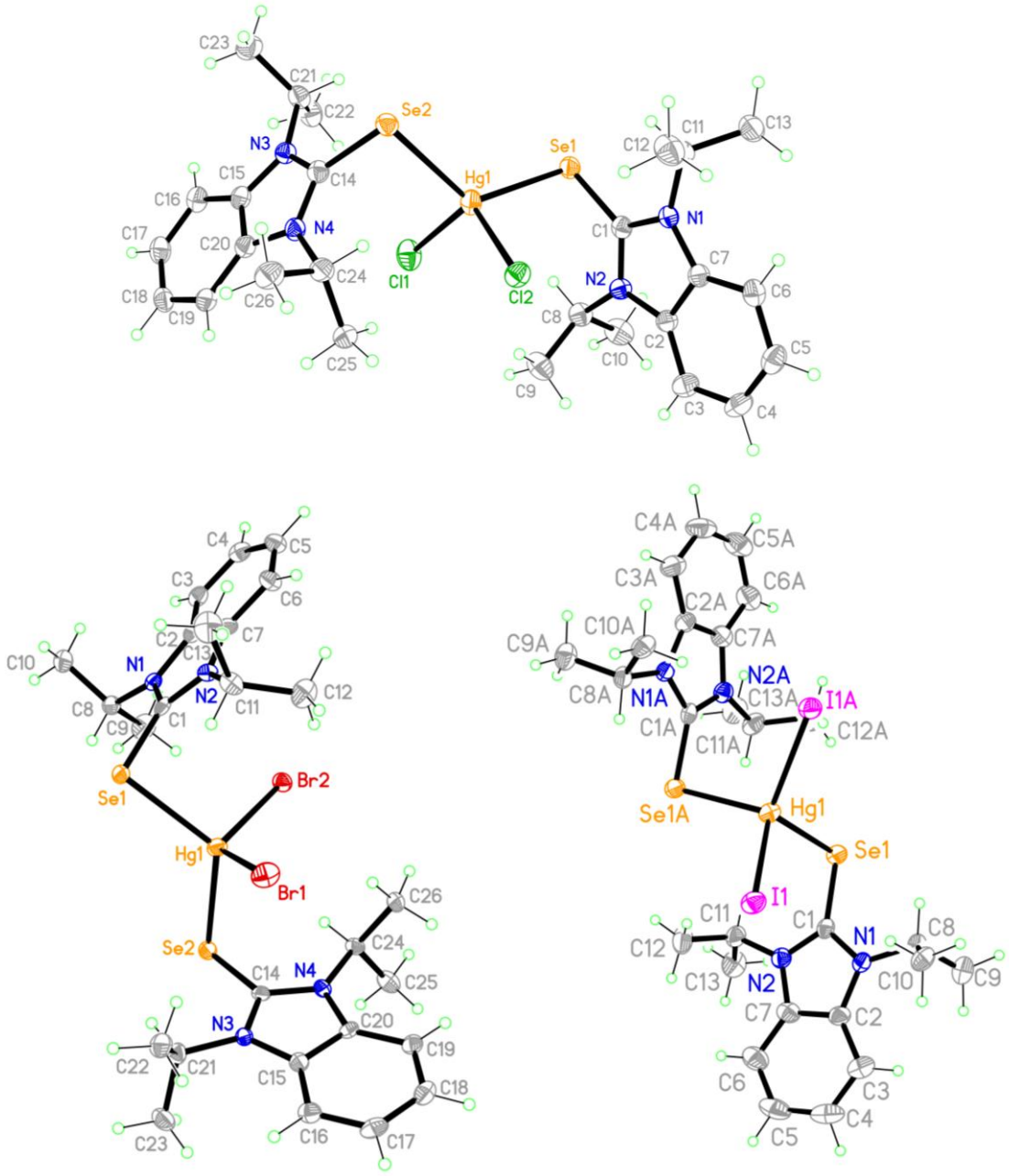

Figure 2.18. Molecular structures of $(iPr_2bimSe)_2HgX_2$ (X = Cl, Br, I)

Moreover, the Hg-S bonds also shorten and thus become stronger as the electronegativity of the corresponding halide increases and its covalent radii decrease. The S–Hg–S bond angles in $(iPr_2bimSe)_2HgX_2$ (X = Cl, Br, I) [114.2, 112.4 and 106.8º,

for X = Cl, Br, I] decrease with increasing size of the halogen atom. Contrarily, the X–Hg–X bond angles slightly increase [111.0, 113.8 and 126.0º, respectively] as the size of the halogen increases.

Table 2.9: Selected Bond Lengths (Å) and Angles (°) for $(iPr_2bimSe)_2HgX_2$ (X= Cl, Br, I)

	X = Cl	X = Br	X = I
Hg(1)–X(1)	2.5151(7)	2.6275(4)	2.7668(4)
Hg(1)–X(2)	2.5263(7)	2.6347(4)	2.7668(4)
Hg(1)–Se(1)	2.6345(3)	2.6484(4)	2.7028(5)
Hg(1)–Se(2)	2.6309(3)	2.6456(4)	2.7028(5)
Se(1)–C(1)	1.874(3)	1.869(3)	1.872(4)
Se(2)–C(14)	1.879(2)	1.877(3)	1.876(3)
X(2)–Hg(1)–X(1)	116.51(2)	117.443(12)	118.622(16)
X(2)–Hg(1)–Se(1)	102.935(18)	102.571(12)	110.865(12)
X(1)–Hg(1)–Se(1)	103.634(19)	105.167(12)	104.638(12)
X(2)–Hg(1)–Se(2)	104.337(17)	103.550(12)	104.639(11)
X(1)–Hg(1)–Se(2)	104.266(18)	106.187(12)	110.864(12)
Se(1)–Hg(1)–Se(2)	126.098(9)	122.811(12)	106.76(2)

2.4 Thiophilicity *vs* Selenophilicity

Recently, the toxicity of mercury has been attributed to its thiophilicity[101-103] and its selenophilicity.[104-106] With respect to the latter, selenium is an important component of antioxidants, and the interaction between mercury(II) and selenium compounds may reduce the bioavailability of selenium via the formation of insoluble mercury selenide species.[103,104] The enhanced affinity of mercury for selenium, selenophilicity, over its affinity for sulfur, thiophilicity, was confirmed through a series of small scale reactions monitored by ^{1}H NMR spectroscopy (Scheme 2.9). When the Hg(II) was coordinated with the Me_2bimS ligand and mixed with an equimolar amount of free iPr_2bimSe, the thione ligand was displaced. Although HSAB theory would predict this outcome, there is

few experimental data available to support mercury's higher selenophilicity than its thiophilicity.[101-106]

Scheme 2.9: Competition Studies of Me_2bimS and iPr_2bimSe with Mercury

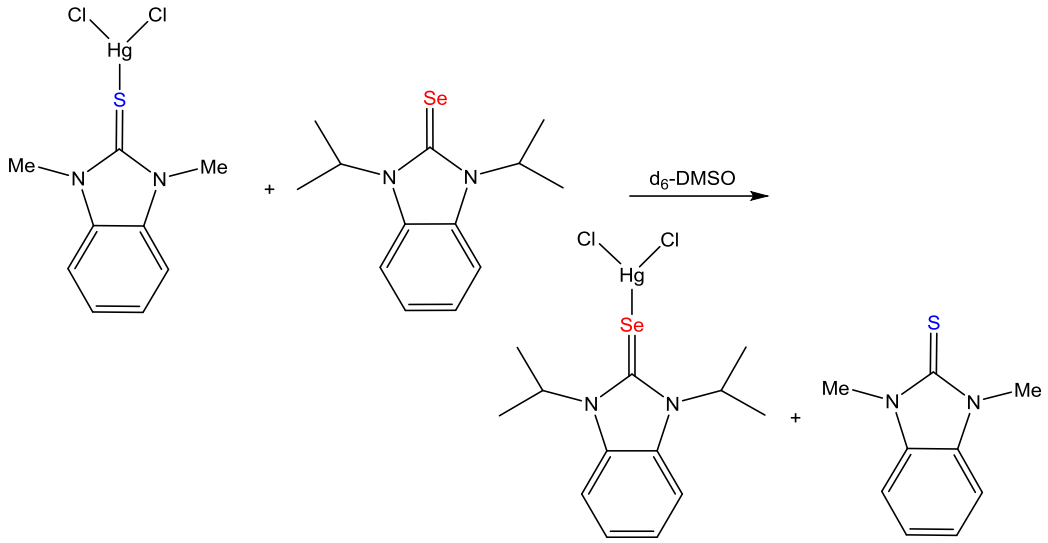

Solutions suitable for ESI-MS studies were prepared by diluting the original NMR samples in LC-MS acetonitrile. Experiments conducted in positive mode at 30 V depicted the expected selone product (Figure 2.19). The presence of the $[(iPr_2bimSe)HgCl]^+$ species (m/z = 517) was observed and, as expected, neither the $[(Me_2bimS)HgCl]^+$ (m/z = 414) or $[(Me_2bimSe)_2HgCl]^+$ (m/z = 593) species was present in solution. Nevertheless, the corresponding 2:1 cationic species, $[(iPr_2bimSe)_2HgCl]^+$, was also shown indicating that an equilibrium between the 1:1 and 1:2 species exists in solution under ESI conditions.

To further confirm that mercury's selenophilicity is greater than its thiophilicity, the reverse reaction of Scheme 2.9 was pursued as a solution of $(iPr_2bimSe)HgCl_2$ in d_6-DMSO was treated with a d_6-DMSO solution of Me_2bimS (Scheme 2.10). This reaction was immediately monitored by ^{1}H NMR spectroscopy as depicted in Figure 2.20.

Remarkably, a reaction took place. The ^{1}H NMR spectrum shows two sets of AA'BB' splitting patterns in the aromatic region corresponding to the two different benzimidazole ligands. Moreover, the septet at 5.58 ppm, corresponding to the two tertiary protons in the isopropyl substitutent, confirms the presence of the iPr_2bimSe ligand backbone and the singlet at 3.78 ppm, corresponding to the twelve methyl protons, confirms the presence of the iPr_2bimSe ligand backbone.

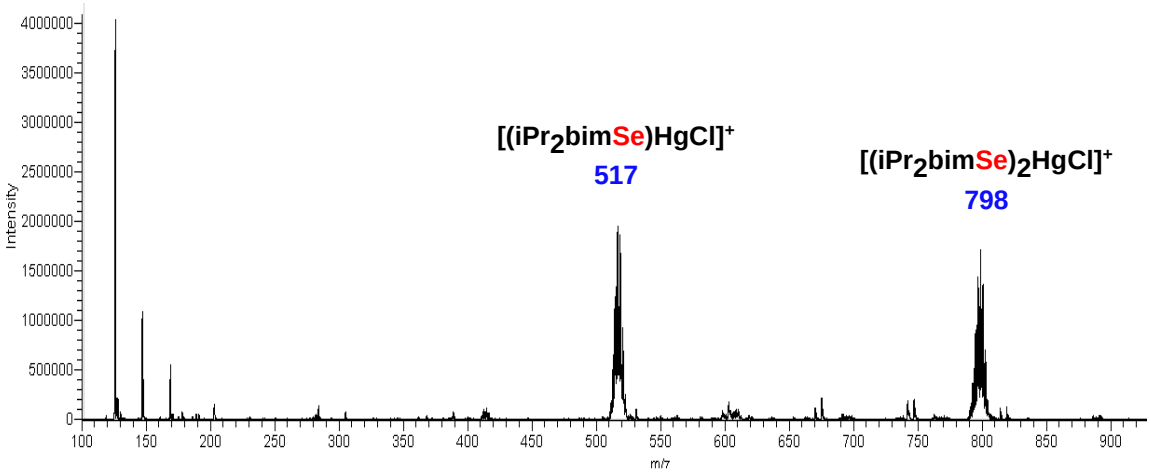

Figure 2.19: ESI-MS spectrum of competition study of iPr_2bimSe and iPr_2bimS with mercury

Scheme 2.10: Crossover Reaction Between $(iPr_2bimSe)HgCl_2$ and Me_2bimS

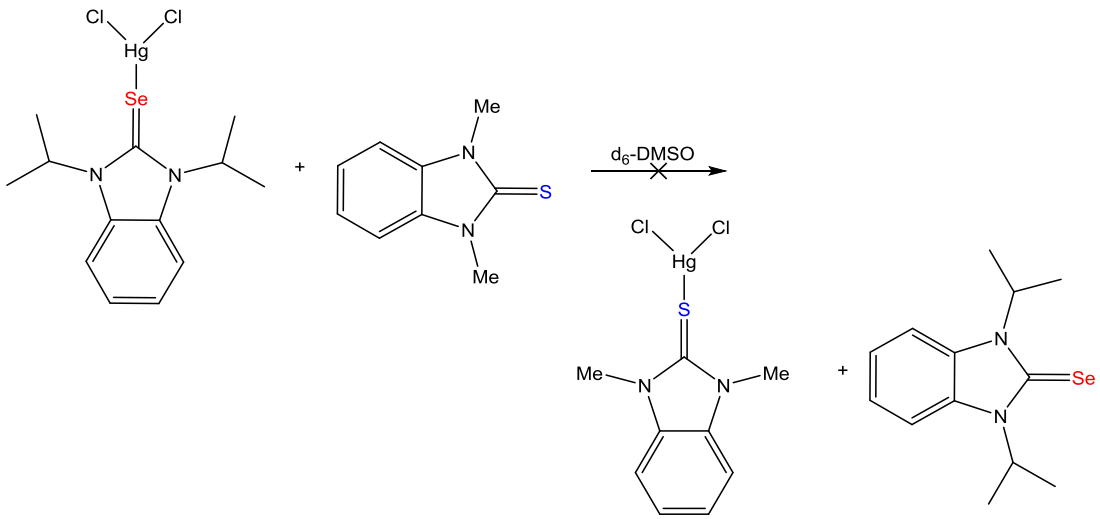

Notably, the chemical shifts observed in the spectrum of the crossover reaction between (iPr_2bimSe)$HgCl_2$ and Me_2bimS do not correspond to those observed in the spectra of the free ligands or the (iPr_2bimSe)$HgCl_2$ and (Me_2bimSe)$HgCl_2$ complexes. This indicates the possible formation of the heteroleptic complex (iPr_2bimSe)(Me_2bimS)$HgCl_2$. Although we did not observe the expected outcome, these results indicate that mercury(II) would rather have four instead of three ligands in its coordination sphere. However, the affinity for four ligands was not observed for the forward reaction as a complete displacement of the thione ligand led to the formation of a three-coordinate mercury selone complex.

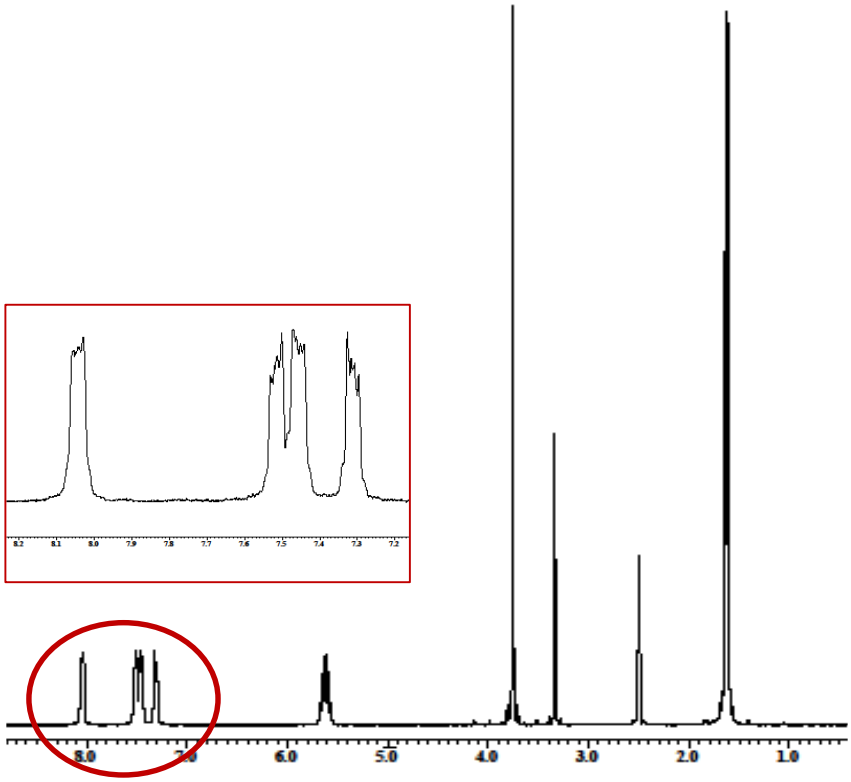

Figure 2.20: ^{1}H NMR spectrum of the reaction between (iPr_2bimSe)$HgCl_2$ and Me_2bimS in d_6-DMSO

In an attempt to purposely synthesize the heteroleptic (iPr_2bimSe)(Me_2bimS)$HgCl_2$ complex, equimolar amounts of iPr_2bimSe and Me_2bimS

were treated with a $HgCl_2$ solution in acetonitrile (Scheme 2.11). The ^1H NMR spectrum of the crude product is shown in Figure 2.21. The peaks and their chemical shits correspond to those observed for the reverse reaction of the competitions studies (Figure 2.20), however, different intensities were observed for the AA'BB' splitting patterns corresponding to the ligand backbones. The peaks corresponding to the iPr_2bimSe ligand are have a higher abundance than the peaks corresponding to the Me_2bimS ligand. This implies that there is partial addition of the thione ligand to the mercury center. The selone ligand, having a higher tendency to bind to mercury, tends to dominate the addition competition between the thione and selone ligands to the mercury coordination site. In order to ensure the complete addition of both the iPr_2bimSe and Me_2bimS ligands to the mercury coordination sphere, a different synthetic route is proposed. The selone (1:1) mercury complex may then be treated with the free thione ligand in order to minimize ligand addition competition, as proposed in Scheme 2.12.

Scheme 2.11: Attempted Synthesis of $(iPr_2bimSe)(Me_2bimS)HgCl_2$

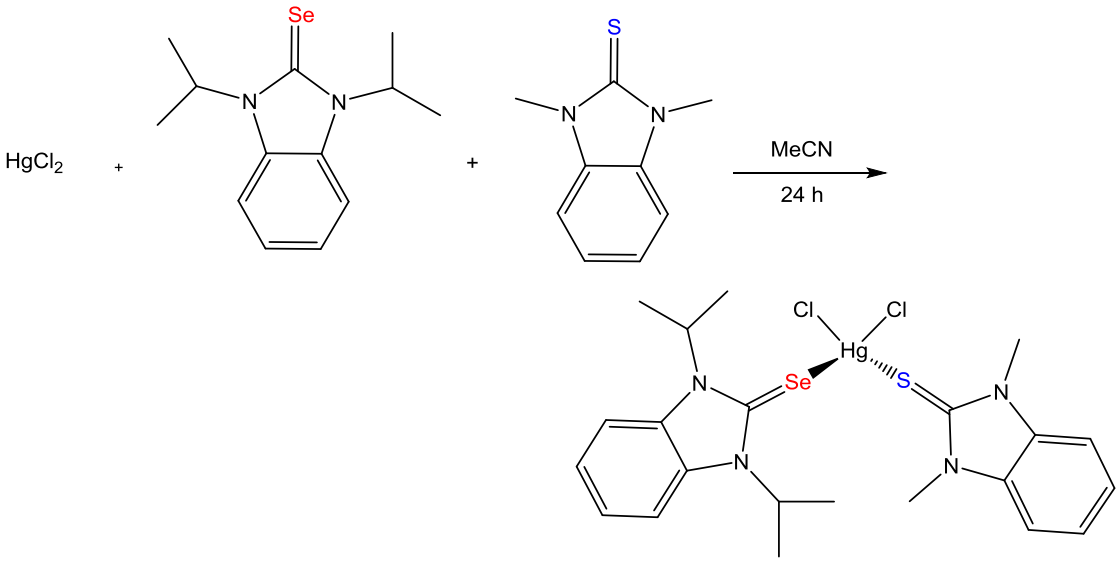

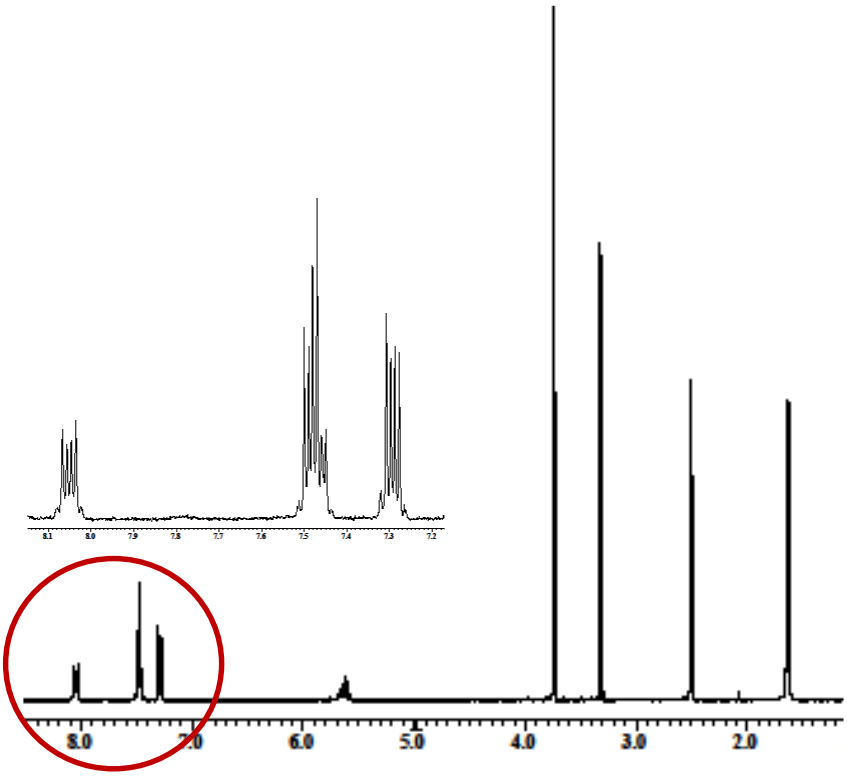

Figure 2.21: ^{1}H NMR spectrum of (iPr_2bimSe)(Me_2bimS)$HgCl_2$ in d_6-DMSO

Scheme 2.12: Proposed Synthesis of (iPr_2bimSe)(Me_2bimS)$HgCl_2$

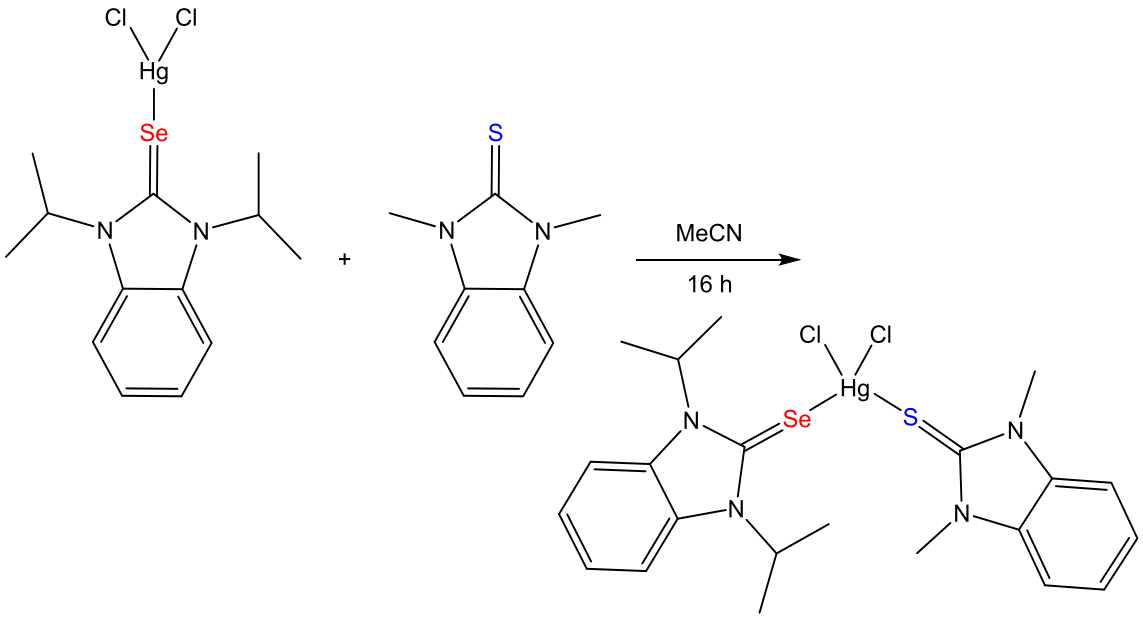

2.5 Synthesis of Copper(I) Complexes

The properties of copper-coordinated compounds, whether in classical inorganic coordination complexes, organometallic compounds, or bioinorganic models are largely determined by the nature of ligand and donor atoms bound to the metal ion.[107,108] Copper may be stabilized in its +1, +2, and +3 oxidation states, but very few examples of copper(III) compounds are reported.[108] Coordination chemistry of copper is therefore dominated by Cu(II) derivatives with little, but important examples of Cu(I) compounds. Due to the closed-shell d^{10} electronic confirmation, Cu(I) complexes are usually colorless solids and strongly prefer ligands having soft donors such as phosphorus and aromatic amines. Although two-coordinated linear and three-coordinated trigonal arrangements are known, Cu(I) complexes are mostly four-coordinated species adopting a tetrahedral geometry.

The first Cu(I) complexes of the iPr_2bimE (E = S, Se) ligand scaffold has been prepared. The synthesis of the $(iPr_2bimE)_2CuX$ (E = S, Se; X = Cl, Br, I) was achieved by treating CuX (X = Cl, I) or $CuBr{\cdot}SMe_2$ and iPr_2bimE (E = S, Se) in a 1:2 stoichiometric ratio under an inert atmosphere (Scheme 2.13). All six complexes were isolated in 62-78% yields and tend to oxidize within 12 h of exposure to air. Additionally, they have all been characterized using analytical and spectroscopic methods such as elemental analysis, IR, ^{1}H and ^{13}C NMR spectroscopies.

Crystal structures of $(iPr_2bimS)_2CuX$ (X = Cl, I) suitable for X-ray diffraction studies have been obtained in which both complexes exhibit a 3-coordinate trigonal planar geometry around the copper metal shown in Figures 2.22 and 2.23. Selected bond lengths and angles are summarized in Table 2.10. Complexes of heterocyclic ligands with

copper in one or both oxidation states (+1 and +2) are of interest in bioinorganic chemistry because of the search for simple model compounds for copper-proteins.[109-111]

Scheme 2.13. Synthesis of Copper(I) Complexes

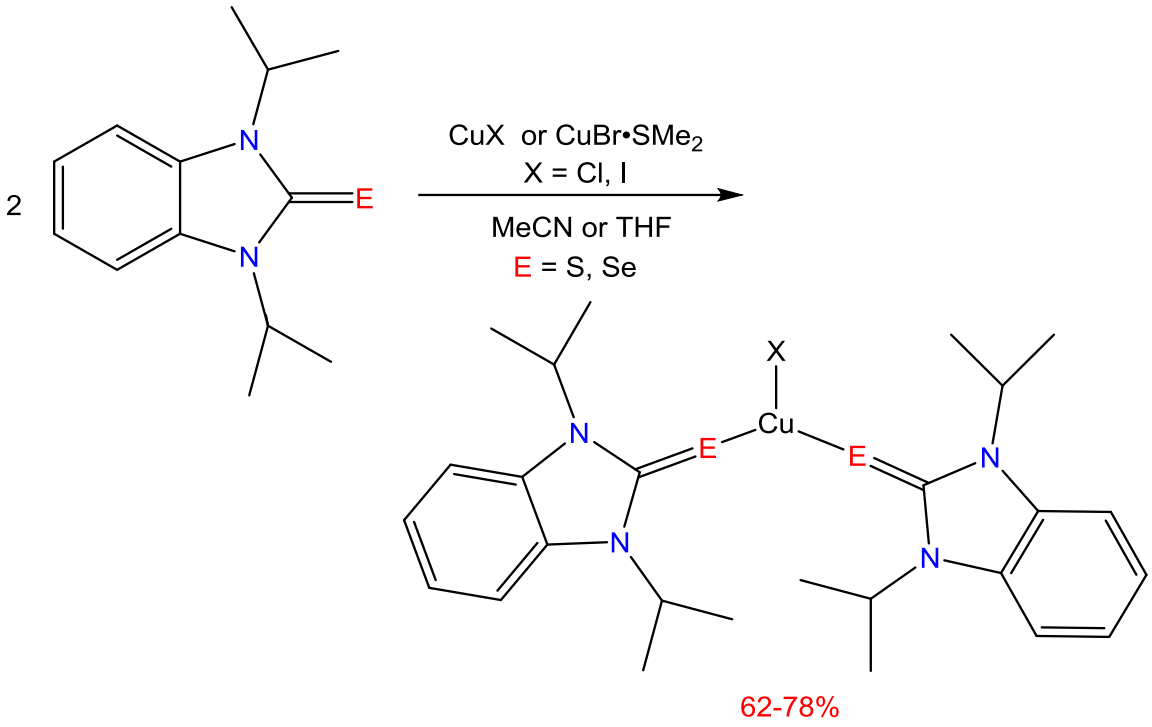

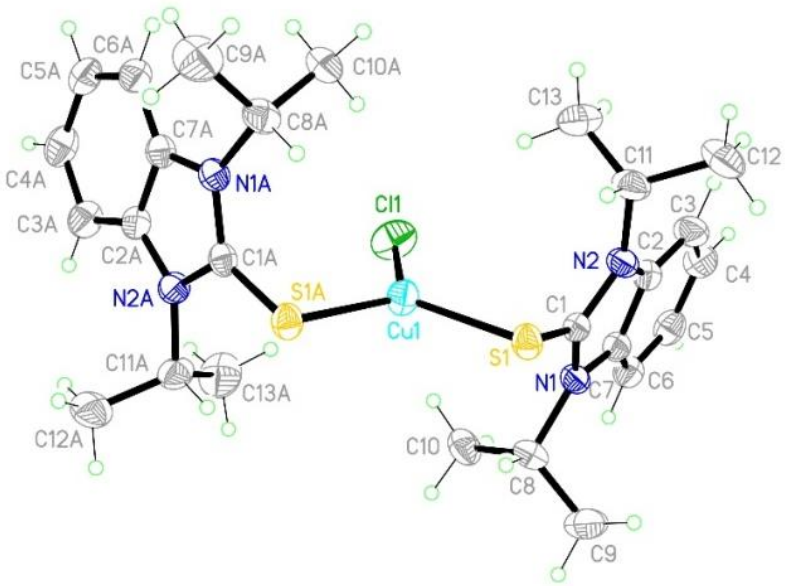

Figure 2.22. Molecular structure of $(iPr_2bimS)_2CuCl$

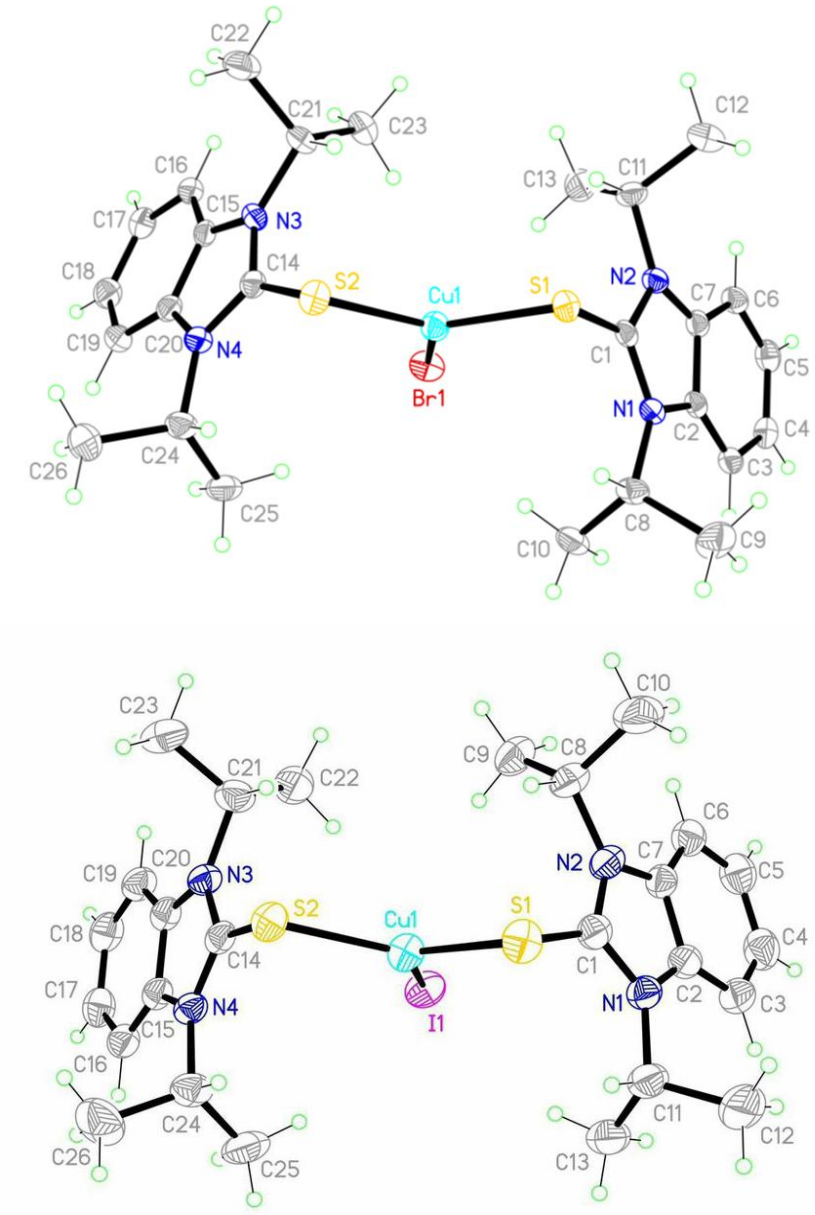

Figure 2.23. Molecular structures of $(iPr_2bimS)_2CuX$ (X = Br, I)

Similarly to the mercury(II) complexes of the iPr_2bimS ligand, the C-S bond distances in $(iPr_2bimS)_2CuX$ (X= Cl, Br, I) [1.71, 1.71, and 1.72 Å for X = Cl, Br, I, respectively] increase in length relative to the C-S bond in the free iPr_2bimS ligand [1.670 Å]. Moreover, the Cu-X bond distances (2.20, 2.34, and 2.52 Å for X = Cl, Br, I, respectively) significantly increase as the electronegativity of the corresponding halide

decreases. Moreover, the S-Cu-S bond angles significantly increases (115.1, 117.3, and 120.3° for X = Cl, Br, I, respectively) to accommodate the increasing covalent radii of the corresponding halide.

Table 2.10: Selected Bond Lengths (Å) and Angles (°) for $(iPr_2bimS)_2CuX$ (X= Cl, Br, I)

	X = Cl	X = Br	X = I
Cu(1)–X(1)	2.2001(6)	2.3413(5)	2.5164(4)
Cu(1)–S(1)	2.2376(4)	2.2419(7)	2.2459(7)
Cu(1)–S(1)#1	2.2377(4)	2.2453(7)	2.2470(7)
S(1)–C(1)	1.711(14)	1.712(2)	1.715(3)
X(1)–Cu(1)–S(1)	122.44(11)	120.06(2)	121.52(2)
X(1)–Cu(1)–S(1)#1	122.44(11)	122.63(2)	118.18(2)
S(1)–Cu(1)–S(1)#1	115.12(2)	117.27(2)	120.25(3)
C(1)–S(1)–Cu(1)	95.69(5)	101.01(8)	95.86(8)

2.6 Synthesis of Gold(I) Complexes

To explore the coordination chemistry of the iPr_2bimE (R = Me, E = S; R = ^{i}Pr, E = S, Se) ligands with gold, the Au(I) complexes $(R_2bimE)AuCl$ (R = Me, E = S; R = ^{i}Pr, E = S, Se) were easily prepared by reacting the respective ligand with an equimolar amount of (tht)AuCl[112] as shown in Scheme 2.14. All three air- and light-stable complexes are beige in color and may be isolated in 53-67% yields.

Single crystals of $(iPr_2bimS)AuCl$ suitable for X-ray diffraction studies were obtained by the slow evaporation of a solution of the compound in toluene. The structure is shown in Figure 2.24 depicting a two-coordinate metal center with a slight deviation from linearity (177.0°). Selected bond lengths and angles are summarized in Table 2.11. Moreover, a distinct bent geometry around the sulfur atom is depicted via the C1-S1-Au1 bond angle of 101.7°. Notably, no aurophillic interactions were observed in this structure

due to the steric bulk of the isopropyl substituents preventing these interactions in the solid state.

Scheme 2.14. Syntheses of (R_2bimE)AuCl (R = Me, E = S; R = ^{i}Pr, E =

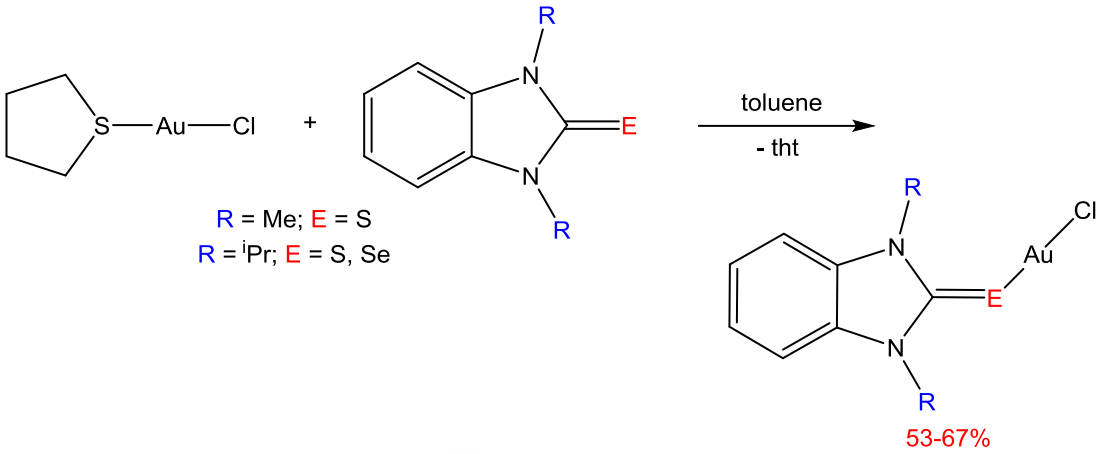

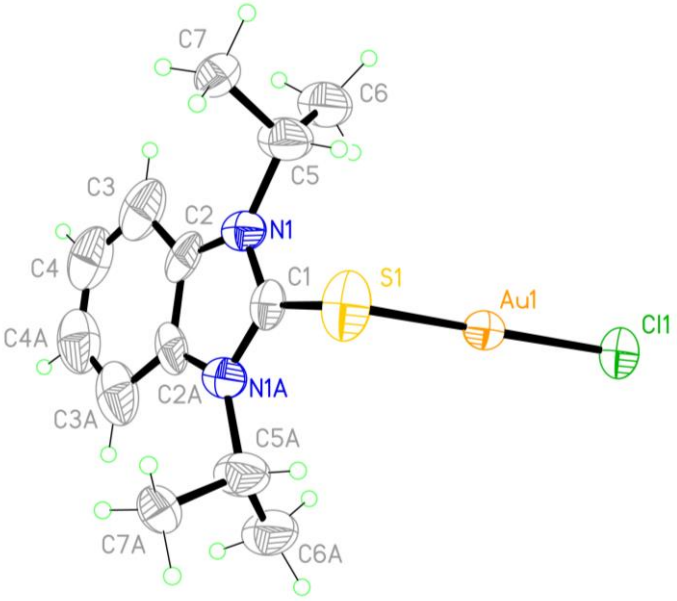

Figure 2.24. Molecular structure of (iPr_2bimS)AuCl

Table 2.11: Selected Bond Lengths (Å) and Angles (°) for (iPr_2bimS)AuCl

Au(1)–S(1)	2.240(3)	S(1)–Au(1)–Cl(1)	176.90(10)
Au(1)–Cl(1)	2.271(3)	C(1)–S(1)–Au(1)	102.60(3)
S(1)–C(1)	1.751(10)	N(1)–C(1)–N(1)#1	109.50(8)

Linear gold(I) complexes are precedented in the literature.[64, 65, 113] Nolan *et al.* recently reported the synthesis of linear gold(I) complexes by treatment of $(Me_2S)AuCl$ with different selenourea ligands in tetrahydrofuran (Figure 2.25).[113] All structures feature the expected two-coordinate linear Se-Au-Cl fragment with the reported Se-Au-Cl bond angles of (170.93-175.46°) and also present a distinct bent geometry around the selenium atom depicted by the reported C-Se-Au bond angles of (103.40-106.94°).

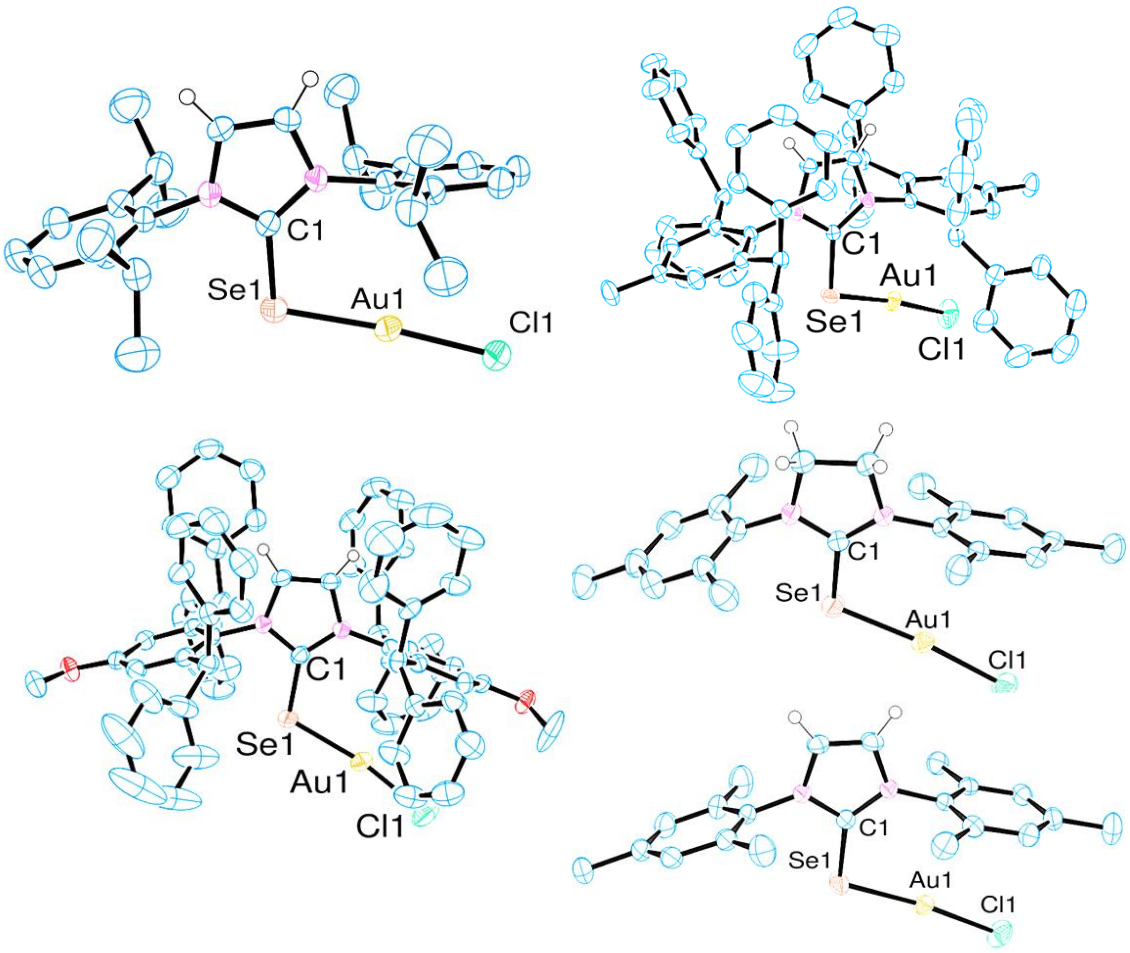

Figure 2.25. Molecular structures of Nolan's (NHSe)AuCl complexes.[113]

2.7 Potential Applications of Copper(I) Complexes

Copper is an essential element for most aerobic organisms, employed as a structural and catalytic cofactor, and consequently it is involved in many biological pathways.[114] Taking this into account, much attention has been given to research on the mechanisms of absorption,[115] distribution,[116] metabolism, and excretion of copper,[117] as well as on its role in development of cancer and other diseases.[118] Copper toxicity comes about from its ability to produce reactive oxygen species (ROS), displace other metal ions, peroxidize lipids, and cleave DNA and RNA.[119] In respect to the former, copper(I) ions can reduce hydrogen peroxide to hydroxyl radical (Equation 2.2). Copper(II) ions may in turn be reduced to Cu(I) by superoxide anion ($O_2^{\bullet-}$), or glutathione. Therefore, it can be concluded that the production of reactive oxygen species such as $OH^{\bullet}$ are driven by the copper, regardless of the form in which it is initially introduced into the body. The highly reactive hydroxyl radical is thus able to interact with any biological molecule by abstracting the hydrogen from an amino-bearing carbon to form a carbon-centered protein radical and from an unsaturated fatty acid to from a lipid radical. This results in oxidative damage of cells. Moreover, elevated levels of copper have been found in many types of human cancers, including prostate, breast, colon, lung, and brain.[120]

$$\begin{aligned} Cu^{2+} + O_2^{-\bullet} &\longrightarrow Cu^{+} + O_2 \\ Cu+ + H_2O_2 &\longrightarrow Cu^{2+} + OH + OH^{-} \end{aligned} \qquad (2.2)$$

With the exception of platinum(II) compounds, there is relatively little mechanistic information on how metal anticancer drugs function, but it is clear that metal ions can work by a variety of different routes. Non-platinum active compounds are likely to have mechanism of action, biodistribution and toxicity which are different from those of

platinum drugs might be effective against human cancers that are poor chemosensitive or have become resistant to conventional platinum drugs. Copper, being an essential element, may be less toxic than non-essential metals such as platinum. In recent years several families of copper complexes have been studies as potential antitumor agents. Although only a little understanding of the molecular basis of their mechanism of action has been documented, copper complexes have attracted attention based on modes of action different from that of cisplatin (covalent binding to DNA). Therefore, copper complexes may provide at least in principle a broader spectrum of antitumor activity. Preliminary studies were conducted to test the potential anti-cancer activity of the copper(I) complexes. To examine the cytotoxicity of iPr_2bimS and $(iPr_2bimS)_2CuCl$, we conducted a cell viability (Guava) test of these materials with live HeLa cells. Due to the low solubility of both the free ligand and copper complex in D-10 cell medium, 10 μL of dimethyl sulfoxide was spiked to the respective compounds before seeding the HeLa cells. The viability of the cells treated with iPr_2bimS, $(iPr_2bimS)_2CuCl$, and cisplatin as a standard was determined by the Guava ViaCount cytometry, data is shown in Figure 2.26.

As expected, the cell growth inhibition effects of cisplatin are dosage dependent. The cell growth inhibition effects of the free iPr_2bimS ligand and $(iPr_2bimS)_2CuCl$ complex are nonexistent, even at the highest tested dosage concentration of 20 μM. These preliminary results suggest that further testing needs to be conducted at higher concentrations, and/or with different cell types; as elevated levels of copper have been

found in many types of human cancers including prostate, breast, colon, lung, and brain

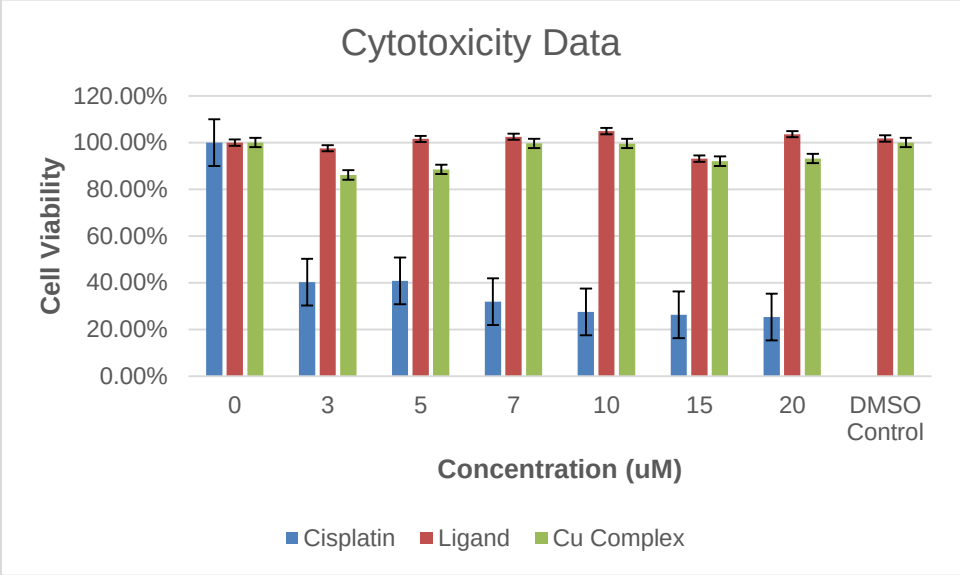

Figure 2.26. Preliminary cytotoxicity data.

Additionally, in order to facilitate the bioavailability of copper into the cell membrane, charge complexes may be synthesized such as the one proposed in Figure 2.27.

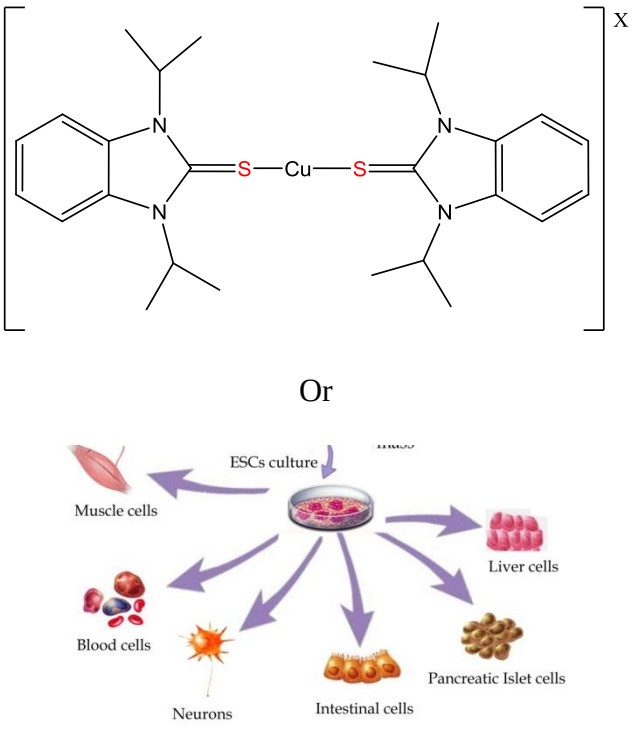

Figure 2.27. Proposed Adjustments for Cytotoxicity Studies

CHAPTER 3: EXPERIMENTAL

3.1 General Considerations

All reactions were performed under aerobic conditions or under dry oxygen-free nitrogen in an Innovative Technology System One-M-DC glove box where indicated. Solvents were purified and degassed by standard procedures and all commercially available reagents were used as received. [Me_2bimH]I,[76] [iPr_2bimH]Br,[77] CuBr·SMe_2[120] and (tht)AuCl[112] were prepared following literature procedures. ^{1}H and ^{13}C NMR spectra were obtained on JEOL ECX-300 (300 MHz) or JEOL ECA-500 (500 MHz) FT spectrometers. ^{1}H and ^{13}C chemical shifts are reported in ppm relative to $SiMe_4$ ($\delta = 0$ ppm) and were referenced internally with respect to the residual solvent resonances (^{1}H: δ 2.50 ppm for d_6-DMSO, 1.94 ppm for CD_2*H*CN; ^{13}C: δ 1.39 ppm for *C*D_3CN, 39.52 ppm for d_6-DMSO); coupling constants are reported in Hertz (Hz). IR spectra were recorded as pure solids on a Perkin-Elmer Spectrum 100 FT-IR spectrometer and are reported in cm^{-1}; relative intensities of the absorptions are indicated in parentheses (vs = very strong, s = strong, m = medium, w = weak, sh = shoulder). Elemental analyses were determined by Atlantic Microlab, Inc. (Norcross, GA).

3.2 Synthesis of Me_2bimS

Under an argon atmosphere, a suspension of the benzimidazolium salt [Me_2bimH]I (0.502 g, 1.831 mmol), K_2CO_3 (0.277 g, 2.006 mmol), and elemental sulfur (0.0709 g, 2.211 mmol) in methanol (35 mL) was heated to reflux for 24 h. The volatiles were removed under vacuum from the reaction mixture to give a white solid. The crude

product was extracted into dichloromethane (5 x 5 mL) and the colorless extract was concentrated under reduced pressure to *ca.* 2 mL and treated with pentane (2 x 10 mL), leading to the separation of the white product, which was isolated by filtration and dried *in vacuo* for 21 h (0.186 g, 57%). Mp = 145-147 °C. NMR data (in d_6-DMSO): ^{1}H δ 3.70 [s, 6 H, C*H*$_3$], 7.22-7.30 (m, 2 H, aromatic *H*), 7.40-7.48 (m, 2 H, aromatic *H*); ^{1}H NMR data (in CD_3CN): δ 3.73 [s, 6 H, C*H*$_3$], 7.22-7.35 (m, 4 H, aromatic *H*); ^{1}H NMR data (in d_6-acetone): δ 3.76 [s, 6 H, C*H*$_3$], 7.23-7.30 (m, 2 H, aromatic *H*), 7.34-7.41 (m, 2 H, aromatic *H*); ^{13}C δ 31.0 [q, $^1J_{C-H}$ = 141, 2 C, *C*H$_3$], 109.5 (d, $^1J_{C-H}$ = 169, 2 C, aromatic *C*), 122.8 (dd, $^1J_{C-H}$ = 163, $^2J_{C-H}$ = 7, 2 C, aromatic *C*), 132.0 (s, 2 C, aromatic *C*), 169.2 (s, 1 C, *C*=S). IR data: 3055 (w), 2931 (w), 1490 (m), 1433 (s), 1397 (s), 1385 (sh), 1336 (vs), 1246 (m), 1189 (w), 1150 (w), 1127 (w), 1111 (m), 1086 (w), 1020 (w), 1010 (m), 914 (w), 811 (m), 735 (vs), 662 (m). Anal. Calcd for $C_9H_{10}N_2S$: C, 60.6; H, 5.7; N, 15.7. Found: C, 60.4; H, 5.6; N, 15.9%.

3.3 Synthesis of iPr_2bimS

Under an argon atmosphere, a suspension of the benzimidazolium salt [iPr_2bimH]Br (0.836 g, 2.951 mmol), K_2CO_3 (0.491 g, 3.555 mmol), and elemental sulfur (0.105 g, 3.268 mmol) in methanol (50 mL) and heated to reflux for 48 h. The volatiles were removed under vacuum from the reaction mixture to give a light brown solid. The crude product was extracted into dichloromethane (25 mL) and the solvent was removed under reduced pressure from the yellow extract to give a brown sticky solid. The residue was treated with diethyl ether (3 x 10 mL) and the solvent was removed under vacuum from the combined extracts to afford the pure product as an off-white powder, which was dried *in vacuo* for 12 h (0.392 g, 57%). Mp = 181-184 °C. NMR data (in d_6-DMSO): ^{1}H δ 1.50 [d, $^3J_{H-H}$ = 7.3, 12 H, CH(C*H*$_3$)$_2$], 5.57 [septet, $^3J_{H-H}$ = 7.3, 2 H, C*H*(CH$_3$)$_2$],

7.18-7.25 (m, 2 H, aromatic *H*), 7.64-7.71 (m, 2 H, aromatic *H*); ^{1}H NMR data (in CD_3CN): δ 1.53 [d, $^{3}J_{H-H}$ = 7.3, 12 H, CH(C*H*$_3$)$_2$], 5.68 [septet, $^{3}J_{H-H}$ = 7.3, 2 H, C*H*(CH$_3$)$_2$], 7.16-7.24 (m, 2 H, aromatic *H*), 7.52-7.59 (m, 2 H, aromatic *H*); ^{1}H NMR data (in d_6-acetone): δ 1.56 [d, $^{1}J_{H-H}$ = 7.2, 12 H, CH(C*H*$_3$)$_2$], 5.73 [septet, $^{3}J_{H-H}$ = 7.2, 2 H, C*H*(CH$_3$)$_2$], 7.18-7.26 (m, 2 H, aromatic *H*), 7.59-7.67 (m, 2 H, aromatic *H*); ^{13}C δ 19.4 [q, $^{1}J_{C-H}$ = 128, 4 C, CH(*C*H$_3$)$_2$], 48.7 [d, $^{1}J_{C-H}$ = 140, 2 C, *C*H(CH$_3$)$_2$], 111.2 (d, $^{1}J_{C-H}$ = 165, 2 C, aromatic *C*), 122.2 (dd, $^{1}J_{C-H}$ = 163, $^{2}J_{C-H}$ = 9, 2 C, aromatic *C*), 130.2 (s, 2 C, aromatic *C*), 167.3 (s, 1 C, *C*=S). IR data: 3074 (w), 2981 (m), 2971 (sh), 2937 (w), 2879 (w), 1939 (w), 1898 (w), 1782 (w), 1672 (m), 1601 (w), 1514 (w), 1478 (s), 1415 (s), 1365 (s), 1338 (vs), 1327 (vs), 1312 (m), 1260 (m), 1227 (w), 1171 (m), 1161 (m), 1140 (s), 1090 (s), 1028 (m), 931 (w), 890 (m), 855 (w), 797 (m), 744 (vs), 664 (s). Anal. Calcd for $C_{13}H_{18}N_2S$: C, 66.6; H, 7.7; N, 12.0. Found: C, 66.5; H, 7.8; N, 11.9%.

3.4 Synthesis of iPr$_2$bimSe

Under an argon atmosphere, a suspension of the benzimidazolium salt [iPr$_2$bimH]Br (0.505 g, 1.766 mmol), K_2CO_3 (0.299 g, 2.119 mmol), and gray selenium (0.154 g, 1.942 mmol) in methanol (35 mL) was heated to reflux for 48 h. The dark reaction mixture was filtered while still warm, and the solvent was removed under reduced pressure from the yellow filtrate to give a pale brown solid. The product was extracted into dichloromethane (4 x 5 mL) and the pale yellow extract was concentrated under reduced pressure to *ca.* 1 mL and treated with pentane (15 mL) to afford the pure product as an off-white solid, which was isolated by filtration and dried *in vacuo* for 24 h (0.208 g, 50%). Mp = 136-138 °C. NMR data (in d_6-DMSO): ^{1}H δ 1.52 [d, $^{3}J_{H-H}$ = 7.0, 12 H, CH(C*H*$_3$)$_2$], 5.74 [septet, $^{3}J_{H-H}$ = 7.2, 2 H, C*H*(CH$_3$)$_2$], 7.21-7.31 (m, 2 H, aromatic *H*), 7.72-7.81 (m, 2 H, aromatic *H*); ^{13}C δ 19.4 [q, $^{1}J_{C-H}$ = 127, 4 C, CH(*C*H$_3$)$_2$], 51.3 [d, $^{1}J_{C-H}$

= 149, 2 C, *C*H(CH_3)$_2$], 111.8 (d, $^1J_{C-H}$ = 162, 2 C, aromatic *C*), 122.7 (dd, $^1J_{C-H}$ = 159, $^2J_{C-H}$ = 9, 2 C, aromatic *C*), 131.3 (s, 2 C, aromatic *C*), *C*=Se not observed. IR data: 3068 (w), 2977 (w), 2931 (w), 2875 (w), 1691 (w), 1603 (w), 1476 (s), 1410 (m), 1370 (s), 1337 (m), 1317 (w), 1304 (vs), 1160 (m), 1140 (m), 1132 (w), 1092 (s), 1069 (w), 1024 (w), 887 (w), 746 (vs), 708 (w), 652 (s). Anal. Calcd for $C_{13}H_{18}N_2Se$: C, 55.5; H, 6.5; N, 10.0. Found: C, 55.7; H, 6.4; N, 10.0%.

3.5 Synthesis of (R_2bimS)I_2

3.5.1 Synthesis of (Me_2bimS)I_2

A solution of I_2 (0.102 g, 0.402 mmol) in tetrahydrofuran (4 mL) was added to a solution of Me_2bimS (0.075 g, 0.421 mmol) in the same solvent (6 mL), resulting in the formation, within 1 minute, of a dark brown solid suspended in a purple solution. After stirring for 16 h, the suspension was concentrated under reduced pressure to *ca.* 1 mL, treated with diethyl ether (10 mL), and the product was isolated by filtration and dried *in vacuo* for 24 h (0.084 g, 48%). Mp = 245-248 °C (dec.). NMR data (in d_6-DMSO): ^{1}H δ 3.72 [s, 6 H, C*H*$_3$], 7.26-7.30 (m, 2 H, aromatic *H*), 7.44-7.49 (m, 2 H, aromatic *H*); ^{13}C δ 31.0 [q, $^1J_{C-H}$ = 141, 2 C, *C*H_3], 109.5 (d, $^1J_{C-H}$ = 168, 2 C, aromatic *C*), 122.9 (dd, $^1J_{C-H}$ = 163, $^2J_{C-H}$ = 7, 2 C, aromatic *C*), 132.0 (s, 2 C, aromatic *C*), *C*=S not observed. IR data: 3052 (w), 2937 (w), 1603 (w), 1484 (w), 1459 (m), 1430 (w), 1423 (w), 1388 (w), 1371 (w), 1353 (w), 1343 (m), 1254 (w), 1187 (w), 1154 (w), 1130 (w), 1100 (m), 1023 (m), 1007 (w), 974 (w), 931 (w), 850 (w), 826 (w), 808 (m), 747 (vs), 664 (m). Anal. Calcd for $C_9H_{10}I_2N_2S$: C, 25.0; H, 2.3; N, 6.5. Found: C, 24.9; H, 2.2; N, 6.4%.

3.5.2 Synthesis of (iPr_2bimS)I_2

A solution of I_2 (0.069 g, 0.272 mmol) in diethyl ether (5 mL) was added to a solution of iPr_2bimS (0.062 g, 0.265 mmol) in the same solvent (5 mL), resulting in the immediate

formation of a dark red solid suspended in a yellow solution. After stirring for 18 h, the suspension was concentrated under reduced pressure to *ca.* 1 mL, treated with pentane (20 mL), and the product was isolated by filtration and dried *in vacuo* for 24 h (0.084 g, 65%). Mp = 170-172 °C (dec.). NMR data (in d_6-DMSO): ^{1}H δ 1.55 [d, $^{3}J_{H-H}$ = 7.3, 12 H, CH(C*H*$_3$)$_2$], 5.55 [septet, $^{3}J_{H-H}$ = 7.3, 2 H, C*H*(CH$_3$)$_2$], 7.25-7.34 (m, 2 H, aromatic *H*), 7.73-7.82 (m, 2 H, aromatic *H*); ^{13}C δ 19.4 [q, $^{1}J_{C-H}$ =128, 4 C, CH(*C*H$_3$)$_2$], 48.9 [d, $^{1}J_{C-H}$ = 141, 2 C, *C*H(CH$_3$)$_2$], 111.2 m[d, $^{1}J_{C-H}$ = 164, 2 C, *C*H(CH$_3$)$_2$], 122.3 [dd, $^{1}J_{C-H}$ = 163, $^{2}J_{C-H}$ = 7, 2 C, aromatic *C*], 130.2 (s, 2 C, aromatic *C*), 166.7 (s, 2 C, *C*=S). IR data: 2983 (w), 2978 (w), 2954 (w), 2932 (w), 2881 (w), 2870 (w), 1707 (w), 1691 (w), 1668 (w), 1604 (w), 1558 (w), 1506 (w), 1471 (w), 1406 (w), 1399 (w), 1355 (m), 1311 (m), 1169 (w), 1141 (m), 1097 (m), 1081 (m), 1023 (w), 971 (w), 919 (w), 886 (w), 841 (w), 734 (vs), 701 (w), 682 (w), 663 (m). Anal. Calcd for $C_{13}H_{18}I_2N_2S$: C, 32.0; H, 3.7; N, 5.7. Found: C, 31.8; H, 3.7; N, 5.7%.

3.6 Synthesis of (iPr$_2$bimSe)X$_2$

3.6.1 Synthesis of (iPr$_2$bimSe)Cl$_2$

A solution of $SOCl_2$ (27 μL, 0.044 g, 0.373 mmol) in dichloromethane (20 mL) was added to a solution of iPr$_2$bimSe (0.075 g, 0.267 mmol) in the same solvent (5 mL), resulting in the immediate formation of a yellow solution. After stirring for 1 h, the solution was concentrated under reduced pressure to dryness, treated with pentane (25 mL), and the pale yellow solid was isolated by filtration and dried *in vacuo* for 24 h (0.044 g, 47%). Mp = 212-214 °C (dec.). NMR data (in d_6-DMSO): ^{1}H δ 1.76 [d, $^{3}J_{H-H}$ = 6.9, 12 H, CH(C*H*$_3$)$_2$], 5.73 [septet, $^{3}J_{H-H}$ = 7.1, 2 H, C*H*(CH$_3$)$_2$], 7.64-7.72 (m, 2 H, aromatic *H*), 7.28-7.38 (m, 2 H, aromatic *H*); ^{13}C δ 20.1 [q, $^{1}J_{C-H}$ = 131, 4 C, CH(*C*H$_3$)$_2$], 55.4 [d, $^{1}J_{C-H}$ = 144 , 2 C, *C*H(CH$_3$)$_2$], 115.6 [d, $^{1}J_{C-H}$ = 172, 2 C, aromatic *C*], 126.7 [dd,

$^{1}J_{C-H}$ = 164, $^{2}J_{C-H}$ = 8, 2 C, aromatic *C*], 129.7 (s, 2 C, aromatic *C*), 151.1 (s, 1 C, *C*=Se). IR data: 3103 (w), 3076 (w), 3048 (w), 2981 (w), 2966 (w), 2937 (w), 2878 (w), 2871 (w), 1600 (w), 1514 (w), 1474 (w), 1460 (w), 1436 (m), 1415 (w), 1391 (w), 1369 (w), 1342 (w), 1298 (m), 1178 (w), 1145 (m), 1096 (s), 1079 (w), 1021 (w), 973 (w), 892 (w), 820 (w), 753 (w), 738 (vs), 684 (w), 654 (w). Anal. Calcd. for $C_{13}H_{18}Cl_2N_2Se$: C, 44.3; H, 5.2; N, 8.0. Found: C, 43.8; H, 5.0; N, 8.0%.

3.6.2 Synthesis of (iPr_2bimSe)Br_2

Elemental bromine (14 µL, 0.044 g, 0.272 mmol) was added to a stirred solution of iPr_2bimSe (0.075 g, 0.267 mmol) in dichloromethane (10 mL), resulting in the immediate formation of a bright yellow solution. After stirring for 1 h, the solution was concentrated under reduced pressure to *ca.* 1 mL and treated with pentane (15 mL), leading to the separation of the product, which was isolated by filtration and dried *in vacuo* for 25 h (0.096 g, 82%). Mp = 249-250 °C (dec.). NMR data (in d_6-DMSO): ^{1}H δ 1.77 [d, $^{3}J_{H-H}$ = 7.0, 12 H, CH(C*H*$_3$)$_2$], 5.69 [septet, $^{3}J_{H-H}$ = 7.0, 2 H, C*H*(CH$_3$)$_2$], 7.60-7.76 [m, 2 H, aromatic *H*], 8.25-8.40 (m, 2 H, aromatic *H*); ^{13}C δ 19.8 [q, $^{1}J_{C-H}$ = 128, 4 C, CH(*C*H$_3$)$_2$], 55.6 [d, $^{1}J_{C-H}$ = 144, 2 C, *C*H(CH$_3$)$_2$], 115.5 (d, $^{1}J_{C-H}$ = 168, 2 C, aromatic *C*), 126.7 (d, $^{1}J_{C-H}$ = 163, 2 C, aromatic *C*), 130.0 (s, 2 C, aromatic *C*), 148.2 (s, 1 C, *C*=Se). IR data: 3103 (w), 3074 (w), 3062 (w), 3044 (w), 2978 (w), 2965 (w), 2937 (w), 2876 (w), 1595 (w), 1470 (w), 1456 (w), 1432 (s), 1416 (m), 1388 (w), 1368 (m), 1297 (m), 1176 (w), 1144 (s), 1095 (s), 1077 (w), 1018 (w), 973 (w), 888 (w), 821 (w), 737 (vs), 650 (m). Anal. Calcd for $C_{13}H_{18}Br_2N_2Se$: C, 35.4; H, 4.1; N, 6.4. Found: C, 35.3; H, 4.0; N, 6.3%.

3.6.3 Synthesis of (iPr_2bimSe)I_2

A solution of I_2 (0.068 g, 0.268 mmol) in diethyl ether (5 mL) was added to a solution of iPr_2bimSe (0.076 g, 0.270 mmol) in the same solvent (5 mL), resulting in the immediate formation of a dark red solid suspended in a colorless solution. After stirring for 20 h, the suspension was concentrated under reduced pressure to *ca.* 1 mL, treated with pentane (20 mL), and the product was isolated by filtration and dried *in vacuo* for 24 h (0.116 g, 81%). Mp = 234-236 °C (dec.). NMR data (in d_6-DMSO): ^{1}H δ 1.68 [d, J_{H-H} = 7.0, 12 H, CH(C*H*$_3$)$_2$], 5.61 [septet, $^3J_{H-H}$ = 7.0, 2 H, C*H*(CH$_3$)$_2$], 7.50-7.60 (m, 2 H, aromatic *H*), 8.10-8.20 (m, 2 H, aromatic *H*); ^{13}C δ 19.6 [d, $^1J_{C-H}$ = 128, 4 C, CH(*C*H$_3$)$_2$], 54.3 [d, $^1J_{C-H}$ = 144, 2 C, *C*H(CH$_3$)$_2$], 114.2 (d, $^1J_{C-H}$ = 163, 2 C, aromatic *C*), 125.4 (d, $^1J_{C-H}$ = 164, 2 C, aromatic *C*), 130.9 (s, 2 C, aromatic *C*), *C*=Se not observed. IR data: 3105 (w), 3078 (w), 3045 (w), 2986 (w), 2974 (w), 2934 (w), 2875 (w), 1603 (w), 1475 (m), 1459 (w), 1431 (s), 1409 (m), 1386 (m), 1368 (s), 1294 (m), 1170 (m), 1142 (s), 1094 (s), 1024 (m), 989 (w), 971 (w), 892 (w), 857 (w), 820 (w), 756 (vs), 734 (s), 651 (m). Anal. Calcd for $C_{13}H_{18}I_2N_2Se$: C, 29.2; H, 3.4; N, 5.2. Found: C, 29.1; H, 3.2; N, 5.2%.

3.7 Synthesis of (Me_2bimS)HgX_2

3.7.1 Synthesis of (Me_2bimS)$HgCl_2$

A stirred suspension of $HgCl_2$ (0.099 g, 0.365 mmol) in ethanol (3 mL) was treated with a solution of Me_2bimS (0.075 g, 0.421 mmol) in the same solvent (7 mL), resulting in the immediate formation of a white solid and a colorless solution. After stirring for 24 h, the suspension was concentrated under reduced pressure to *ca.* 3 mL, treated with diethyl ether (10 mL), and the product was isolated by filtration and dried *in vacuo* for 23 h (0.112 g, 68%). Mp = 263-264 °C. NMR data (in d_6-DMSO): ^{1}H δ 3.81 (s, 6 H, C*H*$_3$),

7.33-7.41 (m, 2 H, aromatic *H*), 7.56-7.63 (m, 2 H, aromatic *H*); ^{13}C δ 32.1 (q, $^{1}J_{C-H}$ = 142, 2 C, *C*H$_3$), 111.2 (d, $^{1}J_{C-H}$ = 171, 2 C, aromatic *C*), 124.5 (dd, $^{1}J_{C-H}$ = 165, $^{2}J_{C-H}$ = 5, 2 C, aromatic *C*), 131.9 (s, 2 C, aromatic *C*), *C*=S peak not observed. IR data: 3090 (w), 3054 (w), 3030 (w), 2944 (w), 1613 (w), 1575 (w), 1472 (s), 1457 (m), 1388 (s), 1376 (sh), 1366 (sh), 1348 (m), 1260 (w), 1188 (w), 1155 (w), 1139 (w), 1128 (w), 1102 (m), 1022 (m), 1016 (m), 926 (w), 825 (w), 806 (m), 762 (vs), 750 (vs), 741 (vs), 672 (w), 656 (w). Anal. Calcd for $C_9H_{10}Cl_2HgN_2S$: C, 24.0; H, 2.2; N, 6.2. Found: C, 24.5; H, 2.5; N, 6.2%.

3.7.2 Synthesis of (Me$_2$bimS)HgBr$_2$

A stirred suspension of HgBr$_2$ (0.132 g, 0.366 mmol) in ethanol (3 mL) was treated with a solution of Me$_2$bimS (0.075 g, 0.421 mmol) in the same solvent (9 mL), resulting in the immediate formation of a white solid and a colorless solution. After stirring for 24 h, the suspension was concentrated under reduced pressure to *ca.* 2 mL and treated with diethyl ether (10 mL), and the product was isolated by filtration and dried *in vacuo* for 23 h (0.156 g, 79%). Mp = 248-250 °C. NMR data (in d$_6$-DMSO): ^{1}H δ 3.87 (s, 6 H, C*H*$_3$), 7.40-7.47 (m, 2 H, aromatic *H*), 7.65-7.72 (m, 2 H, aromatic *H*); ^{13}C δ 32.1 (q, $^{1}J_{C-H}$ = 142, 2 C, *C*H$_3$), 111.0 (dd, $^{1}J_{C-H}$ = 170, $^{2}J_{C-H}$ = 6, 2 C, aromatic *C*), 124.3 (dd, $^{1}J_{C-H}$ = 165, $^{2}J_{C-H}$ = 6, 2 C, aromatic *C*), 131.9 (s, 2 C, aromatic *C*), 162.6 (s, 1 C, *C*=S). IR data: 2939 (w), 1612 (w), 1583 (w), 1488 (w), 1469 (s), 1455 (s), 1426 (w), 1386 (s), 1367 (m), 1346 (s), 1260 (w), 1187 (w), 1154 (w), 1128 (w), 1101 (m), 1021 (w), 1013 (m), 974 (w), 929 (w), 824 (w), 806 (m), 748 (vs), 741 (vs), 669 (w), 654 (w). Anal. Calcd for $C_9H_{10}Br_2HgN_2S$: C, 20.1; H, 1.9; N, 5.2. Found: C, 19.9; H, 1.8; N, 5.1%.

3.7.3 Synthesis of $(Me_2bimS)HgI_2$

A stirred suspension of HgI_2 (0.184 g, 0.405 mmol) in diethyl ether (3 mL) was treated with a solution of Me_2bimS (0.075 g, 0.421 mmol) in the same solvent (9 mL), resulting in the formation, within 1 h, of a pale yellow solid and a colorless solution. After stirring for 24 h, the suspension was concentrated under reduced pressure to *ca.* 2 mL, treated with pentane (10 mL), and the product was isolated by filtration and dried *in vacuo* for 23 h (0.151 g, 59%). Mp = 206-208 °C (dec.). NMR data (in d_6-DMSO): ^{1}H δ 3.84 (s, 6 H, C*H*$_3$), 7.36-7.44 (m, 2 H, aromatic *H*), 7.60-7.67 (m, 2 H, aromatic *H*); ^{13}C δ 31.9 (q, $^1J_{C-H}$ = 142, 2 C, *C*H$_3$), 110.6 (dd, $^1J_{C-H}$ = 170, $^2J_{C-H}$ = 5, 2 C, aromatic *C*), 123.9 (dd, $^1J_{C-H}$ = 164, $^2J_{C-H}$ = 7, 2 C, aromatic *C*), 131.9 (s, 2 C, aromatic *C*), 164.4 (s, 1 C, *C*=S). IR data: 2928 (w), 1463 (m), 1429 (w), 1389 (m), 1367 (w), 1344 (m), 1326 (w), 1253 (w), 1188 (w), 1150 (w), 1128 (w), 1102 (w), 1023 (w), 1009 (w), 930 (w), 843 (w), 824 (w), 806 (w), 743 (vs), 657 (m). Anal. Calcd for $C_9H_{10}HgI_2N_2S$: C, 17.1; H, 1.6; N, 4.4. Found: C, 16.9; H, 1.6; N, 4.3%.

3.7.4 Synthesis of $(Me_2bimS)_2HgCl_2$

A stirred suspension of $HgCl_2$ (0.052 g, 0.192 mmol) in acetonitrile (3 mL) was treated with a solution of Me_2bimS (0.075 g, 0.421 mmol) in the same solvent (9 mL), resulting in the immediate formation of a white solid and a colorless solution. After stirring for 24 h, the suspension was concentrated under reduced pressure to *ca.* 2 mL and treated with diethyl ether (10 mL), and the product was isolated by filtration and dried *in vacuo* for 23 h (0.079 g, 66%). Mp = 248-250 °C. NMR data (in d_6-DMSO): ^{1}H δ 3.81 (s, 12 H, C*H*$_3$), 7.34-7.41 (m, 4 H, aromatic *H*), 7.56-7.64 (m, 4 H, aromatic *H*); ^{13}C δ 31.7 (q, $^1J_{C-H}$ = 142, 4 C, *C*H$_3$), 110.4 (dd, $^1J_{C-H}$ = 170, $^2J_{C-H}$ = 5, 4 C, aromatic *C*), 123.8 (dd, $^1J_{C-H}$ = 164, $^2J_{C-H}$ = 7, 4 C, aromatic *C*), 131.9 (s, 4 C, aromatic *C*), 164.6 (s, 2 C, *C*=S). IR data:

3051 (w), 2928 (w), 1611 (w), 1572 (w), 1462 (s), 1433 (m), 1388 (s), 1373 (w), 1356 (w), 1343 (m), 1256 (w), 1189 (w), 1157 (w), 1133 (w), 1106 (m), 1021 (w), 1015 (w), 947 (w), 932 (w), 863 (w), 851 (w), 826 (w), 808 (m), 761 (vs), 753 (vs), 741 (s), 665 (m), 657 (w). Anal. Calcd for $C_{18}H_{20}Cl_2HgN_4S_2$: C, 34.4; H, 3.2; N, 8.9. Found: C, 34.1; H, 3.1; N, 8.8%.

3.7.5 Synthesis of $(Me_2bimS)_2HgBr_2$

A stirred suspension of $HgBr_2$ (0.065 g, 0.180 mmol) in acetonitrile (3 mL) was treated with a solution of Me_2bimS (0.075 g, 0.421 mmol) in the same solvent (7 mL), resulting in the formation, within 1 h, of a white solid and a colorless solution. After stirring for 21 h, the suspension was concentrated under reduced pressure to *ca.* 2 mL, treated with diethyl ether (10 mL), and the product was isolated by filtration and dried *in vacuo* for 23 h (0.076 g, 59%). Mp = 238-240 °C. NMR data (in d_6-DMSO): ^{1}H δ 3.81 (s, 12 H, C*H*$_3$), 7.33-7.41 (m, 4 H, aromatic *H*), 7.56-7.64 (m, 4 H, aromatic *H*); ^{13}C δ 31.6 (q, $^1J_{C\text{-}H}$ = 140, 4 C, *C*H$_3$), 110.4 (dd, $^1J_{C\text{-}H}$ = 170, $^2J_{C\text{-}H}$ = 5, 4 C, aromatic *C*), 123.7 (dd, $^1J_{C\text{-}H}$ = 164, $^2J_{C\text{-}H}$ = 7, 4 C, aromatic *C*), 131.9 (s, 4 C, aromatic *C*), 165.1 (s, 2 C, *C*=S). IR data: 3103 (w), 3054 (w), 2982 (w), 2935 (w), 1609 (w), 1460 (s), 1431 (s), 1386 (s), 1371 (w), 1355 (m), 1343 (m), 1255 (m), 1189 (m), 1155 (m), 1132 (m), 1104 (m), 1021 (m), 1012 (m), 984 (w), 931 (w), 859 (w), 848 (w), 827 (w), 808 (m), 748 (vs), 741 (vs), 657 (m). Anal. Calcd for $C_{18}H_{20}Br_2HgN_4S_2$: C, 30.2; H, 2.8; N, 7.8. Found: C, 29.9; H, 2.8; N, 7.7%.

3.7.6 Synthesis of $(Me_2bimS)_2HgI_2$

A stirred suspension of HgI_2 (0.096 g, 0.210 mmol) in acetonitrile (3 mL) was treated with a solution of Me_2bimS (0.075 g, 0.420 mmol) in the same solvent (9 mL), resulting in the formation, within 1 hour, of a pale yellow solid and a colorless solution. After

stirring for 24 h, the suspension was concentrated under reduced pressure to *ca.* 2 mL and treated with diethyl ether (10 mL), and the product was isolated by filtration and dried *in vacuo* for 23 h (0.106 g, 62%). Mp = 228-230 °C (dec.). NMR data (in d_6-DMSO): ^{1}H δ 3.79 (s, 12 H, C*H*$_3$), 7.31-7.39 (m, 4 H, aromatic *H*), 7.53-7.61 (m, 4 H, aromatic *H*); ^{13}C δ 31.6 (q, $^1J_{C-H}$ = 144, 4 C, *C*H$_3$), 110.2 (dd, $^1J_{C-H}$ = 171, $^2J_{C-H}$ = 6, 4 C, aromatic *C*), 123.5 (dd, $^1J_{C-H}$ = 163, $^2J_{C-H}$ = 7, 4 C, aromatic *C*), 132.0 (s, 4 C, aromatic *C*), 166.3 (s, 2 C, *C*=S). IR data: 3058 (w), 2977 (w), 2936 (w), 1492 (w), 1459 (s), 1452 (sh), 1426 (m), 1388 (s), 1362 (m), 1341 (s), 1252 (m), 1189 (w), 1151 (m), 1131 (m), 1101 (s), 1023 (m), 1009 (m), 927 (w), 826 (w), 808 (m), 750 (vs), 738 (vs), 680 (w), 657 (m). Anal. Calcd for $C_{18}H_{20}HgI_2N_4S_2$: C, 26.7; H, 2.5; N, 6.9. Found: C, 26.3; H, 2.4; N, 6.6%.

3.8 Synthesis of $(iPr_2bimS)_nHgX_2$

3.8.1 Synthesis of $(iPr_2bimS)HgCl_2$

A stirred suspension of $HgCl_2$ (0.069 g, 0.255 mmol) in diethyl ether (3 mL) was treated with a solution of iPr_2bimS (0.066 g, 0.281 mmol) in the same solvent (6 mL), resulting in the formation, within 15 min, of a colorless solution. After stirring for 22 h, the solution was concentrated under reduced pressure to *ca.* 2 mL and treated with pentane (10 mL), leading to the separation of the white product, which was isolated by filtration, washed with pentane (2 x 5 mL), and dried *in vacuo* for 20 h (0.096 g, 74%). Mp = 194-197 °C (dec.). NMR data (in d_6-DMSO): ^{1}H δ 1.57 [d, $^3J_{H-H}$ = 6.9, 12 H, CH(C*H*$_3$)$_2$], 5.57 [septet, $^3J_{H-H}$ = 7.0, 2 H, C*H*(CH$_3$)$_2$], 7.32-7.39 (m, 2 H, aromatic *H*), 7.81-7.90 (m, 2 H, aromatic *H*); ^{13}C δ 19.6 [q, $^1J_{C-H}$ = 128, 4 C, CH(*C*H$_3$)$_2$], 50.2 [d, $^1J_{C-H}$ = 145, 2 C, *C*H(CH$_3$)$_2$], 112.5 (d, $^1J_{C-H}$ = 163, 2 C, aromatic *C*), 123.5 (d, $^1J_{C-H}$ = 165, 2 C, aromatic *C*), 130.1 (s, 2 C, aromatic *C*), *C*=S not observed. IR data: 3116 (w), 3097

(w), 3040 (w), 2978 (w), 2940 (w), 1606 (w), 1474 (m), 1459 (w), 1416 (vs), 1395 (sh), 1371 (sh), 1356 (s), 1312 (m), 1300 (m), 1174 (w), 1149 (s), 1137 (w), 1096 (s), 1082 (w), 1022 (w), 939 (w), 892 (w), 850 (w), 753 (vs), 744 (sh), 662 (s). Anal. Calcd for $C_{13}H_{18}Cl_2HgN_2S$: C, 30.9; H, 3.6; N, 5.5. Found: C, 30.9; H, 3.5; N, 5.4%.

3.8.2 Synthesis of (iPr_2bimS)$HgBr_2$

A stirred suspension of $HgBr_2$ (0.053 g, 0.148 mmol) in ethanol (3 mL) was treated with a solution of iPr_2bimS (0.041 g, 0.175 mmol) in the same solvent (6 mL), resulting in the formation of a white solid and a colorless solution. After stirring for 22 h, the suspension was concentrated under reduced pressure to *ca.* 3 mL and treated with diethyl ether (10 mL), leading to the separation of the white product, which was isolated by filtration and dried *in vacuo* for 20 h (0.061 g, 69%). Mp = 196-199 °C (dec.). NMR data (in d_6-DMSO): ^{1}H δ 1.59 [d, $^3J_{H-H}$ = 6.9, 12 H, CH(C*H*$_3$)$_2$], 5.57 [septet, $^3J_{H-H}$ = 7.0, 2 H, C*H*(CH$_3$)$_2$], 7.33-7.42 (m, 2 H, aromatic *H*), 7.84-7.93 (m, 2 H, aromatic *H*); ^{13}C δ 19.7 [q, $^1J_{C-H}$ = 128, 4 C, CH(*C*H$_3$)$_2$], 50.3 [d, $^1J_{C-H}$ = 143, 2 C, *C*H(CH$_3$)$_2$], 112.7 (d, $^1J_{C-H}$ = 164, 2 C, aromatic *C*), 123.6 (dd, $^1J_{C-H}$ = 164, $^2J_{C-H}$ = 8, 2 C, aromatic *C*), 130.1 (s, 2 C, aromatic *C*), 160.8 (s, 1 C, *C*=S). IR data: 2978 (w), 2901 (w), 1471 (w), 1442 (w), 1411 (s), 1392 (w), 1372 (w), 1353 (m), 1309 (m), 1260 (m), 1171 (w), 1141 (m), 1131 (w), 1093 (s), 1080 (m), 1065 (sh), 1057 (sh), 1049 (sh), 1024 (m), 933 (w), 888 (w), 802 (w), 755 (w), 738 (vs), 660 (s). Anal. Calcd for $C_{13}H_{18}Br_2HgN_2S$: C, 26.3; H, 3.1; N, 4.7. Found: C, 26.5; H, 3.2; N, 4.6%.

3.8.3 Synthesis of (iPr_2bimS)HgI_2

A stirred suspension of HgI_2 (0.026 g, 0.057 mmol) in ethanol (3 mL) was treated with a solution of iPr_2bimS (0.016 g, 0.070 mmol) in the same solvent (6 mL), resulting in the formation, within 5 min, of a pale yellow solution. After stirring for 22 h, the solution

was concentrated under reduced pressure to *ca.* 3 mL and treated with diethyl ether (10 mL), leading to the separation of the pale yellow product, which was isolated by filtration and dried *in vacuo* for 20 h (0.028 g, 71%). Mp = 224-226 °C (dec.). NMR data (in d_6-DMSO): ^{1}H δ 1.58 [d, $^{3}J_{H-H}$ = 7.1, 12 H, CH(C*H*$_3$)$_2$], 5.56 [septet, $^{3}J_{H-H}$ = 7.0, 2 H, C*H*(CH$_3$)$_2$], 7.30-7.38 (m, 2 H, aromatic *H*), 7.80-7.88 (m, 2 H, aromatic *H*); ^{13}C δ 19.9 [q, $^{1}J_{C-H}$ = 128, 4 C, CH(*C*H$_3$)$_2$], 49.9 [d, $^{1}J_{C-H}$ = 145, 2 C, *C*H(CH$_3$)$_2$], 112.2 (d, $^{1}J_{C-H}$ = 165, 2 C, aromatic *C*), 123.2 (dd, $^{1}J_{C-H}$ = 162, $^{2}J_{C-H}$ = 6, 2 C, aromatic *C*), 130.2 (s, 2 C, aromatic *C*), 162.8 (s, 1 C, *C*=S). IR data: 2977 (w), 2931 (w), 2901 (w), 1471 (w), 1406 (s), 1390 (w), 1374 (w), 1349 (m), 1308 (m), 1295 (w), 1261 (w), 1173 (w), 1141 (m), 1131 (m), 1092 (s), 1079 (m), 1024 (m), 931 (w), 892 (w), 803 (w), 738 (vs), 660 (m). Anal. Calcd for $C_{13}H_{18}HgI_2N_2S$: C, 22.7; H, 2.6; N, 4.1. Found: C, 22.9; H, 2.6; N, 4.0%.

3.8.4 Synthesis of (iPr$_2$bimS)$_2$HgCl$_2$

A stirred suspension of $HgCl_2$ (0.024 g, 0.089 mmol) in acetonitrile (5 mL) was treated with a solution of iPr$_2$bimS (0.046 g, 0.198 mmol) in the same solvent (15 mL), resulting in the formation of a white solid suspended in a colorless solution. After stirring the suspension for 24 h, the product was isolated by filtration and dried *in vacuo* for 24 h (0.050 g, 76%). Mp = 160-162 °C (dec.). NMR data (in d_6-DMSO): ^{1}H δ 1.55 [d, $^{3}J_{H-H}$ = 7.1, 24 H, CH(C*H*$_3$)$_2$], 5.57 [septet, $^{3}J_{H-H}$ = 7.1, 4 H, C*H*(CH$_3$)$_2$], 7.26-7.34 (m, 4 H, aromatic *H*), 7.75-7.84 (m, 4 H, aromatic *H*); ^{13}C δ 19.5 [q, $^{1}J_{C-H}$ = 128, 8 C, CH(*C*H$_3$)$_2$], 49.6 [d, $^{1}J_{C-H}$ = 140, 4 C, *C*H(CH$_3$)$_2$], 111.9 (d, $^{1}J_{C-H}$ = 164, 4 C, aromatic *C*), 122.9 (dd, $^{1}J_{C-H}$ = 162, $^{2}J_{C-H}$ = 7, 4 C, aromatic *C*), 130.2 (s, 4 C, aromatic *C*), 163.7 (s, 2 C, *C*=S). IR data: 3108 (w), 3054 (w), 2979 (w), 2961 (w), 2938 (w), 2875 (w), 1474 (m), 1443 (w), 1410 (vs), 1391 (w), 1372 (m), 1354 (vs), 1313 (s), 1300 (w), 1169 (m), 1144 (s),

1095 (s), 1081 (m), 1021 (w), 977 (w), 935 (w), 889 (w), 842 (w), 757 (vs), 747 (vs), 687 (w), 661 (s). Anal. Calcd for $C_{26}H_{36}Cl_2HgN_4S_2$: C, 42.2; H, 4.9; N, 7.6. Found: C, 42.5; H, 4.9; N, 7.7%.

3.8.5 Synthesis of $(iPr_2bimS)_2HgBr_2$

A stirred suspension of $HgBr_2$ (0.037 g, 0.102 mmol) in acetonitrile (3 mL) was treated with a solution of iPr_2bimS (0.050 g, 0.214 mmol) in the same solvent (6 mL), resulting in the formation of a colorless solution. After stirring for 22 h, the solution was concentrated under reduced pressure to *ca.* 2 mL and treated with diethyl ether (10 mL), leading to the separation of the white product, which was isolated by filtration and dried *in vacuo* for 20 h (0.063 g, 75%). Mp = 164-166 °C (dec.). NMR data (in d_6-DMSO): ^{1}H δ 1.52 [d, $^3J_{H-H}$ = 7.1, 24 H, CH(C*H*$_3$)$_2$], 5.56 [septet, $^3J_{H-H}$ = 7.1, 4 H, C*H*(CH$_3$)$_2$], 7.22-7.30 (m, 4 H, aromatic *H*), 7.70-7.78 (m, 4 H, aromatic *H*); ^{13}C δ 20.2 [q, $^1J_{C-H}$ = 127, 8 C, CH(*C*H$_3$)$_2$], 50.4 [d, $^1J_{C-H}$ = 143, 4 C, *C*H(CH$_3$)$_2$], 112.8 (d, $^1J_{C-H}$ = 165, 4 C, aromatic *C*), 123.7 (dd, $^1J_{C-H}$ = 163, $^2J_{C-H}$ = 8, 4 C, aromatic *C*), 130.7 (s, 4 C, pyridine *C*), 163.3 (s, 2 C, *C*=S). IR data: 3105 (w), 3074 (w), 3052 (w), 2978 (w), 2958 (w), 2937 (w), 2876 (w), 1474 (m), 1444 (w), 1409 (s), 1401 (s), 1372 (m), 1353 (vs), 1312 (s), 1299 (w), 1168 (m), 1143 (s), 1094 (s), 1081 (m), 1022 (w), 888 (w), 841 (w), 755 (s), 740 (vs), 661 (s). Anal. Calcd for $C_{26}H_{36}Br_2HgN_4S_2$: C, 37.7; H, 4.4; N, 6.8. Found: C, 37.6; H, 4.5; N, 6.7%.

3.8.6 Synthesis of $(iPr_2bimS)_2HgI_2$

A stirred suspension of HgI_2 (0.075 g, 0.165 mmol) in acetonitrile (3 mL) was treated with a solution of iPr_2bimS (0.081 g, 0.346 mmol) in the same solvent (8 mL), resulting in the formation, within 30 min, of a pale yellow solution. After stirring for 24 h, the solution was concentrated under reduced pressure to *ca.* 5 mL and treated with diethyl

ether (10 mL), leading to the separation of the pale yellow product, which was isolated by filtration and dried *in vacuo* for 23 h (0.099 g, 65%). Mp = 174-176 °C (dec.). NMR data (in d_6-DMSO): ^{1}H δ 1.55 [d, $^{3}J_{H-H}$ = 7.1, 24 H, CH(C*H*$_3$)$_2$], 5.57 [septet, $^{3}J_{H-H}$ = 7.1, 4 H, C*H*(CH$_3$)$_2$], 7.25-7.33 (m, 4 H, aromatic *H*), 7.74-7.82 (m, 4 H, aromatic *H*); ^{13}C δ 19.7 [q, $^{1}J_{C-H}$ = 128, 8 C, CH(*C*H$_3$)$_2$], 49.5 [d, $^{1}J_{C-H}$ = 144, 4 C, *C*H(CH$_3$)$_2$], 111.9 (d, $^{1}J_{C-H}$ = 163, 4 C, aromatic *C*), 122.9 (dd, $^{1}J_{C-H}$ = 163, $^{2}J_{C-H}$ = 9, 4 C, aromatic *C*), 130.2 (s, 4 C, aromatic *C*), 164.5 (s, 2 C, *C*=S). IR data: 2977 (w), 2936 (w), 2901 (w), 1473 (m), 1408 (s), 1397 (s), 1391 (s), 1373 (w), 1350 (s), 1313 (m), 1296 (w), 1168 (w), 1143 (s), 1094 (s), 1081 (m), 1065 (sh), 1057 (w), 1026 (w), 930 (w), 892 (w), 847 (w), 738 (vs), 660 (s). Anal. Calcd for $C_{26}H_{36}HgI_2N_4S_2$: C, 33.8; H, 3.9; N, 6.1. Found: C, 33.5; H, 3.7; N, 6.1%.

3.9 Synthesis of (iPr$_2$bimSe)$_n$HgX$_2$

3.9.1 Synthesis of (iPr$_2$bimSe)HgCl$_2$

A stirred suspension of $HgCl_2$ (0.072 g, 0.265 mmol) in ethanol (3 mL) was treated with a solution of iPr$_2$bimSe (0.076 g, 0.270 mmol) in the same solvent (7 mL), resulting in the formation, within 1 minute, of a white solid suspended in a colorless solution. After stirring for 20 h, the suspension was concentrated under reduced pressure to *ca.* 3 mL, treated with diethyl ether (10 mL), and the product was isolated by filtration and dried *in vacuo* for 24 h (0.097 g, 66%). Mp = 241-243 °C (dec.). NMR data (in d_6-DMSO): ^{1}H δ 1.65 [d, $^{1}J_{H-H}$ = 7.1, 12 H, CH(C*H*$_3$)$_2$], 5.63 [septet, $^{1}J_{H-H}$ = 7.1, 2 H, C*H*(CH$_3$)$_2$], 7.45-7.53 (m, 2 H, aromatic *H*), 8.04-8.12 (m, 2 H, aromatic *H*); ^{13}C δ 19.9 [q, $^{1}J_{C-H}$ = 128, 4 C, CH(*C*H$_3$)$_2$], 53.7 [d, $^{1}J_{C-H}$ = 140, 2 C, *C*H(CH$_3$)$_2$], 114.0 (d, $^{1}J_{C-H}$ = 171, 2 C, aromatic *C*), 124.7 (dd, $^{1}J_{C-H}$ = 164, $^{2}J_{C-H}$ = 8, 2 C, aromatic *C*), 131.0 (s, 2 C, aromatic *C*), 150.6 (s, 1 C, *C*=Se). IR data: 3037 (w), 2976 (w), 2938 (w), 1603 (w), 1472 (w),

1457 (w), 1416 (s), 1389 (w), 1372 (w), 1355 (m), 1298 (m), 1173 (w), 1147 (m), 1138 (w), 1094 (s), 1072 (w), 1021 (w), 935 (w), 890 (w), 849 (w), 822 (w), 755 (vs), 737 (m), 709 (w), 651 (m). Anal. Calcd for $C_{13}H_{18}Cl_2HgN_2Se$: C, 28.3; H, 3.3; N, 5.1. Found: C, 28.4; H, 3.2; N, 5.2%

3.9.2 Synthesis of (iPr_2bimSe)$HgBr_2$

A stirred suspension of $HgBr_2$ (0.088 g, 0.243 mmol) in acetonitrile (3 mL) was treated with a solution of iPr_2bimSe (0.075 g, 0.267 mmol) in the same solvent (7 mL), resulting in the formation, within 1 minute, of a white solid suspended in a colorless solution. After stirring for 25 h, the suspension was concentrated under reduced pressure to *ca.* 3 mL, treated with diethyl ether (10 mL), and the product was isolated by filtration and dried *in vacuo* for 24 h (0.112 g, 72%). Mp = 231-233 °C (dec.). NMR data (in d_6-DMSO): ^{1}H δ 1.65 [d, $^1J_{H-H}$ = 7.3, 12 H, CH(C*H*$_3$)$_2$], 5.62 [septet, $^1J_{H-H}$ = 7.0, 2 H, C*H*(CH$_3$)$_2$], 7.45-7.53 (m, 2 H, aromatic *H*), 8.04-8.11 (m, 2 H, aromatic *H*); ^{13}C δ 20.0 [q, $^1J_{C-H}$ = 128, 4 C, CH(*C*H$_3$)$_2$], 53.6 [d, $^1J_{C-H}$ = 144, 2 C, *C*H(CH$_3$)$_2$], 113.3 (d, $^1J_{C-H}$ = 139, 2 C, aromatic *C*), 124.7 (dd, $^1J_{C-H}$ = 164, $^2J_{C-H}$ = 8, 2 C, aromatic *C*), 131.1 (s, 2 C, aromatic *C*), 151.4 (s, 1 C, *C*=Se). IR data: 3083 (w), 2988 (w), 2936 (w), 2876 (w), 1605 (w), 1473 (w), 1419 (s), 1392 (m), 1375 (w), 1354 (m), 1300 (m), 1244 (w), 1174 (w), 1143 (m), 1134 (w), 1095 (s), 1073 (w), 1026 (w), 973 (w), 936 (w), 890 (w), 847 (w), 821 (w), 751 (s), 743 (vs), 670 (w). Anal. Calcd for $C_{13}H_{18}Br_2HgN_2Se$: C, 24.3; H, 2.8; N, 4.4. Found: C, 24.9; H, 2.7; N, 4.4%.

3.9.3 Synthesis of (iPr_2bimSe)HgI_2

A stirred suspension of HgI_2 (0.121 g, 0.266 mmol) in ethanol (3 mL) was treated with a solution of iPr_2bimSe (0.075 g, 0.267 mmol) in the same solvent (7 mL), resulting in the formation, within 1 minute, of a pale yellow solid suspended in a colorless solution.

After stirring for 20 h, the suspension was concentrated under reduced pressure to *ca.* 3 mL, treated with diethyl ether (10 mL), and the product was isolated by filtration and dried *in vacuo* for 4 h (0.166 g, 85%). Mp = 247-249 °C (dec.). NMR data (in d_6-DMSO): ^{1}H δ 1.66 [d, $^{1}J_{H-H}$ = 7.1, 12 H, CH(C*H*$_3$)$_2$], 5.62 [septet, $^{1}J_{H-H}$ = 7.0, 2 H, C*H*(CH$_3$)$_2$], 7.42-7.52 (m, 2 H, aromatic *H*), 8.01-8.10 (m, 2 H, aromatic *H*); ^{13}C δ 20.4 [q, $^{1}J_{C-H}$ = 129, 4 C, CH(*C*H$_3$)$_2$], 53.5 [d, $^{1}J_{C-H}$ = 141, 2 C, *C*H(CH$_3$)$_2$], 114.0 (d, $^{1}J_{C-H}$ = 167, 2 C, aromatic *C*), 124.7 (dd, $^{1}J_{C-H}$ = 164, $^{2}J_{C-H}$ = 7, 2 C, aromatic *C*), 131.2 (s, 2 C, aromatic *C*), 152.8 (s, 1 C, *C*=Se). IR data: 2977 (w), 2932 (w), 1471 (w), 1408 (s), 1389 (w), 1373 (w), 1353 (m), 1302 (m), 1175 (w), 1142 (m), 1134 (w), 1093 (s), 1071 (w), 1023 (w), 933 (w), 889 (w), 881 (w), 739 (vs), 695 (w), 677 (w). Anal. Calcd for $C_{13}H_{18}HgI_2N_2Se$: C, 21.2; H, 2.5; N, 3.8. Found: C, 21.1; H, 2.4; N, 3.8%.

3.9.4 Synthesis of (iPr$_2$bimSe)$_2$HgCl$_2$

A stirred suspension of $HgCl_2$ (0.035 g, 0.129 mmol) in methanol (3 mL) was treated with a solution of iPr$_2$bimSe (0.076 g, 0.270 mmol) in the same solvent (7 mL), resulting in the immediate formation of a white solid suspended in a colorless solution. After stirring for 24 h, the suspension was concentrated under reduced pressure to *ca.* 3 mL, treated with diethyl ether (10 mL), and the product was isolated by filtration and dried *in vacuo* for 21 h (0.055 g, 52%). Mp = 228-230 °C (dec.). NMR data (in d_6-DMSO): ^{1}H δ 1.61 [d, $^{1}J_{H-H}$ = 7.3, 24 H, CH(C*H*$_3$)$_2$], 5.66 [septet, $^{1}J_{H-H}$ = 7.1, 4 H, C*H*(CH$_3$)$_2$], 7.36-7.47 (m, 4 H, aromatic *H*), 7.94-7.85 (m, 4 H, aromatic *H*); ^{13}C δ 19.8 [q, $^{1}J_{C-H}$ = 128, 8 C, CH(*C*H$_3$)$_2$], 53.0 [d, $^{1}J_{C-H}$ = 140, 4 C, *C*H(CH$_3$)$_2$], 113.4 (d, $^{1}J_{C-H}$ = 166, 4 C, aromatic *C*), 124.1 (dd, $^{1}J_{C-H}$ = 163, $^{2}J_{C-H}$ = 7, 4 C, aromatic *C*), 131.1 (s, 4 C, aromatic *C*), 154.5 (s, 2 C, *C*=Se). IR data: 2981 (w), 2969 (w), 2957 (w), 2937 (w), 2871 (w), 1602 (w), 1473 (m), 1443 (w), 1415 (m), 1397 (m), 1368 (w), 1347 (m), 1326 (m), 1310

(m), 1166 (w), 1139 (m), 1094 (s), 1072 (m), 1024 (w), 936 (w), 892 (w), 854 (w), 748 (vs), 674 (w), 650 (m). Anal. Calcd for $C_{26}H_{36}Cl_2HgN_4Se_2$: C, 37.4; H, 4.4; N, 6.7. Found: C, 36.9; H, 4.4; N, 6.6%.

3.9.5 Synthesis of $(iPr_2bimSe)_2HgBr_2$

A stirred suspension of $HgBr_2$ (0.044 g, 0.122 mmol) in acetonitrile (3 mL) was treated with a solution of iPr_2bimSe (0.075 g, 0.267 mmol) in the same solvent (7 mL), resulting in the formation, within 1 minute, of a white solid suspended in a colorless solution. After stirring for 25 h, the suspension was concentrated under reduced pressure to *ca.* 3 mL, treated with diethyl ether (10 mL), and the product was isolated by filtration and dried *in vacuo* for 24 h (0.053 g, 49%). Mp = 232-234 °C (dec.). NMR data (in d_6-DMSO): ^{1}H δ 2.17 [d, $^1J_{H-H}$ = 7.1, 24 H, CH(C*H*$_3$)$_2$], 6.31 [septet, $^1J_{H-H}$ = 7.0, 4 H, C*H*(CH$_3$)$_2$], 7.84-7.92 (m, 4 H, aromatic *H*), 8.38-8.46 (m, 4 H, aromatic *H*); ^{13}C δ 19.9 [q, $^1J_{C-H}$ = 128, 8 C, CH(*C*H$_3$)$_2$], 52.9 [d, $^1J_{C-H}$ = 140, 4 C, *C*H(CH$_3$)$_2$], 113.3 (d, $^1J_{C-H}$ = 164, 4 C, aromatic *C*), 124.0 (dd, $^1J_{C-H}$ = 164, $^2J_{C-H}$ = 7, 4 C, aromatic *C*), 131.1 (s, 4 C, aromatic *C*), 155.5 (s, 2 C, *C*=Se). IR data: 2979 (w), 2935 (w), 1471 (w), 1455 (w), 1403 (s), 1375 (w), 1348 (m), 1328 (m), 1304 (m), 1173 (w), 1144 (m), 1095 (s), 1073 (w), 1024 (w), 975 (w), 936 (w), 891 (w), 850 (w), 819 (w), 747 (vs), 738 (w), 675 (w), 653 (m). Anal. Calcd for $C_{26}H_{36}Br_2HgN_4Se_2$: C, 33.8; H, 3.9; N, 6.1. Found: C, 33.6; H, 3.7; N, 6.0%.

3.9.6 Synthesis of $(iPr_2bimSe)_2HgI_2$

A stirred suspension of HgI_2 (0.053 g, 0.117 mmol) in acetonitrile (3 mL) was treated with a solution of iPr_2bimSe (0.075 g, 0.267 mmol) in the same solvent (7 mL), resulting in the formation, within 1 minute, of a pale yellow solid suspended in a colorless solution. After stirring for 25 h, the suspension was concentrated under reduced pressure

to *ca.* 3 mL, treated with diethyl ether (10 mL), and the product was isolated by filtration and dried *in vacuo* for 24 h (0.075 g, 63%). Mp = 247-249 °C (dec.). NMR data (in d_6-DMSO): ^{1}H δ 1.61 [d, $^{1}J_{H-H}$ = 7.1, 24 H, CH(C*H*$_3$)$_2$], 5.67 [septet, $^{1}J_{H-H}$ = 5.7, 4 H, C*H*(CH$_3$)$_2$], 7.34-7.44 (m, 4 H, aromatic *H*), 7.90-8.00 (m, 4 H, aromatic *H*); ^{13}C δ 20.0 [q, $^{1}J_{C-H}$ = 126, 8 C, CH(*C*H$_3$)$_2$], 52.6 [d, $^{1}J_{C-H}$ = 144, 4 C, *C*H(CH$_3$)$_2$], 113.0 (d, $^{1}J_{C-H}$ = 163, 4 C, aromatic *C*), 123.8 (dd, $^{1}J_{C-H}$ = 163, $^{2}J_{C-H}$ = 7, 4 C, aromatic *C*), 131.2 (s, 4 C, aromatic *C*), 157.6 (s, 2 C, *C*=Se). IR data: 2975 (w), 2935 (w), 2874 (w), 1471 (m), 1404 (s), 1390 (m), 1374 (m), 1344 (m), 1327 (w), 1302 (m), 1259 (m), 1175 (w), 1142 (m), 1095 (s), 1072 (w), 1044 (w), 1021 (m), 933 (w), 892 (w), 880 (w), 869 (w), 852 (w), 799 (m), 738 (vs), 650 (m). Anal. Calcd for $C_{26}H_{36}HgI_2N_4Se_2$: C, 30.7; H, 3.6; N, 5.5. Found: C, 30.6; H, 3.5; N, 5.4%.

3.10 Synthesis of (iPr$_2$bimS)$_2$CuX

3.10.1 Synthesis of (iPr$_2$bimS)$_2$CuCl

Under a nitrogen atmosphere, a stirred suspension of copper(I) chloride (0.048 g, 0.485 mmol) in acetonitrile (4 mL) was treated with a solution of iPr$_2$bimS (0.264 g, 1.126 mmol) in the same solvent (6 mL). The ensuing yellow suspension was stirred for 18 h, concentrated under reduced pressure to *ca.* 3 mL, treated with diethyl ether (10 mL), and the yellow product was isolated by filtration and dried *in vacuo* for 23 h (0.220 g, 76%). Mp = 162-164 °C (dec.). NMR data (in d_6-DMSO): ^{1}H δ 1.51 [d, $^{3}J_{H-H}$ = 7.8, 24 H, CH(C*H*$_3$)$_2$], 5.57 [septet, $^{3}J_{H-H}$ = 6.7, 4 H, C*H*(CH$_3$)$_2$], 7.20-7.26 (m, 4 H, aromatic *H*), 7.66-7.73 (m, 4 H, aromatic *H*); ^{13}C δ 19.4 [q, $^{1}J_{C-H}$ = 127, 8 C, CH(*C*H$_3$)$_2$], 48.9 [d, $^{1}J_{C-H}$ = 143, 4 C, *C*H(CH$_3$)$_2$], 111.4 (d, $^{1}J_{C-H}$ = 166, 4 C, aromatic *C*), 122.4 (dd, $^{1}J_{C-H}$ = 161, $^{2}J_{C-H}$ = 7, 4 C, aromatic *C*), 130.1 (s, 4 C, pyridine *C*), 166.1 (s, 2 C, *C*=S) . IR data: 3075 (w), 2979 (w), 2938 (w), 1596 (w), 1474 (m), 1417 (m), 1387 (s), 1340 (s), 1317

(s), 1296 (w), 1175 (w), 1160 (m), 1141 (s), 1132 (s), 1092 (s), 1023 (w), 930 (w), 889 (w), 847 (w), 744 (vs), 659 (s). Anal. Calcd for $C_{26}H_{36}ClCuN_4S_2$: C, 55.0; H, 6.4; N, 9.9. Found: C, 54.8; H, 6.6; N, 9.7%.

3.10.2 Synthesis of $(iPr_2bimS)_2CuBr$

Under a nitrogen atmosphere, a stirred suspension of $CuBr{\cdot}SMe_2$ (0.050 g, 0.243 mmol) in acetonitrile (4 mL) was treated with a solution of iPr_2bimS (0.123 g, 0.511 mmol) in the same solvent (6 mL). The ensuing white suspension was stirred for 3 h, concentrated under reduced pressure to *ca.* 2 mL, treated with diethyl ether (10 mL), and the product was isolated by filtration and dried *in vacuo* for 24 h (0.089 g, 60%). Mp = 202-204 °C (dec.). NMR data (in d_6-DMSO): ^{1}H δ 1.53 [d, $^3J_{H\text{-}H}$ = 7.1, 24 H, CH(C*H*$_3$)$_2$], 5.59 [septet, $^3J_{H\text{-}H}$ = 7.0, 4 H, C*H*(CH$_3$)$_2$], 7.23-7.31 (m, 4 H, aromatic *H*), 7.71-7.79 (m, 4 H, aromatic *H*); ^{13}C δ 19.5 [q, $^1J_{C\text{-}H}$ = 128, 8 C, CH(*C*H$_3$)$_2$], 49.4 [d, $^1J_{C\text{-}H}$ = 142, 4 C, *C*H(CH$_3$)$_2$], 111.8 (d, $^1J_{C\text{-}H}$ = 163, 4 C, aromatic *C*), 122.8 (dd, $^1J_{C\text{-}H}$ = 163, $^2J_{C\text{-}H}$ = 7, 4 C, aromatic *C*), 130.1 (s, 4 C, pyridine *C*), 164.0 (s, 2 C, *C*=S). IR data: 2970 (w), 2938 (w), 2872 (w), 1474 (s), 1417 (m), 1388 (s), 1375 (w), 1341 (vs), 1321 (s), 1296 (w), 1173 (w), 1161 (m), 1142 (s), 1134 (sh), 1093 (s), 1081 (w), 1023 (w), 931 (w), 892 (w), 846 (w), 744 (vs), 682 (w), 659 (s). Anal. Calcd for $C_{26}H_{36}BrCuN_4S_2$: C, 51.0; H, 5.9; N, 9.2. Found: C, 50.8; H, 5.8; N, 9.2%.

3.10.3 Synthesis of $(iPr_2bimS)_2CuI$

Under a nitrogen atmosphere, a stirred suspension of copper(I) iodide (0.072 g, 0.380 mmol) in acetonitrile (5 mL) was treated with a solution of iPr_2bimS (0.205 g, 0.875 mmol) in the same solvent (5 mL), resulting in the formation of a yellow solution and, within 1 min, a yellow solid. After stirring for 4 h, the suspension was concentrated under reduced pressure to *ca.* 3 mL, treated with diethyl ether (10 mL), and the product

was isolated by filtration and dried *in vacuo* for 21 h (0.189 g, 75%). Mp = 173-175 °C (dec.). NMR data (in CD_3CN): ^1H δ 1.56 [d, $^3J_{H-H}$ = 7.1, 24 H, $CH(CH_3)_2$], 5.69 [septet, $^3J_{H-H}$ = 7.1, 4 H, $CH(CH_3)_2$], 7.19-7.27 (m, 4 H, aromatic *H*), 7.56-7.63 (m, 4 H, aromatic *H*); ^{13}C δ 20.0 [q, $^1J_{C-H}$ = 133, 8 C, $CH(CH_3)_2$], 50.4 [d, $^1J_{C-H}$ = 148, 4 C, $CH(CH_3)_2$], 112.4 (d, $^1J_{C-H}$ = 142, 4 C, aromatic *C*), 123.2 (dd, $^1J_{C-H}$ = 162, $^2J_{C-H}$ = 8, 4 C, aromatic *C*), 131.8 (s, 4 C, pyridine *C*), 168.2 (s, 2 C, *C*=S). IR data: 3068 (w), 3051 (w), 2975 (w), 2935 (w), 2873 (w), 1597 (w), 1474 (m), 1416 (m), 1407 (w), 1387 (s), 1373 (w), 1342 (s), 1318 (s), 1296 (m), 1173 (w), 1161 (m), 1141 (s), 1093 (s), 1081 (m), 1023 (w), 930 (w), 892 (w), 847 (w), 743 (vs), 683 (w), 661 (s). Anal. Calcd for $C_{26}H_{36}N_4S_2CuI$: C, 47.4; H, 5.5; N, 8.5. Found: C, 47.3; H, 5.6; N, 8.5%.

3.11 Synthesis of $(iPr_2bimSe)_2CuX$

3.11.1 Synthesis of $(iPr_2bimSe)_2CuCl$

Under a nitrogen atmosphere, a stirred suspension of CuCl (0.012 g, 0.121 mmol) in tetrahydrofuran (4 mL) was treated with a solution of iPr_2bimSe (0.075 g, 0.266 mmol) in the same solvent (6 mL), resulting in the formation of a pale blue solution. After stirring for 24 h, the solution was concentrated under reduced pressure to *ca.* 1 mL and treated with diethyl ether (10 mL), leading to the separation of the off-white product, which was isolated by filtration and dried *in vacuo* for 21 h (0.054 g, 61%). Mp = 178-180 °C (dec.). NMR data (in d_6-DMSO): ^1H δ 1.53 [d, $^3J_{H-H}$ = 7.4, 24 H, $CH(CH_3)_2$], 5.74 [septet, $^3J_{H-H}$ = 7.0, 4 H, $CH(CH_3)_2$], 7.21-7.30 (m, 4 H, aromatic *H*), 7.73-7.82 (m, 4 H, aromatic *H*); ^{13}C δ 19.5 [q, $^1J_{C-H}$ = 127, 8 C, $CH(CH_3)_2$], 51.9 [d, $^1J_{C-H}$ = 139, 4 C, $CH(CH_3)_2$], 112.3 (d, $^1J_{C-H}$ = 165, 4 C, aromatic *C*), 123.1 (dd, $^1J_{C-H}$ = 163, $^2J_{C-H}$ = 6 , 4 C, aromatic *C*), 131.2 (s, 4 C, aromatic *C*), 161.2 (s, 2 C, *C*=Se). IR data: 2975 (w), 2954 (w), 2937 (w), 2923 (w), 2870 (w), 1593 (w), 1474 (m), 1414 (m), 1396 (s), 1385 (sh),

1374 (w), 1339 (s), 1322 (w), 1309 (vs), 1296 (sh), 1229 (w), 1216 (w), 1174 (w), 1162 (w), 1141 (s), 1134 (sh), 1092 (s), 1070 (m), 1023 (w), 972 (w), 931 (w), 889 (w), 850 (w), 823 (w), 746 (vs), 736 (s), 672 (w), 650 (s). Anal. Calcd for $C_{26}H_{36}ClCuN_4Se_2$: C, 47.2; H, 5.5; N, 8.5. Found: C, 46.9; H, 5.5; N, 8.4%.

3.11.2 Synthesis of $(iPr_2bimSe)_2CuBr$

Under a nitrogen atmosphere, a stirred suspension of $CuBr{\cdot}SMe_2$ (0.050 g, 0.243 mmol) in acetonitrile (4 mL) was treated with a solution of iPr_2bimSe (0.144 g, 0.511 mmol) in the same solvent (6 mL). The ensuing white suspension was stirred for 3 h, concentrated under reduced pressure to *ca.* 2 mL, treated with diethyl ether (10 mL), and the product was isolated by filtration and dried *in vacuo* for 22 h (0.106 g, 70%). Mp = 216-218 °C (dec.). NMR data (in d_6-DMSO): ^{1}H δ 1.55 [d, $^3J_{H\text{-}H}$ = 6.9, 24 H, CH(C*H*$_3$)$_2$], 5.74 [septet, $^3J_{H\text{-}H}$ = 7.1, 4 H, C*H*(CH$_3$)$_2$], 7.27-7.33 (m, 4 H, aromatic *H*), 7.80-7.87 (m, 4 H, aromatic *H*); ^{13}C δ 19.5 [q, $^1J_{C\text{-}H}$ = 127, 8 C, CH(*C*H$_3$)$_2$], 51.7 [d, $^1J_{C\text{-}H}$ = 142, 4 C, *C*H(CH$_3$)$_2$], 112.2 (d, $^1J_{C\text{-}H}$ = 168, 4 C, aromatic *C*), 123.0 (d, $^1J_{C\text{-}H}$ = 163, 4 C, aromatic *C*), 131.1 (s, 4 C, pyridine *C*), *C*=Se peak not observed. IR data: 2976 (w), 2937 (w), 2875 (w), 1473 (m), 1414 (s), 1399 (s), 1387 (sh), 1373 (w), 1348 (m), 1341 (m), 1325 (w), 1310 (s), 1297 (sh), 1174 (w), 1165 (w), 1143 (s), 1094 (s), 1073 (w), 1022 (w), 975 (w), 933 (w), 893 (w), 844 (w), 814 (w), 746 (vs), 738 (m), 674 (w), 650 (m). Anal. Calcd for $C_{26}H_{36}BrCuN_4Se_2$: C, 44.2; H, 5.1; N, 7.9. Found: C, 43.7; H, 5.0; N, 7.9%.

3.11.3 Synthesis of $(iPr_2bimSe)_2CuI$

Under a nitrogen atmosphere, a stirred suspension of CuI (0.025 g, 0.131 mmol) in tetrahydrofuran (4 mL) was treated with a solution of iPr_2bimSe (0.076 g, 0.270 mmol) in the same solvent (6 mL), resulting in the formation of a yellow solution. After stirring for 24 h, the solution was concentrated under reduced pressure to *ca.* 1 mL and treated

with diethyl ether (10 mL), leading to the separation of the pale yellow product, which was isolated by filtration and dried *in vacuo* for 22 h (0.054 g, 56%). Mp = 208-210 °C (dec.). NMR data (in d_6-DMSO): ^{1}H δ 1.56 [d, $^3J_{H-H}$ = 7.3, 24 H, CH(C*H*$_3$)$_2$], 5.74 [septet, $^3J_{H-H}$ = 6.9, 4 H, C*H*(CH$_3$)$_2$], 7.25-7.36 (m, 4 H, aromatic *H*), 7.79-7.90 (m, 4 H, aromatic *H*); ^{13}C δ 19.6 [q, $^1J_{C-H}$ = 126, 8 C, CH(*C*H$_3$)$_2$], 51.8 [d, $^1J_{C-H}$ = 145, 4 C, *C*H(CH$_3$)$_2$], 112.2 (d, $^1J_{C-H}$ = 166, 4 C, aromatic *C*), 123.0 (dd, $^1J_{C-H}$ = 163, $^2J_{C-H}$ = 7 , 4 C, aromatic *C*), 131.2 (s, 4 C, pyridine *C*), 161.2 (s, 4 C, pyridine *C*). IR data: 3078 (w), 2982 (w), 2938 (w), 2871 (w), 1603 (w), 1474 (m), 1445 (w), 1416 (m), 1397 (m), 1368 (w), 1348 (m), 1326 (w), 1311 (s), 1166 (w), 1140 (m), 1095 (s), 1072 (w), 1095 (w), 937 (w), 893 (w), 855 (w), 748 (vs), 737 (w), 674 (w), 650 (m). Anal. Calcd for $C_{26}H_{36}CuIN_4Se_2$: C, 41.5; H, 4.8; N, 7.4. Found: C, 41.4; H, 4.8; N, 7.7%.

3.12 Synthesis of (R_2bimE)AuX

3.12.1 Synthesis of (Me_2bimS)AuCl

Under a nitrogen atmosphere, toluene (10 mL) was added to a mixture of (tht)AuCl (0.129 g, 0.402 mmol) and Me_2bimS (0.075 g, 0.421 mmol), resulting in the immediate formation of a white solid and a colorless solution. The suspension was stirred for 2 h, concentrated under reduced pressure to *ca.* 3 mL, treated with pentane (10 mL), and the product was isolated by filtration and dried *in vacuo* for 7 h (0.112 g, 67%). Mp = 160-162 °C (dec.). NMR data (in d_6-DMSO): ^{1}H δ 4.03 (s, 6 H, C*H*$_3$), 7.48-7.53 (m, 2 H, aromatic *H*), 7.76-7.80 (m, 2 H, aromatic *H*); ^{13}C δ 32.5 (q, $^1J_{C-H}$ = 139, 2 C, *C*H$_3$), 111.6 (d, $^1J_{C-H}$ = 167, 2 C, aromatic *C*), 124.9 (d, $^1J_{C-H}$ = 164, 2 C, aromatic *C*), 131.9 (s, 2 C, aromatic *C*), C=S peak not observed. IR data: 3105 (w), 3053 (w), 3032 (w), 2939 (w), 1591 (w), 1574 (w), 1492 (w), 1468 (s), 1461 (sh), 1435 (s), 1388 (s), 1369 (m), 1345 (s), 1258 (m), 1184 (w), 1153 (w), 1131 (w), 1105 (m), 1020 (m), 1012 (w), 974

(w), 933 (m), 877 (w), 848 (w), 822 (w), 805 (m), 705 (vs), 671 (w), 654 (m). Anal. Calc. for $C_9H_{10}AuClN_2S$: C, 26.3; H, 2.5; N, 6.8%. Found: C, 26.1; H, 2.4; N, 6.8%.

3.12.2 Synthesis of (iPr_2bimS)AuCl

Under a nitrogen atmosphere, toluene (10 mL) was added to a mixture of (tht)AuCl (0.098 g, 0.305 mmol) and iPr_2bimS (0.076 g, 0.324 mmol), resulting in the formation of a white solid and a pale yellow solution. The suspension was stirred for 2 h and the product was isolated by filtration, washed with pentane (2 x 3 mL), and dried *in vacuo* for 6 h (0.086 g, 60%). Mp = 180-183 °C (dec.). NMR data (in d_6-DMSO): ^{1}H δ 1.64 [d, $^3J_{H-H}$ = 6.9, 12 H, CH(C*H*$_3$)$_2$], 5.68 [septet, $^3J_{H-H}$ = 6.9, 2 H, C*H*(CH$_3$)$_2$], 7.46-7.51 (m, 2 H, aromatic *H*), 8.02-8.07 (m, 2 H, aromatic *H*); ^{13}C δ 19.6 [q, $^1J_{C-H}$ = 128, 4 C, CH(*C*H$_3$)$_2$], 51.3 [d, $^1J_{C-H}$ = 141, 2 C, *C*H(CH$_3$)$_2$], 113.8 (d, $^1J_{C-H}$ = 168, 2 C, aromatic *C*), 124.8 (dd, $^1J_{C-H}$ = 163, $^2J_{C-H}$ = 6, 2 C, aromatic *C*), 130.1 (s, 2 C, aromatic *C*), 154.7 (s, 1 C, *C*=S). IR data: 3104 (w), 3073 (w), 3054 (w), 3032 (w), 2977 (w), 2938 (w), 2872 (w), 1591 (w), 1467 (w), 1445 (m), 1419 (s), 1405 (m), 1386 (m), 1373 (m), 1360 (m), 1319 (m), 1303 (m), 1235 (w), 1174 (w), 1161 (w), 1145 (m), 1134 (m), 1104 (m), 1099 (m), 1081 (w), 1022 (w), 978 (w), 940 (w), 886 (w), 844 (w), 802 (w), 737 (vs), 692 (w), 669 (w), 659 (m). Anal. Calcd for $C_{13}H_{18}AuClN_2S$: C, 33.5; H, 3.9; N, 6.0. Found: C, 33.2; H, 3.8; N, 5.9%.

3.12.3 Synthesis of (iPr_2bimSe)AuCl

Under a nitrogen atmosphere, toluene (10 mL) was added to a mixture of (tht)AuCl (0.081 g, 0.253 mmol) and iPr_2bimSe (0.074 g, 0.263 mmol), resulting in the formation of an off-white solid and a pale orange solution. The suspension was stirred for 2 h and the product was isolated by filtration, washed with pentane (5 mL), and dried *in vacuo* for 5 h (0.084 g, 64%). Mp = 238-240 °C (dec.). NMR data (in d_6-DMSO): ^{1}H δ 1.63 [d,

$^{3}J_{H\text{-}H}$ = 7.1, 12 H, CH(C*H*$_3$)$_2$], 5.72 [septet, $^{3}J_{H\text{-}H}$ = 7.0, 2 H, C*H*(CH$_3$)$_2$], 7.46-7.58 (m, 2 H, aromatic *H*), 8.02-8.16 (m, 2 H, aromatic *H*); ^{13}C δ 19.6 [q, $^{1}J_{C\text{-}H}$ = 128, 4 C, CH(*C*H$_3$)$_2$], 53.5 [d, $^{1}J_{C\text{-}H}$ = 139, 2 C, *C*H(CH$_3$)$_2$], 114.1 (d, $^{1}J_{C\text{-}H}$ = 165, 2 C, aromatic *C*), 125.0 (dd, $^{1}J_{C\text{-}H}$ = 164, $^{2}J_{C\text{-}H}$ = 6, 2 C, aromatic *C*), 130.9 (s, 2 C, aromatic *C*), 147.7 (s, 1 C, *C*=Se). IR data: 2977 (w), 2938 (w), 2879 (w), 1471 (w), 1464 (w), 1412 (m), 1389 (w), 1372 (w), 1359 (m), 1306 (m), 1173 (w), 1147 (m), 1095 (m), 1020 (w), 926 (w), 892 (w), 819 (w), 741 (vs), 675 (w). Anal. Calcd for $C_{13}H_{18}AuClN_2Se$: C, 30.4; H, 3.5; N, 5.5. Found: C, 30.4; H, 3.4; N, 5.5%.

3.13 Cytotoxicity Measurements

Viability assays of the HeLa cells in the presence and absence of iPr$_2$bimS and (iPr$_2$bimS)$_2$CuCl were studied by Guava ViaCount assay (Guava Technologies, Inc.). HeLa cells were first seeded in ninety-six-well plates with a density of 1 x 10^4 cells/mL in 3 mL of D-10 medium (Dulbecco Modified Eagle's Medium plus horse serum, L-alanyl-L-glutamine, gentamicin sulfate, and penicillin–streptomycin solution), and set in an incubator at 37 °C in a 5% CO_2 atmosphere for 24 h. The media of the wells was then replaced with freshly prepared D-10 media containing different concentrations of iPr$_2$bimS and (iPr$_2$bimS)$_2$CuCl ranging from 0 to 20 mg/mL, and the wells were set back into the incubator at 37 °C and 5% CO_2 for 2 days. The plates were then removed from the incubator, the media of each well was discarded, each well was washed with phosphate saline buffer (PBS) and the cells were trypsinized, centrifuged, and re-suspended in D-10 medium. The cells in the re-suspended media were then counted using a Bright-Line hemocytometer and their viability was determined by the Guava ViaCount cytometry assay.

CHAPTER 4: CONCLUSIONS

4.1 Conclusions

In summary, the coordination chemistry of heterocyclic sulfur- and selenium-containing compounds has been a very attractive area of study for the last three decades. Due to their applications arising from the relevance of these compounds to biological systems, their coordination chemistry with heavy metals is attractive. Within this field of research, we have been engaged in the investigation of molecular architectures realized by thione-ligated mercury(II), copper(I), and gold(I) complexes aiming to gain insight into the interplay between the ligand's characteristic and the structural diversity observed. The new iPr_2bimS ligand has been prepared and syntheses of the R_2bimE (R = Me, E = S; R = ^{i}Pr, E = Se) ligands has successfully been optimized. The three ligands are air-stable, exhibit good solubility in a wide variety of organic solvents, thus making them convenient candidates for coordination chemistry studies.

The coordination chemistry of the iPr_2bimS ligand with mercury(II), copper(I), and gold(I) has been established, creating the first metal complexes of the R_2bimE ligands. A total of 18 new complexes of the mercury halides, $LHgX_2$ and L_2HgX_2 (L = Me_2bimS, iPr_2bimS, iPr_2bimSe; X = Cl, Br, I), have been prepared and fully characterized by elemental analysis, NMR and IR spectroscopies, and some by ESI-MS and X-ray crystal diffraction. Complexes of Me_2bimS show slightly higher solubilites in organic solvents than the free ligand and tend to favor the formation of extended

structures in the solid state more than those of iPr_2bimE (E = S, Se), a likely effect of the less bulky Me substituent. Moreover, the thione and selone complexes, $(iPr_2bimE)_nHgX_2$ (n = 1,2; E = S, Se; X = Cl, Br, I), do not show significant solubility or structural differences when comparing the two donor atoms. The enhanced mercury affinity for selenium, selenophilicity, over its affinity for sulfur, thiophilicity, of the Hg(II) complexes was confirmed through a series of small scale reactions monitored by ^1H NMR spectroscopy and ESI-MS.

The dihalogen derivatives $(R_2bimE)I_2$ (R = Me, E = S; R = ^{i}Pr, E = S, Se) were made by treatment of the respective N-heterocyclic thione and selone ligands with elemental iodine. Moreover, the bromide and chloride derivatives of $(iPr_2bimSe)X_2$ (X = Br, Cl) were successfully synthesized by treatment of the ligand with Br_2 or $SOCl_2$. Utilization of $SOCl_2$ optimizes the synthesis of the dichloride derivative as it is less toxic and easier to handle than Cl_2 gas or SO_2Cl_2 employed in similar reactions. The R_2bimE (R = Me, E = S; R = ^{i}Pr; E = S, Se) ligands formed charge-transfer derivatives upon complexation with I_2. Crystal structures of their bromide and chloride complexes exhibit a T-shaped geometry around the chalcogen donor indicative of oxidative-addition products previously reported by Devillanova and Singh.

The coordination chemistry studies of the three ligands towards copper(I) and gold(I) was also explored. A total of six new compounds of copper(I) $(iPr_2bimE)_2CuX$ (E = S, Se; X = Cl, Br, I) were prepared and fully characterized. All of these complexes depict a three-coordinate geometry around the copper center. Although three-coordinate copper(I) complexes have been reported in the literature, their occurrence is relatively

rare in comparison to four-coordinate complexes. Similar three-coordinate copper(I) complexes are precedented.[101b, 119] Syntheses of the $(Me_2bimE)_2CuX$ complexes (X = Cl, Br, I) were not feasible as the methyl substituents were not effective in sterically stabilizing the copper(I) species. Furthermore, all three $(R_2bimE)AuCl$ complexes (R = Me, E = S; R = iPr, E = S, Se) have been successfully synthesized and characterized by a combination of different analytical and spectroscopic methods. Crystal structures of the $(iPr_2bimS)AuCl$ depict a linear geometry around the metal center.

Preliminary biological activity of the $(iPr_2bimS)_2CuCl$ complex against HeLa cervical cancer cells did not show any anticancer activity. Further biological studies at higher concentrations against HeLa and other different cell lines such as breast or colon is needed to continue the cytotoxicity assessment of these new complexes. Moreover, the $(Me_2bimE)_2AuCl$ can also be tested as molecular linear Au(I) complexes have been reported to depict antitumor activity.[120, 121]

4.2 Future Work

The straightforward and short synthetic procedure for the preparation of the R_2bimE ligands (R = Me, E = S; R = iPr, E = S, Se), along with their stability in air and solubility in a variety of organic solvents make them useful ligands for future coordination studies.

Reactivity studies of R_2bimE (R = Me, E = S; R = iPr, E = S, Se) with strong acids (HCl, HBr, HBF_4, HPF_6 and $HClO_4$) will show if these N-heterocyclic ligands are stable in acidic environments. Future modifications of the three ligands include changing the thione or selone donor group to a telone functionality. This would increase the 'softness' of the new ligand, which would display different reactivities, which has already

been observed by changing from sulfur to selenium. Moreover, alteration of the methyl and isopropyl substituents on the benzimidazolium nitrogens to symmetric *n*-butyl substituents would increase the solubility of the ligands and complexes in organic solvents.

Additionally, the copper(I) complexes synthesized, $(iPr_2bimE)_2CuX$ (E = S, Se; X = Cl, Br, I), may be used as precursors to generate three coordinate copper(I) hydroxide analogues shown in Scheme 4.1. Although a number of copper hydroxide complexes have been reported, these have been bimetallic or Cu(II) derivatives.[122] It was not until recently, were Nolan and collaborators have reported examples of 14-electron dicoordinate NHC complexes, (NHC)Cu(L)OH (L = two-electron donor).[123] Within this area of chemistry, the versatile reactivity of a Cu-OH moiety associated with the stabilizing properties of an NHT/NHSe ancillary ligand could be explored by utilizing such analogues as precursors to synthesize a wide variety of organocopper complexes, as illustrated in Scheme 4.2. The reactivity of the hydroxide derivatives towards H-C bond activation may be investigated by treating the precursor with nitromethane to generate $(iPr_2bimE)_2CuCH_2NO_2$ (E = S, Se). Activation of the CH_2 moiety of cyclopentadiene may result in the formation of a new three-legged piano-stool complexes. Similarly, activation of an aromatic sp^2 C-H bond may be explored with 1,2,4,5-tetrafluorobenzene. Formation of a Cu-Si bond may be accomplished via the reaction of the hydroxide precursor with $Me_2N\text{-}SiMe_3$ to produce the $(iPr_2bimE)_2CuSiMe_3$ (E = S, Se) complexes. Furthermore, the activation of alcohols may be pursued to yield three coordinate copper(I) methoxide complexes, $(iPr_2bimE)_2CuOR$ (E = S, Se; R = ^{t}Bu, Me).

Scheme 4.1. Proposed Synthesis of Copper(I) Hydroxide Complexes

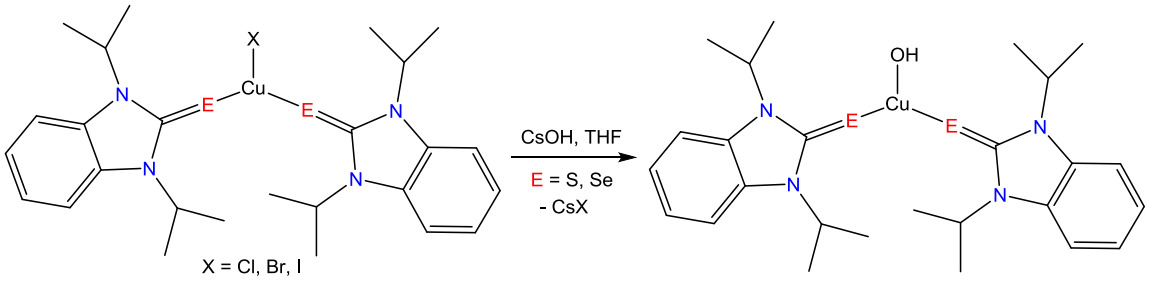

Scheme 4.2. Summary of Proposed Complexes Synthesized Utilizing Copper(I) Hydroxide Complexes

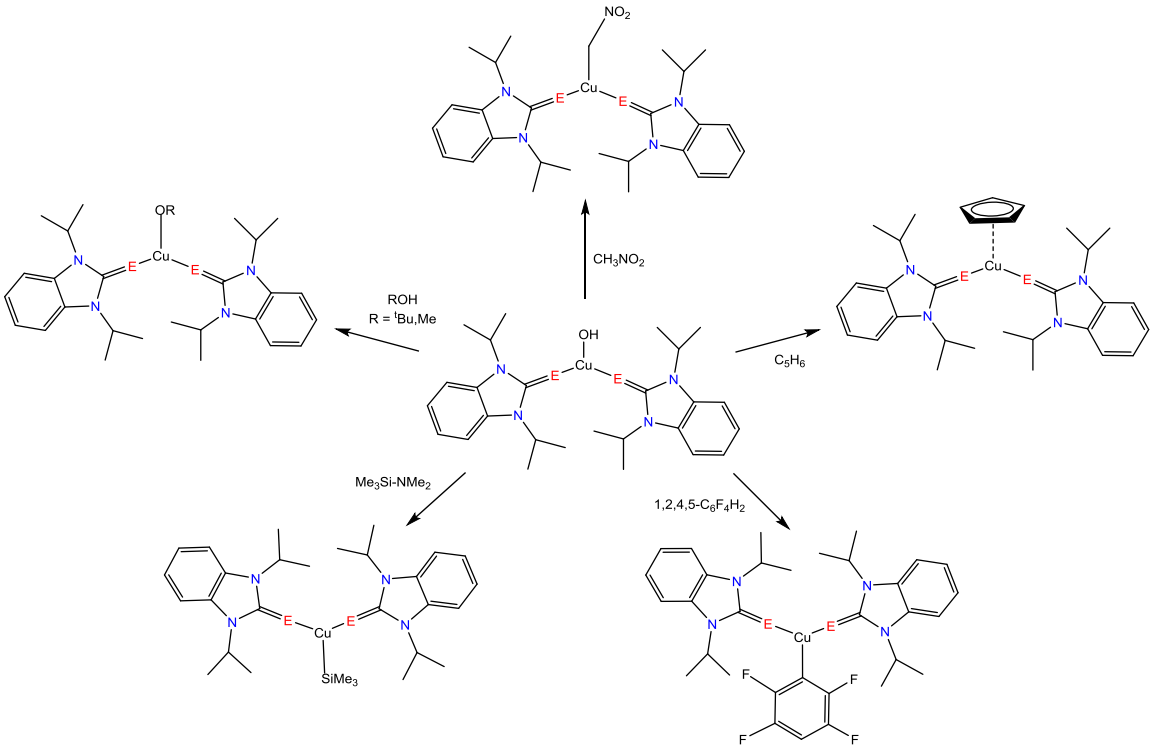

In addition, the copper(I) halide complexes, $(iPr_2bimS)_2CuX$ (X = Cl, Br, I), may also be used as precursors to generate three coordinate copper(I) thiolate mimics of blue Cu proteins. Blue Cu proteins are responsible for biological electron transfer where the copper center exhibits a conserved ligand set that consists of a trigonal planar arrangement around the metal.[109-111] The metal center is thus surrounded by two N-His

imidazolys and one Cys thiolate.[109] We propose synthesizing blue Cu protein mimics via a salt metathesis route where our previously synthesized $(iPr_2bimS)_2CuX$ (X = Cl, Br, I) compounds may be treated with an alkali metal thiolate to produce an alkali metal halide and the desired Cu(I) thiolate depicted in Scheme 4.3.

Scheme 4.3. Proposed Synthesis of Copper(I) Thiolate Complexes

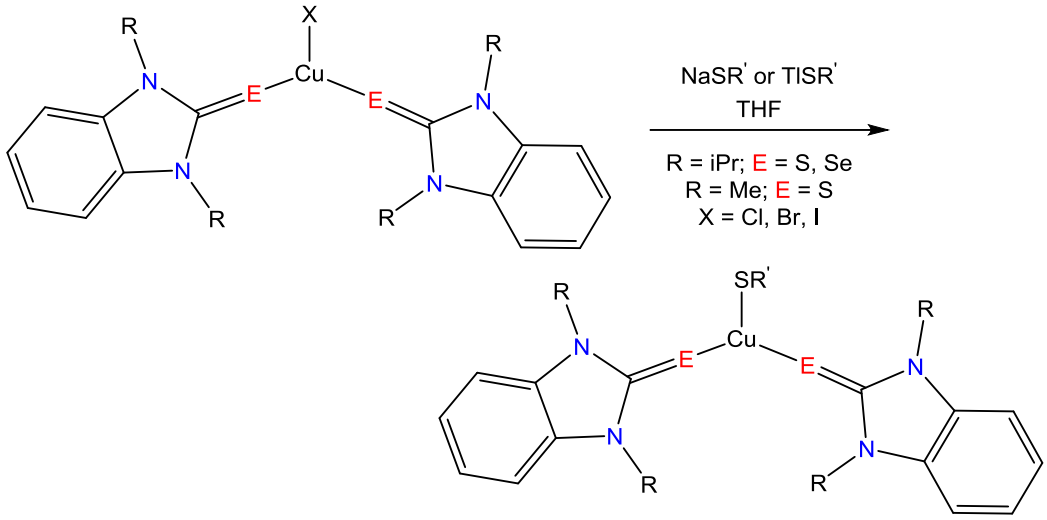

Additionally, coordination chemistry of the R_2bimE ligands (R = Me, E = S; R = iPr, E = S, Se) will be extended to early transition metal centers like chromium, molybdenum, and relatively hard metals like platinum and palladium (Figure 4.1). Group 6 metal carbonyls $(R_2bimE)M(CO)_5$ (M = Cr, Mo W; R = Me, E = S; R = iPr, E = S, Se) may be prepared to further explore the coordination of the ligand through the π-backbonding between the metal and carbon of the carbonyl groups. Other potential metals that can be coordinated include manganese(I) and rhenium(I) to form the corresponding metal carbonyl derivatives, $(R_2bimE)M(CO)_3Br$ (M = Mn, Re; R = Me, E = S; R = iPr, E = S, Se). Such manganese and rhenium complexes of the R_2bimE thiones and selone (R = Me, E = S; R = iPr, E = S, Se) could potentially be utilized as the

photosensitizers and homogenous catalysts for the photochemical reduction of CO_2 to CO.[124, 125] The photosensitizing performance of these Mn(I) and Re(I) complexes may be investigated under visible light irradiation and their photophysical and electrochemical properties can be analyzed via UV/Vis and cyclic voltammetry. Finally, coordination complexes of Ni, Pd, and Pt could potentially be used as anti-cancer agents. Potential structures of all these coordinated complexes are illustrated in Figure 4.1.

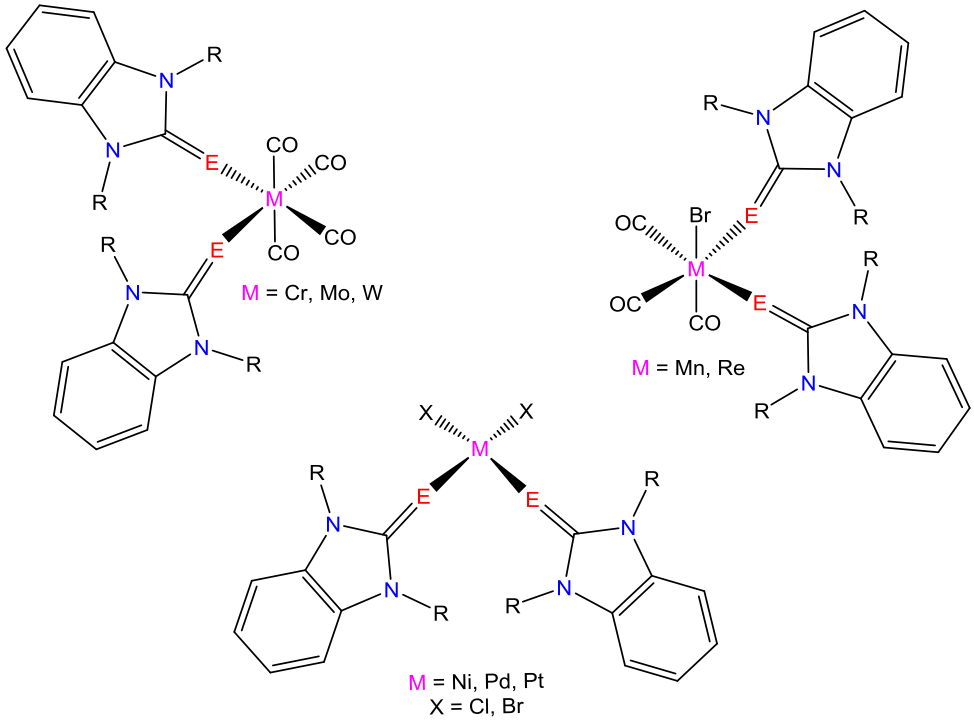

Figure 4.1. Potential structures of R_2bimE complexes (R = Me, E = S; R = iPr, E = S, Se) with other transition metals

REFERENCES

1. *Handbook of Chalcogen Chemistry*; Devillanova, F. A., Ed.; Royal Society of Chemistry: Cambridge, 2007; Chapter 2.3, pp 107-134.

2. Cremlyn, R. J. *An Introduction to Organosulfur Chemistry*; John Wiley & Sons, Inc.: New York, 1996.

3. Maciejewski, A.; Steer, R. P. *Chem. Rev*. **1993**, *93*, 67-98.

4. Serrano-Andres, L.; Pou-Amerigo, R.; Fulscher, M. P.; Borin, A. C. *J. Chem. Phys. A* **2001**, *117*, 1649-1659.

5. Bourissou, D.; Guerret, O.; Gabbaï, F. P.; Bertrand, G. *Chem. Rev.* **2000**, *100*, 39-92.

6. Hopkinson, N. M.; Richter, C.; Schedler, M.; Glorius, F. *Nature* **2014**, *510*, 485-496.

7. Enders, D.; Niemeier, O.; Henseler, A. *Chem. Rev*. **2007**, *107*, 5606-5655.

8. Díez-González, S.; Marion, N.; Nolan, S. P. *Chem Rev.* **2009**, *109*, 3612-3676.

9. Öfele, K. *J. Organomet. Chem*. **1968**, *12*, 42-43.

10. Wanzlick, H.-W. and Schönherr, H. J. *Angew Chem., Int. Ed. Engl*. **1968**, *7*, 141-142.

11. Arduengo, A. J.; Harlow, R. L.; Kline, M. *J. Am. Chem. Soc*. **1991**, *113*, 361-363.

12. Arduengo, A. J.; Dias, H. V. R.; Harlow, R. L.; Kline, M. *J. Am. Chem. Soc*. **1992**, *114*, 5530-5534.

13. Arduengo, A. J.; Bock, H.; Chen, H.; Denk, M.; Dixon, D. A.; Green, J. C.; Herrmann, W. A.; Jones, N. L.; Wagner, M.; West, R. *J. Am. Chem. Soc*. **1994**, *116*, 6641-6649.

14. Arca, M.; Aragoni, C. M.; Devillanova, F. A.; Garau, A.; Isaia, F.; Lippolis, V.; Mancini, A.; Verani, G. *Bioinorg. Chem. Appl*. **2006**, *13*, 1-12.

15. Demartin, F.; Deplano, P.; Devillanova, F. A.; Isaia, F.; Lipolis, V.; Gaetano, V. *Inorg. Chem*. **1993**, *32*, 3694-3702.

16. Crossley, R. I.; Hill, F. A.; Humphrey R. E.; Smith, K. M. *Organometallics* **2006**, *25*, 2242-2253.

17. Jia, W.-G.; Huang, Y.-B.; Lin, Y.-J.; Wang, G.-L.; Jin, G.-X. *Eur. J. Inorg. Chem*. **2008**, 4063-4074.

18. Landry, V. K; Parkin, G. *Polyhedron* **2007**, *26*, 4751-4757.

19. Li, D.; Shi, W. J.; Hou, L. *Inorg. Chem*. **2005**, *44*, 3907-3913.

20. (a) Raper, E. S. *Coord. Chem. Rev*. **1994**, *129*, 91-156. (b) Raper, E. S. *Coord. Chem. Rev*. **1997**, *165*, 475-567.

21. (a) Han, L.; Wu, B.; Xu, Y.; Wu, M.; Gong, Y.; Lou, B.; Chen, B.; Hong, M. *Inorg. Chim. Acta* **2005**, *358*, 2005-2013. (b) Hong, M.; Zhao, Y.; Su, W.; Cao, R.; Fujita, M.; Chan, A. S. C. *Angew. Chem. Int. Ed*. **2000**, *39*, 2468-2470. (c) Lobana, T. S.; Sultana, R.; Castineiras, A.; Butcher, R. J. *Inorg. Chim. Acta* **2009**, *362*, 5265-5270.

22. (a) Majhi, P. K.; Schnakenburg, G.; Steubel, R. *Dalton Trans.* **2014**, *43*, 16673-16679. (b) Stadelman, B. S.; Kimani, M. M.; Bayse, C. A.; McMillen, C. D.; Brumaghim J. L. *Dalton Trans.* **2016**, *45*, 4697-4711. (c) Kimani, M. M.; Watts, D.; Graham, L. A.; Rabinovich, D.; Yap, G. P. A.; Brumaghim, J. L. *Dalton Trans*. **2015**, *44*, 16313-16324. (d) Stadelman, B. S.; Brumaghim, J. L. *Biochalcogen Chemistry: The Biological Chemistry of Sulfur, Selenium, and Tellurium*; ACS Symposium Series; American Chemical Society: Washington, DC, 2013; pp 33-64.

23. (a) Chen, S.; He, B.; Liu, Y.; Wang, Y.; Zhu, J. *Int. J. Electrochem. Sci.* **2014**, *9*, 5400-5408. (b) Ibáñez, S.; Vrečko, D. N.; Estevan, F.; Hirva, P.; Sanaú, M.; Úbeda, M. A. *Dalton Trans*. **2014**, *43*, 2961-2970. (c) Rong, Y.; Palmer, J. H.; Parkin, G. *Dalton Trans.* **2014**, *43*, 1397-1407.

24. (a) Altun, A.; Kuliyev, E.; Aghatabay, N. M. *Spectrochim. Acta Mol. Biomol. Spectrosc.* **2016**, *152*, 181-191. (b) Cherta, L.; Portolés, T.; Pitarch, E.; Beltran, J.; López, F. J.; Calatayud, C.; Company, B.; Hernández, F. *Food Chem*. **2015**, *188*, 301-308. (c) Aslandis, P.; Hatzidimitriou, A. G.; Andreadou, E. G.; Pantazaki, A. A.; Voulgarakis, N. *Mater. Sci. Eng*. **2015**, *50*, 187-193. (d) Evaggelinou, U.; Hatzidimitriou, A. G.; Velali, A.; Pantazaki, A. A.; Voulgarakis, N.; Aslanidis, P. *Polyhedron* **2014**, *72*, 122-129.

25. Oae, S.; Doi, J. C. *Organic sulfur Chemistry: Structure and Mechansism*; CRC Press Inc.: Boca Raton, FL, 1992; Chapter 2, pp 31-63.

26. Krebs, B.; Henkel, B. *Angew. Chem., Int. Ed. Engl*. **1991**, *30*, 769-788.

27. Litvinov, P. V.; Dyachenko, D. V. *Russ. Chem. Rev*. **1997**, *66*, 923-951.

28. Koketsu, M.; Ishihara, H. *Curr. Org. Chem*. **2003**, *7*, 175-185.

29. Ximenez-Embun, P.; Alonso, I.; Madrid-Albarran, Y.; Camara, C. *J. Agric. Food Chem*. **2004**, *52*, 832-838.

30. Xu, Y.; Kool, E. T. *J. Am. Chem. Soc*. **2000**, *122*, 9040-9041.

31. Mugesh, G.; Du Mont, W. W.; Sies, H. *Chem. Rev*. **2001**, *101*, 2125-2179.

32. Parnham, J. M.; Graf, E. *Prog. Drug Res*. **1991**, *36*, 9-47.

33. Koketsu, M.; Ishihara, H.; Wu, W.; Murekami, K. Saiki, I. *Eur. J. Pharm. Sci.* **1999**, *9*, 157-161.

34. Park, J. Y.; Koketsu, M.; Kim, M. J.; Yeo, H. J.; Ishihara, H.; Lee, G. K.; Kim, Y. S.; Kim, K. C. *Biol. Pharm. Bull***. 2003**, *26*, 1657-1660.

35. Banerjee, M.; Karri, R.; Rawat, S. K.; Muthuvel, K.; Pathak, B.; Roy, G. *Angew. Chem. Int. Ed.* **2015**, *54*, 9323-9327.

36. (a) Weerdenburg, J. A. B.; Eshius, N.; Tessari, M.; Rutjes, F. P. J.; Feiters C. M. *Dalton Trans.* **2015**, *44*, 15387-15390. (b) Srinivas, K.; Babu, N. C.; Prabusankar, G. *Dalton Trans*. **2015**, *44*, 15636-15644.

37. Braun, M.; Frank, W.; Ganter, C. *Organometallics* **2012**, *31*, 1927-1934.

38. Khrustalev, N. V.; Ismaylova, R. S.; Aysin, R. R.; Matsulevich, V. Z.; Osmanov, K. V.; Peregudov, S. A.; Borisov, V. A. *Eur. J. Inorg. Chem*. **2012**, 5456-5460.

39. Cristiani, F.; Devillanova, F. A.; Diaz, A.; Verani, G. *J. Org. Chem*. **1963**, *28*, 1642-1644.

40. Hahn, E. F.; Wittenbecher, L.; Boese, R.; Blaser, D. *Chem. Eur. J*. **1999**, *5*, 1931-1935.

41. Manjare, S. T.; Sharma, S; Singh, H. B.; Butcher, R. J. *J. Organomet. Chem*. **2012**, *717*, 61-74.

42. (a) Popova, A.; Sokolova, E.; Raicheva, S.; Christov, M. *Corros. Sci*. **2003**, *45*, 33-58. (b) Wang, Z. *J. Electrochem. Sci.* **2012**, *7*, 11149-11160.

43. Antonijevic, M. M.; Petrovic, B. M. Int. *J. Electrochem. Sci*. **2008**, *3*, 1-28.

44. Popova, A.; Christov, M.; Raicheva, S.; Sokolova, E. *Corros. Sci*. **2004**, *46*, 1333-1350.

45. Mohamed, O. M.; M'rabet, H.; Hernissi, H; El-Elfrit, M. *Acta Crystallogr., Sect. E: Struct. Rep. Online* **2009**, *65*, o2947.

46. Rivera, A.; Mejia-Camacho, A.; Rios-Motta, J.; Dusek, M.; Fejfarova, K. *Acta Crystallogr., Sect. E: Struct. Rep. Online* **2010**, *66*, o1135.

47. Ingec, K. S.; Soylu, H.; Kucukbay, H.; Ercan, Akkurt, M. *Anal. Sci*. **1999**, *15*, 927-936.

48. (a) Criado, A.; Conde, A.; Marquez, R. *Eur. Cyrst. Meeting* 1982, 7, 122. (b) Criado, A.; Conde, A.; Marquez, R. *Acta Crystallogr., Sect. C: Cryst. Struct. Commun*. **1984**, *40*, 188-190.

49. Korotkikh, I. N.; Rayenko, G. F.; Pekhtereva, M. T.; Shvaika, P. O.; Cowley, H. A.; Jones, N. J. *Russ. J. Org. Chem*. **2006**, *42*, 1833-1851.

50. Cristiani, F.; Devillanova, F. A.; Diaz, A.; Verani, G. *Phosphorus Sulfur Relat. Elem*. **1984**, *20*, 231-240.

51. Cristiani, F.; Devillanova, F. A.; Diaz, A.; Verani, G. *J. Chem. Soc., Perkin Trans. 2* **1984**, 1383-1386.

52. Mammadova, G. Z.; Matsulevich, Z. V.; Osmanov, V. K.; Borisov, A. V.; Khrustalev, V. N. *Acta Crystallogr*. **2012**, *68*, o1381.

53. Palmer, J. H.; Parkin, G. *Polyhedron* **2013**, *52*, 658-668.

54. Al-Janabi, M. S. A.; Abdullah, H. B.; Al-Jibori, A. S. *Orient. J. Chem*. **2009**, *25*, 277-286.

55. Popovic, Z.; Soldin, Z.; Matkovic-Calogovic, G. Pavlovic, Rajic, M. Giester, G. , *Eur. J. Inorg. Chem*. **2002**, 171-180.

56. Palmer, J. H.; Parkin, G. *J. Am. Chem. Soc*. **2015**, *137*, 4503-4516.

57. Singh, S.; Bhattacharya S. *RSC Advances* **2014**, *4*, 49491-49500.

58. Aslanidis, P.; Cox, J. P.; Karagiannidis, P.; Hadjikakou, K. S.; Antoniadis, C. D. *Eur. J. Inorg. Chem*. **2002**, 2216-2229.

59. Raper, S. E.; Creighton, R. J.; Wilson, D. J.; Clegg, E.; Milne, A. *Inorg. Chim. Acta* **1988**, *149*, 265-271.

60. Al-Harbi, A.; Rong, Yi; Parkin, G. *Dalton Trans*. **2013**, *42*, 11117-11123.

61. Qi-Ming Q.; Min, L.; Zhong-Feng, L.; Qiong-Hua, J.; Xu, H.; Zhen-Wei, Z.; Cun-Lin, Z. Qing-Xuan, M. *J. Mol. Struct*. **2014**, *1062*, 125.

62. Skoulika, S.; Aubry, A.; Karagianidis, P.; Aslanidis, P.; Papastefanou, S. *Inorg. Chim. Acta* **1991**, *183*, 207-213.

63. Lobana, S. T.; Sultana, R.; Hundal, G. *Polyhedron* **2008**, *27*, 1008-1015.

64. Dennehy, M.; Quinzani, V. O.; Faccio, R.; Freire, E.; Mombru, W. A. *Acta Crystallogr., Sect. C: Cryst. Struct. Commun*. **2012**, *68*, m12-m16.

65. Han, S.; Yoon, Y. Y.; Jung, O. S.; Lee, Y. A. *Chem. Commun*. **2011**, *47*, 10689-10691.

66. Schneider, J.; Lee, Y. A.; Perez, J.; Brennessel, W. W.; Flaschenriem, C.; Eisenberg, R. *Inorg. Chem*. **2008**, *47*, 957-966.

67. Yue, C.-Y.; Yin, X.-C.; Li, B.-C.; Jiang, F.-L.; Hong, M.-C. *Chin. J. Struct. Chem*. **2010**, *29*, 1001-1019.

68. (a) Xie, J.; Wu, C.; Christopher, B. W.; Quan, J.; Zhu, L. *Phosphorus, Sulfur Silicon Relat. Elem.* **2011**, *186*, 31-37. (b) Aragoni, M. C.; Arca, M.; Demartin, F.; Devillanova, F. A.; Garau, A.; Isaia, F. Lelj, F.; Lippolis, V.; Verani, G. *Chem. Eur. J*. **2001**, *7*, 3122-3133.

69. Aragoni, M. C.; Arca, M.; Demartin, F.; Devillanova, F. A.; Garau, A.; Isaia, F.; Lippolis, V.; Verani, G. *Dalton Trans*. **2005**, 2252-2258.

70. (a) Manjare, S. T.; Yadav, S.; Singh, H. B.; Butcher, R. J. *Eur. J. Inorg. Chem*. **2013**, 5344-5357. (b) Liske, A.; Verlinden, K.; Buhl, H.; Schaper, K.; Ganter, C. *Organometallics* **2013**, *32*, 5269-5272.

71. Melnick, J. G.; Parkin, G. *Science* **2007**, *317*, 225-227.

72. Melnick, J. G.; Yurkerwich, K.; Buccella, D.; Sattler, W.; Parkin, G. *Inorg. Chem*. **2008**, *47*, 6421-6426.

73. Melnick, J. G.; Yurkerwich, K.; Parkin, G. *Inorg. Chem*. **2009**, *48*, 6763-6772.

74. Melnick, J. G.; Yurkerwich, K; Parkin, G. *J. Am. Chem. Soc.* **2010**, *132*, 647-655.

75. Choudhury, J.; Sinha, P.; Prabhakar, S.; Vairamani, M.; Roy S. *Phosphorus Sulfur Silicon Relat. Elem*. **2008**, *12*, 2943-2955.

76. (a) Huynh, V. H; Holtgrewe, C.; Pape, T.; Koh, L. L.; Hahn, E. *Organometallics* **2006**, *25*, 245-249. (b) Huynh, V. H.; Han, Y.; Hui Hui Ho, J.; Tan, K. G. *Organometallics* **2006**, *25*, 3267-3274.

77. (a) Günther, H. *Angew. Chem. Int. Ed. Engl.* **1972**, *10*, 861-874. (b) Garbisch, E. W. *J. Chem. Educ*. **1968**, *45*, 480.

78. *March's Advanced Organic Chemistry: Reactions, Mechanisms, and Structure*; Smith, M. B.; March, J. John Wiley & Sons, Inc.: New York, 2007; pp 24-25.

79. Powell, B. M.; Torrie, B. H. *Acta Crystallogr*. **1983**, *C39*, 963-965.

80. Panda, A.; Mugesh, G.; Singh, H. B.; Butcher, R. J. *Organometallics* **1999**, *18*, 1986-1993.

81. Kienitz, C. O.; Thöne, C.; Jones, P. G. *Inorg. Chem*. **1996**, *35*, 3990-3997.

82. Osborne, A. G.; Hollands, R. E.; Bryan, R. F.; Lockhart, S. *J. Organomet. Chem*. **1982**, *226*, 129-142.

83. Landry, V. K.; Minoura, M.; Pang, K.; Buccella, D.; Kelly, B. V.; Parkin, G. *J. Am. Chem. Soc*. **2006**, *128*, 12490-12497.

84. Boyle, P. D.; Godfrey, S. M. *Coord. Chem. Rev*. **2001**, *223*, 265-299.

85. Jeske, J.; Mont, W.; Jones, P. G. *Chem. Eur. J*. **1995**, *5*, 385-389.

86. Vaughan, G. B. M.; Jora, A. J.; Fitch, A. N.; Gates, P. N.; Muir A. S. *J. Chem. Soc., Dalton Trans*. **1999**, 79-84.

87. Freeman, F.; Ziller, J. W.; Po, H. N.; Keindl, M. C. *J. Am Chem. Soc*. **1988**, *110*, 2586-2591.

88. Cristiani, F.; Devillanova, F. A.; Isaia, F.; Lippolis, V.; Verani, G.; Demartin, F. *Polyhedron* **1995**, *14*, 2937-2943.

89. Deplano, P.; Devillanova, F. A.; Lippolis, V.; Mercuri M. L.; Trogu, E. F. *Gazz. Chim. Ital*. **1994**, *124*, 445-454.

90. Bigoli, F.; Deplano, P.; Devillanova, F. A.; Lippolis, v.; Mercuri, M.L.; Pelllinghelli, M.A.; Trogu, E. F. *Eur. J. Inorg. Chem*. **1998**, *1*, 137-141.

91. Perkins, C. W.; Martin, J. C.; Arduengo, A. J.; Alegria, A.; Lau, W.; Kochi, J. K. *J. Am. Chem. Soc*. **1980**, *102*, 7753-7759.

92. Demartin, F.; Devillanova, F. A.; Isaia, F.; Lippolis, V.; Verani, G. *Inorg. Chim. Acta* **1997**, *255*, 203-205.

93. Deplano, P.; Devillanova, F. A.; Ferraro, J. R.; Isaia, F.; Lippolis, V.; Mercuri, L. *Appl. Spectrosc*. **1992**, *46*, 1625-1629.

94. Godfrey, S. M.; Jackson, S. L.; Mcauliffe, C. A.; Pritchard, R. G. *J. Chem. Soc., Dalton Trans*. **1997**, 4499-4502.

95. (a) Iwaoka, M.; Komatsu, H.; Tomoda, *J. Organomet. Chem*. **2000**, *611*, 164-171. (b) Dutton, L. J.; Tabeshi, R.; Jennings, C. M.; Lough, J. A.; Ragogna, J. P. *Inorg. Chem*. **2007**, *46*, 8594-8602.

96. Klapötke, M. T.; Krumm, B.; Polborn, K. *Anorg. Allg. Chem*. **2008**, *634*, 1287-1290.

97. (a) Klapötke, M. T.; Krumm, B.; Polborn, K. *J. Am. Chem. Soc*. **2004**, *126*, 710-711. (b) Gushwa, F. A.; Richards, F. A. *Eur. J. Inorg. Chem*. **2008**, 728-736. (c) Dutton, L. J.; Martin, D. C.; Sgro J. M.; Jones, D. N.; Ragogna, J. *Inorg. Chem*. **2009**, *48*, 3239-3247.

98. (a) Juárez-Pérez, E. J.; Aragoni, M. C.; Arca, M.; Blake, A. J.; Devillanova, F. A.; Garau, A.; Isaia, F.; Lippolis, V.; Núñez, R.; Pintus, A.; Wilson, C. *Chem. Eur. J.* **2011**, *17*, 11497-11514. (b) Aragoni, M. C.; Arca, M.; Devillanova, F. A.; Grimaldi, P.; Isaia, F.; Lelj, F.; Lippolis, V. *Eur. J. Inorg. Chem.* **2006**, 2166-2174. (c) Aragoni, M. C.; Arca, M.; Demartin, F.; Devillanova, F. A.; Garau, A.; Grimaldi, P.; Isaia, F.; Lelj, F.; Lippolis, V.; Verani, G. *Eur. J. Inorg. Chem.* **2004**, 2363-2368.

99. (a) Mutter, J.; Naumann, J.; Guethlin, C. *Crit. Rev. Toxicol*. **2007**, *37*, 537-549. (b) Sanmartin, D. P.; Font, M.; Palop, A. J. *Curr. Med. Chem*. **2011**, *18*, 4635-4650.

100. Yang, L.; Powell, D. R.; Houser, R. P. *Dalton Trans*. **2007**, 955-964.

101. (a) Wang, C.; Tong, Y.; Huang, Y.; Zhang, H.; Yang, Y. *RSC Advances* **2015**, *5*, 63087-63094. (b) Kimani, M. M.; Bayse, C. A.; Brumaghim, J. L. *Dalton Trans.* **2011**, *40*, 3711-3723. (c) Aroz, M. T.; Gimeno, M. C.; Kulcsar, M.; Laguna, A.; Lippolis, V. *Eur. J. Inorg. Chem.* **2011**, 2884-2894.

102. (a) Syverson, T.; Kaur, P. *J. Trace Elem. Med. Biol*. **2012**, *26*, 215-226. (b) Tai, H. C.; Lim, C. *J. Phys. Chem. A* **2006**, *110*, 452-462.

103. Guzzi, G.; La Porta, C. A. A. *Toxicology* **2008**, *244*, 1-12.

104. Falnoga, I.; Tusek-Znidaric, M. *Biol. Trac. Elem. Res*. **2007**, *119*, 212-220.

105. Wang, F.; Lemes, M.; Khan, M. A. K. In *Environmental Chemistry and Toxicology of Mercury*; Cai, Y., Liu, G., O'Driscoll, N., Eds.; John Wiley & Sons: Hoboken, NJ, 2012; Chapter 16, pp 106-111.

106. Ralston, N. V. C.; Ralston, C. R.; , J. L., III; Raymond, L. J. *Neurotoxicology* **2008**, *29*, 802-811.

107. Hathaway, B. J. In *Comprehensive Coordination Chemistry*, Wilkinson, G.; Gillard, R. D.; McCleverty, J. A., Eds. Pergamon Press: Oxford (UK), **1987**; Vol. 5; pp 533-594.

108. Mukherjee, R. In *Comprehensive Coordination Chemistry II – From Biology to Nanotechnology*, McCleverty, J. A.; Meyer, T. J., Eds. Elsevier Ltd.; Oxford (UK), **2004**; Vol. 6; pp 747-910.

109. Hwang, H. J.; Berry, S. M.; Nilges, M. J.; Lu, Y. *J. Am. Chem. Soc*. **2005**, *127*, 7274-7275.

110. Clark, K. M.; Yu, Y.; Van der Donk, W. A.; Blackburn, N. J; Lu, Y. *Inorg. Chem. Front*. **2014**, *1*, 153-158.

111. Wilson, T. D.; Yu, Y.; Lu, Y. *Coord. Chem. Rev*. **2013**, 257, 260-276.

112. Usón, R.; Laguna, A.; Laguna, M. *Inorg. Synth*. **1989**, *26*, 85-91.

113. Ahrland, S.; Dreisch, K.; Noren, B.; Oskarsson, A. *Mater. Chem. Phys*. **1993**, *35*, 281-289.

114. Nelson, D. J.; Nahra, F.; Patrick, S. R.; Cordes, D. B.; Slawin, A. M. Z.; Nolan, S. P. *Organometallics* **2014**, *33*, 3640-3645.

115. Kraatz, H.-B.; Metzler-Nolte,N. *Concepts and Models in Bioinorganic Chemistry*; Wiley-VCH: Weinheim, Germany, 2006; Chapter 16, pp 363-391.

116. Wang, T.; Guo, Z. *J. Curr. Med. Chem*. **2006**, *13*, 525-536.

117. Tapiero, H.; Townsend, D. M.; Tew, K. D. *Biomed. Pharmacother*. **2003**, *57*, 386-391.

118. Gupte, A.; Mumper, R. J. *Cancer Treat. Rev*. **2009**, 35, 32-39.

119. (a) Bowmaker, G. A.; Hanna, J. V.; Pakawatchai, C.; Skelton, B. W. Thanyasirikul, Y.; White, A. H. *Inorg. Chem*. **2009**, *48*, 350-368. (b) Aslandis, P.; Kyritsis, S.; Lalia-Kantouri, M.; Wicher, B.; Gdaniec, M. *Polyhedron* **2012**, *48*, 140-145. (c) Ramaprabhu, S.; Lucken, E. A. C.; Bernardinelli, G. *J. Chem. Soc. Dalton Trans*. **1993**, 1185-1193. (d) Devillanova, F. A.; Verani, G. *Transition Met. Chem*. **1980**, *5*, 362-364. (e) Hussain, M. S.; Al-Arfaj, A. R.; Hossain, M. L. *Transition Met. Chem.* **1990**, *15*, 264-269. (f) Kim, H. R.; Jung, I. G.; Yoo, K.; Jang, K.; Lee, E. S.; Yun, J.; Son, S. U. *Chem. Commun*. **2010**, *46*, 758-760.

120. Tisato, F.; Marzano, C.; Porchia, M.; Pellei, M.; Santini, C. *Med. Res. Rev*. **2010**, *30*, 708-712.

121. Tisato, F.; Santini, C.; Pellei, M. *Anti-Cancer Agents Med. Chem*. **2009**, *9*, 185-211.

122. (a) Liu, B.; Zhou, Y. Chen W. *Organometallics* **2010**, *29*, 1457-1464. (b) Yamaguchi, K.; Oishi, T.; Katayama, T.; Mizuno, N. *Chem. Eur. J*. **2009**, *15*, 10464-10472. (c) Shahid, M.; Mazhar, M.; Brien, P. O.; Malik, M. A.; Raftery, J. *Polyhedron* **2009**, *28*, 807-811. (d) Balboa, S.; Carballo, R.; Castiñeiras, A.; González-Pérez, J. M.; Niclós-Gutiérrez, J. *Polyhedron* **2008**, *27*, 2921-2930.

123. Fortman, G. C.; Slawin, A. M. Z.; Nolan, S. P. *Organometallics* **2010**, *29*, 3966-3972.

124. (a) Hawecker, J.; Lehn, J. M.; Ziessel, R. *J. Chem Soc., Chem. Commun.* **1983**, 536-538. (b) Portenkirchner, E.; Oppelt, K.; Ulbricht, C.; Egbe, D. A. M.; Nuegebauer, H.; Knör, G.; Sariciftci, N. S. *J. Organomet. Chem.* **2012**, *716*, 19-25. (c) Reimer J. K.; Shaver, A.; Quick, H. M.; Angelici, J. R. *Inorg. Synth*. **2007**, *28*, 154-159.

125. Eisenberg, R.; McCormick, T. M.; Calitree, B. D.; Orchard, A.; Kraut, N. D.; Bright, F. V.; Detty, M. R. *J. Am. Chem. Soc*. **2010**, *132*, 15480-15483.

APPENDIX A: CRYSTAL DATA FOR iPr_2bimS

Empirical formula	$C_{13}H_{18}N_2S$
Formula weight	234.36
Temperature	120(2) K
Wavelength	1.54178 Å
Crystal system, space group	Orthorhombic, *Pna*2_1 (No. 33)
Unit cell dimensions	a = 22.8522(11) Å α = 90º b = 9.9222(5) Å β = 90º c = 33.7824(18) Å γ = 90º
Volume	7660.0(7) $Å^3$
Z, Calculated density	24, 1.273 Mg/m^3
Absorption coefficient	2.004 mm^{-1}
Crystal size	0.22 x 0.08 x 0.05 mm^3
Reflections collected / unique	42936 / 13207 [R(int) = 0.0654]
Completeness to theta = 68.25°	99.8%
Final R indices [I>2sigma(I)]	R1 = 0.0704, wR2 = 0.1801
R indices (all data)	R1 = 0.0831, wR2 = 0.1887
Largest diff. peak and hole	0.906 and -0.681 e. $Å^{-3}$

APPENDIX B: CYRSTAL DATA FOR iPr_2bimSe

Empirical formula	$C_{13}H_{18}N_2Se$
Formula weight	281.25
Temperature	120(2) K
Wavelength	0.71073 Å
Crystal system, space group	Orthorhombic, *Pbca* (No. 61)
Unit cell dimensions	a = 15.1465(7) Å α = 90° b = 10.998(4) Å β = 90° c = 15.6946(8) Å γ = 90°
Volume	2614.6(2) $Å^3$
Z, Calculated density	8, 2.849 Mg/m^3
Absorption coefficient	2.849 mm^{-1}
Crystal size	0.20 x 0.20 x 0.10 mm^3
Reflections collected / unique	39148 / 2497 [R(int) = 0.0401]
Completeness to theta = 25.25°	99.8%
Final R indices [I>2sigma(I)]	R1 = 0.0199, wR2 = 0.0464
R indices (all data)	R1 = 0.0271, wR2 = 0.0499
Largest diff. peak and hole	0.266 and -0.246 e. $Å^{-3}$

APPENDIX C: CYRSTAL DATA FOR ($iPr_2bimS)I_2$

Empirical formula	$C_{13}H_{18}I_2N_2S$
Formula weight	488.15
Temperature	120(2) K
Wavelength	0.71073 Å
Crystal system, space group	Triclinic, $P\bar{1}$ (No. 2)
Unit cell dimensions	a = 8.7620(14) Å α = 68.132(6)° b = 9.2199(14) Å β = 77.250(7)° c = 11.3309(18) Å γ = 74.024(6)°
Volume	809.5(2) $Å^3$
Z, Calculated density	2, 2.003 Mg/m^3
Absorption coefficient	4.001 mm^{-1}
Crystal size	0.28 x 0.15 x 0.08 mm^3
Reflections collected / unique	3090 / 3090 [R(int) = 0.0000]
Completeness to theta = 25.25°	99.6%
Final R indices [I>2sigma(I)]	R1 = 0.0240, wR2 = 0.0524
R indices (all data)	R1 = 0.0372, wR2 = 0.0595
Largest diff. peak and hole	0.585 and -0.634 e. $Å^{-3}$

APPENDIX D: CYRSTAL DATA FOR $(Me_2bimS)HgCl_2$

Empirical formula	$C_9H_{10}Cl_2HgN_2S$
Formula weight	449.74
Temperature	228(2) K
Wavelength	0.71073 Å
Crystal system, space group	Monoclinic, $P2_1/c$ (No. 14)
Unit cell dimensions	a = 11.4491(7) Å α = 90º b = 5.9784(3) Å β = 95.507(2)º c = 17.3412(12) Å γ = 90º
Volume	1181.48(12) $Å^3$
Z, Calculated density	4, 2.528 Mg/m^3
Absorption coefficient	13.623 mm^{-1}
Crystal size	0.28 x 0.06 x 0.04 mm^3
Reflections collected / unique	17875 / 2173 [R(int) = 0.0345]
Completeness to theta = 25.25°	99.9%
Final R indices [I>2sigma(I)]	R1 = 0.0204, wR2 = 0.0494
R indices (all data)	R1 = 0.0277, wR2 = 0.0540
Largest diff. peak and hole	0.724 and -0.650 e. $Å^{-3}$

APPENDIX E: CRYSTAL DATA FOR $(Me_2bimS)HgBr_2$

Empirical formula	$C_9H_{10}Br_2HgN_2S$
Formula weight	538.66
Temperature	228(2) K
Wavelength	0.71073 Å
Crystal system, space group	Monoclinic, $P2_1/c$ (No. 14)
Unit cell dimensions	a = 11.4410(4) Å α = 90º b = 6.2068(2) Å β = 96.1800(10)º c = 17.5860(6) Å γ = 90º
Volume	1241.56(7) $Å^3$
Z, Calculated density	4, 2.882 Mg/m^3
Absorption coefficient	18.970 mm^{-1}
Crystal size	0.15 x 0.07 x 0.07 mm^3
Reflections collected / unique	30355 / 6172 [R(int) = 0.0407]
Completeness to theta = 25.25°	99.9%
Final R indices [I>2sigma(I)]	R1 = 0.0171, wR2 = 0.0374
R indices (all data)	R1 = 0.0224, wR2 = 0.0391
Largest diff. peak and hole	0.648 and -0.635 e. $Å^{-3}$

APPENDIX F: CYRSTAL DATA FOR $(Me_2bimS)HgI_2$

Empirical formula	$C_{18}H_{20}Hg_2I_4N_4S_4$
Formula weight	1265.28
Temperature	120(2) K
Wavelength	0.71073 Å
Crystal system, space group	Triclinic, $P\bar{1}$ (No. 2)
Unit cell dimensions	a = 8.0015(5) Å α = 68.709(2)° b = 8.6337(6) Å β = 71.479(2)° c = 11.5953(7) Å γ = 83.809(3)°
Volume	707.68(8) $Å^3$
Z, Calculated density	1, 2.969 Mg/m^3
Absorption coefficient	15.357 mm^{-1}
Crystal size	0.18 x 0.12 x 0.10 mm^3
Reflections collected / unique	15062 / 2692 [R(int) = 0.0343]
Completeness to theta = 25.25°	99.8%
Final R indices [I>2sigma(I)]	R1 = 0.0180, wR2 = 0.0392
R indices (all data)	R1 = 0.0229, wR2 = 0.0408
Largest diff. peak and hole	0.578 and -0.842 e. $Å^{-3}$

APPENDIX G: CYRSTAL DATA FOR $(Me_2bimS)_2HgCl_2$

Empirical formula	$C_{18}H_{20}Cl_2HgN_4S_2$
Formula weight	667.99
Temperature	120(2) K
Wavelength	0.71073 Å
Crystal system, space group	Triclinic, $P\bar{1}$ (No. 2)
Unit cell dimensions	a = 7.3786(4) Å α = 80.014(2)° b = 8.9469(5) Å β = 78.432(2)° c = 16.3901(8) Å γ = 84.895(2)°
Volume	1042.32(10) $Å^3$
Z, Calculated density	2, 2.001 Mg/m^3
Absorption coefficient	7.851 mm^{-1}
Crystal size	0.10 x 0.08 x 0.06 mm^3
Reflections collected / unique	29984 / 3932 [R(int) = 0.0311]
Completeness to theta = 25.25°	99.7%
Final R indices [I>2sigma(I)]	R1 = 0.0338, wR2 = 0.0922
R indices (all data)	R1 = 0.0359, wR2 = 0.0933
Largest diff. peak and hole	2.899 and -0.860 e. $Å^{-3}$

APPENDIX H: CYRSTAL DATA FOR $(Me_2bimS)_2HgBr_2$

Empirical formula	$C_{18}H_{20}Br_2HgN_4S_2$
Formula weight	716.91
Temperature	120(2) K
Wavelength	1.54178 Å
Crystal system, space group	Triclinic, $P\bar{1}$ (No. 2)
Unit cell dimensions	a = 7.5882(3) Å α = 80.755(2)° b = 8.9734(4) Å β = 78.187(2)° c = 16.5616(8) Å γ = 84.971(2)°
Volume	1087.74(8) $Å^3$
Z, Calculated density	2, 2.189 Mg/m^3
Absorption coefficient	18.876 mm^{-1}
Crystal size	0.15 x 0.15 x 0.10 mm^3
Reflections collected / unique	15095 / 4114 [R(int) = 0.0390]
Completeness to theta = 68.25°	99.6%
Final R indices [I>2sigma(I)]	R1 = 0.0280, wR2 = 0.0739
R indices (all data)	R1 = 0.0295, wR2 = 0.0750
Largest diff. peak and hole	1.407 and -1.358 e. $Å^{-3}$

APPENDIX I: CRYSTAL DATA FOR $(Me_2bimS)_2HgI_2$

Empirical formula	$C_{18}H_{20}HgI_2N_4S_2$
Formula weight	810.89
Temperature	120(2) K
Wavelength	0.71073 Å
Crystal system, space group	Monoclinic, $P2_1/m$ (No. 11)
Unit cell dimensions	a = 7.8904(7) Å α = 90º b = 9.0300(8) Å β = 91.978(2)º c = 31.930(3) Å γ = 90º
Volume	2273.7(3) $Å^3$
Z, Calculated density	4, 2.369 Mg/m^3
Absorption coefficient	9.680 mm^{-1}
Crystal size	0.16 x 0.14 x 0.14 mm^3
Reflections collected / unique	40201 / 4309 [R(int) = 0.0309]
Completeness to theta = 25.25°	99.9%
Final R indices [I>2sigma(I)]	R1 = 0.0206, wR2 = 0.0489
R indices (all data)	R1 = 0.0249, wR2 = 0.0505
Largest diff. peak and hole	0.480 and -0.791 e. $Å^{-3}$

APPENDIX J: CYRSTAL DATA FOR (iPr_2bimS)$HgCl_2$

Empirical formula	$C_{26}H_{36}Cl_4Hg_2N_4S_2$
Formula weight	1011.69
Temperature	120(2) K
Wavelength	0.71073 Å
Crystal system, space group	Monoclinic, $P2_1/m$ (No. 11)
Unit cell dimensions	a = 11.1667(19) Å α = 90° b = 13.147(2) Å β = 92.039(6)° c = 11.336(2) Å γ = 90°
Volume	1663.1(5) $Å^3$
Z, Calculated density	2, 2.020 Mg/m^3
Absorption coefficient	9.690 mm^{-1}
Crystal size	0.19 x 0.14 x 0.10 mm^3
Reflections collected / unique	28366 / 3260 [R(int) = 0.0348]
Completeness to theta = 25.50°	99.9%
Final R indices [I>2sigma(I)]	R1 = 0.0137, wR2 = 0.0305
R indices (all data)	R1 = 0.0169, wR2 = 0.0315
Largest diff. peak and hole	0.319 and -0.686 e. $Å^{-3}$

APPENDIX K: CYRSTAL DATA FOR (iPr_2bimS)$HgBr_2$

Empirical formula	$C_{26}H_{36}Br_4Hg_2N_4S_2$
Formula weight	1189.49
Temperature	100(2) K
Wavelength	0.71075 Å
Crystal system, space group	Orthorombic, *Pbca* (No. 61)
Unit cell dimensions	a = 9.6256(12) Å α = 90º b = 14.3128(16) Å β = 90º c = 24.450(3) Å γ = 90º
Volume	3368.5(7) $Å^3$
Z, Calculated density	8, 2.346 Mg/m^3
Absorption coefficient	13.996 mm^{-1}
Crystal size	0.21 x 0.20 x 0.14 mm^3
Reflections collected / unique	32294 / 3868 [R(int) = 0.0556]
Goodness-of-fit on F^2	1.005
Final R indices [I>2sigma(I)]	R1 = 0.0185, wR2 = 0.0358
R indices (all data)	R1 = 0.0286, wR2 = 0.0381
Largest diff. peak and hole	0.78 and -0.67 e. $Å^{-3}$

APPENDIX L: CYRSTAL DATA FOR (iPr_2bimS)HgI_2

Empirical formula	$C_{13}H_{18}HgI_2N_2S$
Formula weight	688.74
Temperature	100(2) K
Wavelength	0.71075 Å
Crystal system, space group	Orthorhombic, *Pbca* (No. 61)
Unit cell dimensions	a = 9.9121(9) Å α = 90º b = 14.7843(15) Å β = 90º c = 24.109(3) Å γ = 90º
Volume	3533.0(7) $Å^3$
Z, Calculated density	8, 2.590 Mg/m^3
Absorption coefficient	12.316 mm^{-1}
Crystal size	0.48 x 0.35 x 0.18 mm^3
Reflections collected / unique	22845 / 3228 [R(int) = 0.0508]
Goodness-of-fit on F^2	1.056
Final R indices [I>2sigma(I)]	R1 = 0.0271, wR2 = 0.0629
R indices (all data)	R1 = 0.0302, wR2 = 0.0638
Largest diff. peak and hole	2.87 and -2.14 e. $Å^{-3}$

APPENDIX M: CRYSTAL DATA FOR $(iPr_2bimS)_2HgCl_2$

Empirical formula	$C_{13}H_{18}ClHg_{0.50}N_2S$
Formula weight	370.10
Temperature	120(2) K
Wavelength	0.71073 Å
Crystal system, space group	Orthorhombic, *Pna*2_1 (No. 33)
Unit cell dimensions	a = 25.469(3) Å α = 90º b = 10.2631(14) Å β = 90º c = 11.3846(14) Å γ = 90º
Volume	2975.9(7) $Å^3$
Z, Calculated density	8, 1.652 Mg/m^3
Absorption coefficient	5.514 mm^{-1}
Crystal size	0.10 x 0.10 x 0.05 mm^3
Reflections collected / unique	39537 / 5370 [R(int) = 0.0675]
Completeness to theta = 25.25°	99.8%
Final R indices [I>2sigma(I)]	R1 = 0.0347, wR2 = 0.0721
R indices (all data)	R1 = 0.0448, wR2 = 0.0752
Largest diff. peak and hole	1.657 and -2.289 e. $Å^{-3}$

APPENDIX N: CYRSTAL DATA FOR $(iPr_2bimS)_2HgBr_2$

Empirical formula	$C_{26}H_{36}Br_2HgN_4S_2$
Formula weight	829.12
Temperature	120(2) K
Wavelength	0.71073 Å
Crystal system, space group	Orthorhombic, *Pna*2_1 (No. 33)
Unit cell dimensions	a = 25.5873(17) Å α = 90º b = 10.22506) Å β = 90º c = 11.6012(7) Å γ = 90º
Volume	3035.2(3) $Å^3$
Z, Calculated density	4, 1.814 Mg/m^3
Absorption coefficient	7.863 mm^{-1}
Crystal size	0.14 x 0.10 x 0.05 mm^3
Reflections collected / unique	38488 / 5725 [R(int) = 0.0678]
Completeness to theta = 25.00°	99.8%
Final R indices [I>2sigma(I)]	R1 = 0.0312, wR2 = 0.0454
R indices (all data)	R1 = 0.0451, wR2 = 0.0483
Largest diff. peak and hole	0.630 and -0.639 e. $Å^{-3}$

APPENDIX O: CYRSTAL DATA FOR $(iPr_2bimS)_2HgI_2$

Empirical formula	$C_{26}H_{36}HgI_2N_4S_2$
Formula weight	923.10
Temperature	120(2) K
Wavelength	0.71073 Å
Crystal system, space group	Orthorhombic, *Pbcn* (No. 60)
Unit cell dimensions	a = 20.3312(6) Å α = 90º b = 10.1827(3) Å β = 90º c = 15.0889(5) Å γ = 90º
Volume	3123.80(17) $Å^3$
Z, Calculated density	4, 1.963 Mg/m^3
Absorption coefficient	7.059 mm^{-1}
Crystal size	0.20 x 0.16 x 0.14 mm^3
Reflections collected / unique	35978 / 2988 [R(int) = 0.0386]
Completeness to theta = 25.25°	99.8%
Final R indices [I>2sigma(I)]	R1 = 0.0194, wR2 = 0.0412
R indices (all data)	R1 = 0.0245, wR2 = 0.0432
Largest diff. peak and hole	1.111 and -0.415 e. $Å^{-3}$

APPENDIX P: CYRSTAL DATA FOR (iPr_2bimSe)$HgCl_2$

Empirical formula	$C_{26}H_{36}Cl_4Hg_2N_4Se_2$
Formula weight	1105.49
Temperature	120(2) K
Wavelength	0.71073 Å
Crystal system, space group	Monoclinic, $P2_1/m$ (No. 11)
Unit cell dimensions	a = 11.2024(4) Å α = 90º b = 13.2179(5) Å β = 91.2900(10)º c = 11.2639(4) Å γ = 90º
Volume	1667.45(11) $Å^3$
Z, Calculated density	2, 2.202 Mg/m^3
Absorption coefficient	11.722 mm^{-1}
Crystal size	0.18 x 0.06 x 0.05 mm^3
Reflections collected / unique	26114 / 3179 [R(int) = 0.0501]
Completeness to theta = 25.25°	99.9%
Final R indices [I>2sigma(I)]	R1 = 0.0191, wR2 = 0.0322
R indices (all data)	R1 = 0.0272, wR2 = 0.0339
Largest diff. peak and hole	0.437 and -0.486 e. $Å^{-3}$

APPENDIX Q: CYRSTAL DATA FOR (iPr_2bimSe)$HgBr_2$

Empirical formula	$C_{26}H_{36}Br_2HgN_4S_2$
Formula weight	829.12
Temperature	120(2) K
Wavelength	0.71073 Å
Crystal system, space group	Orthorhombic, *Pna*2_1 (No. 33)
Unit cell dimensions	a = 25.5873(17) Å α = 90º b = 10.22506) Å β = 90º c = 11.6012(7) Å γ = 90º
Volume	3035.2(3) $Å^3$
Z, Calculated density	4, 1.814 Mg/m^3
Absorption coefficient	7.863 mm^{-1}
Crystal size	0.14 x 0.10 x 0.05 mm^3
Reflections collected / unique	38488 / 5725 [R(int) = 0.0678]
Completeness to theta = 25.00°	99.8%
Final R indices [I>2sigma(I)]	R1 = 0.0312, wR2 = 0.0454
R indices (all data)	R1 = 0.0451, wR2 = 0.0483
Largest diff. peak and hole	0.630 and -0.639 e. $Å^{-3}$

APPENDIX R: CYRSTAL DATA FOR (iPr_2bimSe)HgI_2

Empirical formula	$C_{13}H_{18}HgI_2N_2Se$
Formula weight	735.64
Temperature	120(2) K
Wavelength	0.71073 Å
Crystal system, space group	Orthorhombic, *Pbca* (No. 61)
Unit cell dimensions	a = 10.0137(3) Å α = 90º b = 15.0221(4) Å β = 90º c = 23.9234(6) Å γ = 90º
Volume	3598.72(17) $Å^3$
Z, Calculated density	8, 2.716 Mg/m^3
Absorption coefficient	13.998 mm^{-1}
Crystal size	0.14 x 0.10 x 0.08 mm^3
Reflections collected / unique	41873 / 3424 [R(int) = 0.0667]
Completeness to theta = 25.25°	99.8%
Final R indices [I>2sigma(I)]	R1 = 0.0217, wR2 = 0.0321
R indices (all data)	R1 = 0.0323, wR2 = 0.0340
Largest diff. peak and hole	0.616 and -0.549 e. $Å^{-3}$

APPENDIX S: CYRSTAL DATA FOR $(iPr_2bimSe)_2HgCl_2$

Empirical formula	$C_{26}H_{36}Cl_2HgN_4Se_2$
Formula weight	834.00
Temperature	120(2) K
Wavelength	0.71073 Å
Crystal system, space group	Orthorhombic, *Pna*2_1 (No. 33)
Unit cell dimensions	a = 25.5345(17) Å α = 90º b = 10.3184(7) Å β = 90º c = 11.4531(8) Å γ = 90º
Volume	3017.6(4) $Å^3$
Z, Calculated density	4, 1.836 Mg/m^3
Absorption coefficient	7.712 mm^{-1}
Crystal size	0.20 x 0.20 x 0.18 mm^3
Reflections collected / unique	37318 / 5656 [R(int) = 0.0264]
Completeness to theta = 25.25°	99.7%
Final R indices [I>2sigma(I)]	R1 = 0.0137, wR2 = 0.0289
R indices (all data)	R1 = 0.0155, wR2 = 0.0293
Largest diff. peak and hole	0.263 and -0.476 e. $Å^{-3}$

APPENDIX T: CYRSTAL DATA FOR $(iPr_2bimSe)_2HgBr_2$

Empirical formula	$C_{26}H_{36}Br_2HgN_4Se_2$
Formula weight	922.92
Temperature	120(2) K
Wavelength	0.71073 Å
Crystal system, space group	Orthorhombic, *Pna*2_1 (No. 33)
Unit cell dimensions	a = 25.6750(16) Å α = 90º b = 10.2579(7) Å β = 90º c = 11.7262(8) Å γ = 90º
Volume	3088.3(4) $Å^3$
Z, Calculated density	4, 1.985 Mg/m^3
Absorption coefficient	9.950 mm^{-1}
Crystal size	0.20 x 0.19 x 0.18 mm^3
Reflections collected / unique	39186 / 6071 [R(int) = 0.0426]
Completeness to theta = 25.25°	99.8%
Final R indices [I>2sigma(I)]	R1 = 0.0177, wR2 = 0.0320
R indices (all data)	R1 = 0.0212, wR2 = 0.0329
Largest diff. peak and hole	0.342 and -0.439 e. $Å^{-3}$

APPENDIX U: CYRSTAL DATA FOR $(iPr_2bimSe)_2HgI_2$

Empirical formula	$C_{26}H_{36}HgI_2N_4Se_2$
Formula weight	1016.90
Temperature	120(2) K
Wavelength	0.71073 Å
Crystal system, space group	Orthorhombic, *Pbcn* (No. 60)
Unit cell dimensions	a = 20.114(2) Å α = 90º b = 10.2005(9) Å β = 90º c = 15.3011(13) Å γ = 90º
Volume	3139.3(5) $Å^3$
Z, Calculated density	4, 2.152 Mg/m^3
Absorption coefficient	9.210 mm^{-1}
Crystal size	0.14 x 0.10 x 0.05 mm^3
Reflections collected / unique	41744 / 2995 [R(int) = 0.0638]
Completeness to theta = 25.25°	99.8%
Final R indices [I>2sigma(I)]	R1 = 0.0249, wR2 = 0.0538
R indices (all data)	R1 = 0.0328, wR2 = 0.0566
Largest diff. peak and hole	0.422 and -0.930 e. $Å^{-3}$

APPENDIX V: CYRSTAL DATA FOR $(iPr_2bimS)_2CuCl$

Empirical formula	$C_{26}H_{36}ClCuN_4S_2$
Formula weight	567.70
Temperature	200(2) K
Wavelength	1.54178 Å
Crystal system, space group	Orthorhombic, *Aba*2 (No. 41)
Unit cell dimensions	a = 17.4183(7) Å α = 90º b = 15.0933(5) Å β = 90º c = 10.6026(17) Å γ = 90º
Volume	2787.42(17) $Å^3$
Z, Calculated density	4, 1.353 Mg/m^3
Absorption coefficient	3.545 mm^{-1}
Crystal size	0.21 x 0.16 x 0.15 mm^3
Reflections collected / unique	20366 / 2521 [R(int) = 0.0227]
Completeness to theta = 68.25°	99.2%
Final R indices [I>2sigma(I)]	R1 = 0.0201, wR2 = 0.0522
R indices (all data)	R1 = 0.0202, wR2 = 0.0524
Largest diff. peak and hole	0.145 and -0.336 e. $Å^{-3}$

APPENDIX W: CYRSTAL DATA FOR $(iPr_2bimS)_2CuBr$

Empirical formula	$C_{26}H_{36}BrCuN_4S_2$
Formula weight	612.16
Temperature	133(2) K
Wavelength	0.71073 Å
Crystal system, space group	Monoclinic, $P2_1/m$ (No. 11)
Unit cell dimensions	a = 9.0543(14) Å α = 90º b = 34.428(5) Å β = 108.672(5)º c = 9.5064(15) Å γ = 90º
Volume	2807.4(7) $Å^3$
Z, Calculated density	4, 1.448 Mg/m^3
Absorption coefficient	2.371 mm^{-1}
Crystal size	0.28 x 0.14 x 0.10 mm^3
Reflections collected / unique	50122 / 5387 [R(int) = 0.0355]
Completeness to theta = 25.25°	99.8%
Final R indices [I>2sigma(I)]	R1 = 0.0303, wR2 = 0.0691
R indices (all data)	R1 = 0.0382, wR2 = 0.0721
Largest diff. peak and hole	0.302 and -0.327 e. $Å^{-3}$

APPENDIX X: CYRSTAL DATA FOR $(iPr_2bimS)_2CuI$

Empirical formula	$C_{26}H_{36}CuIN_4S_2$
Formula weight	659.15
Temperature	200(2) K
Wavelength	1.54178 Å
Crystal system, space group	Monoclinic, $P2_1/m$ (No. 11)
Unit cell dimensions	a = 9.1403(2) Å α = 90º b = 34.8866(9) Å β = 107.6610(10)º c = 9.6292(2) Å γ = 90º
Volume	2925.78(12) $Å^3$
Z, Calculated density	4, 1.496 Mg/m^3
Absorption coefficient	10.823 mm^{-1}
Crystal size	0.28 x 0.12 x 0.10 mm^3
Reflections collected / unique	18597 / 5337 [R(int) = 0.0269]
Completeness to theta = 68.25°	99.5%
Final R indices [I>2sigma(I)]	R1 = 0.0259, wR2 = 0.0640
R indices (all data)	R1 = 0.0301, wR2 = 0.0662
Largest diff. peak and hole	0.414 and -0.418 e. $Å^{-3}$

APPENDIX Y: CYRSTAL DATA FOR (iPr_2bimS)AuCl

Empirical formula	$C_{13}H_{18}AuClN_2S$
Formula weight	466.77
Temperature	120(2) K
Wavelength	0.71073 Å
Crystal system, space group	Orthorhombic, *Pnma* (No. 62)
Unit cell dimensions	a = 8.7711(3) Å α = 90° b = 10.4174(4) Å β = 90° c = 16.5414(6) Å γ = 90°
Volume	1511.42(10) $Å^3$
Z, Calculated density	4, 2.051 Mg/m^3
Absorption coefficient	10.033 mm^{-1}
Crystal size	0.14 x 0.10 x 0.08 mm^3
Reflections collected / unique	17727 / 1520 [R(int) = 0.0533]
Completeness to theta = 25.20°	99.7%
Final R indices [I>2sigma(I)]	R1 = 0.0290, wR2 = 0.0629
R indices (all data)	R1 = 0.0371, wR2 = 0.0671
Largest diff. peak and hole	1.714 and -1.256 e. $Å^{-3}$